

Republic of Iraq
Ministry of Higher Education and
Scientific Research
University of Babylon
College of Materials Engineering
Department of Polymers Engineering and Petrochemical Industries



Preparation and Characterization of Shape Memory Polymer Materials in Industrial Applications

A Thesis

Submitted to the Council of the Department of Polymers Engineering and Petrochemical Industries / College of Materials Engineering / University of Babylon as a Partial Fulfillment of the Requirements for the Degree of Doctorate of Philosophy (Ph.D.) in Polymeric materials Technologies

By

Rola Abdul Al Khader Abbas Al Saffi

Supervised by

Prof. Dr. Mohammed H.D. Al Maamori

2022 A.D

1444 A.H

بِسْمِ اللَّهِ الرَّحْمَنِ الرَّحِيمِ

الرَّحْمَنُ ① عَلَّمَ الْقُرْآنَ ② خَلَقَ الْإِنْسَانَ ③
عَلَّمَهُ الْبَيَانَ ④ الشَّمْسُ وَالْقَمَرُ بِحُسْبَانٍ ⑤ وَالنَّجْمُ
وَالشَّجَرُ يَسْجُدَانِ ⑥ وَالسَّمَاءَ رَفَعَهَا وَوَضَعَ الْمِيزَانَ ⑦

اللَّهُ
صَادِقٌ
الْعَظِيمُ

((سورة الرحمن))

**In the name of Allah, the
Compassionate, the Merciful.**

**1. The Compassionate. 2. Has taught the
Quran. 3. He created the human being. 4.
And taught him clear expression. 5. The
sun and the moon—by calculations. 6. And
the stars and the trees prostrate. 7. And
the sky, He raised. And He set up the
balance.**

God Almighty has spoken the truth

Supervisor's Certification

I certify that thesis entitled "***Preparation and Characterization of Shape Memory Polymer Materials in Industrial Applications***" was presented by(***Rola Abdul Al Khader Abbas Al Saaffi***) under my supervision at the department of polymer engineering and petrochemical industries, College of Materials Engineering, University of Babylon, in a partial fulfillment of the requirements for the Degree of Doctor of Philosophy in polymeric materials technologies.

Supervisor

Signature:

Name: Prof. Dr. Mohammed H.D. Al Maamori

Supervisor's Certification

I certify that this thesis was prepared by "**Rola Abdul Al Khader Abbas Al Saffi**" under my supervision at the department of polymer engineering and petrochemical industries, College of materials, Engineering, University of Babylon. as a partial requirement for the Degree of Doctor of Philosophy in polymeric materials technologies.

Signature:

Name: Dr. Mohammed H.D. Al Maamori

Title: Professor

Address: Department of Polymers engineering and Petrochemical industries /
College of Engineering of Materials / University of Babylon.

Date: / / 2022

"Chairman of Polymers Engineering and Petrochemical Department"

In view of the available recommendation, I forward this thesis for debate by the examination committee.

Signature:

Name: Dr. Zoalfokkar Kareem Mezaal

Title: Professor

Date: / / 2022

Dedication

To Your Honorable Face...Allah

To the Origin of Geniuses...The Land of Mesopotamia (My Country)

To the Source of Renewed Thought ... University of Babylon

*To all those Who Presented Their Hands to Get Me out of this Deep, Dark Well
in Which I Was Suffering Alone*

To Prof. Dr. Abdul Hameed Al Sarraf (My Husband)

To Raed Al Saffi (My Brother)

And To All Of My Family

Rola

2022

Acknowledgements

To the one from whom the salvation is asked and given, glory be to Allah. the compassionate, the merciful ... to the one who gave me the determination. patience and will to accomplish this thesis and overcome obstacle...

*I cannot but extend my thanks and appreciation to **the Presidency of the University of Babylon, the Deanship of the College of Materials Engineering the Presidency of the University of Technology, and finally the Department of Applied Sciences** for giving me the opportunity to complete in studies,*

*I also extend my deepest and sincere appreciation to the supervisor **Dr. Mohammed Al-Mamouri**. As well as I do not forget to give thanks to **Dr. Abdel Raheem Kazem**, the scientific assistant at the college of Materials Engineering, and to **Mr. Sobhi**.*

*I would also like to extend my thanks and gratitude to **Dr. Abdul Hameed Al-Serraf, Dr. Karim Ali, Dr. Adel Ismail and Dr. Farouk Ibrahim** from the College of Education for Pure Science/Ibn Al-Haitham, as well as to **Dr. Uday Hatem**, head of the Remote Sensitization Department at the University of Baghdad, and to **Dr. Hanan Jemil** at AL.Iraqia University.*

*I also thank **Dr. Ali Mutashar** (may God have mercy on him), **Dr. Raed Abdul Wahab**, head of the Department of Applied Sciences**Dr, Nahida J.H, Dr. Shehab Ahmed Zeidan, Dr. Enas Mohi and Mr. Muayid**.*

*In conclusion, I extend my thanks. to **Dr. Abeer and Dr. Omer** from the Ministry of Industry), **Mr. Ali Mahdi, Eng. Donna and Eng. Ansam** from the Ministry of Science and Technology, to **Eng. Basher**, and to my brother, **Raed AlSaffi**.*

Rola

Abstract

Shape-memory polymers, SMPs were prepared by the vulcanized natural rubber swelling with fatty acid according to the elastomer/small molecular blend SMP technique. Two types of elastomeric products were used as a stationary phase, or what is also called hard segment, in the preparation of the shape memory smart natural rubber, which are:

- 1- The commercial elastomeric product represented by the natural rubber band of type Latex, which is denoted in this study with the symbol (Virgin RB).
- 2- The laboratory elastomer product, represented by the natural rubber of type ribbed smoke sheet (RSS-5) that is laboratory vulcanized with different sulfur ratios ranging between (0.75-2) phr, which is denoted as Virgin RSS. Two types of natural and saturated fatty acids were used, which are Stearic acid and Palmitic acid, with different weight percentages (wt% fatty acid) ranging between (3.8-43.9%) according to a swelling time ranging of (5-180) min as a switching phase or what called as soft segment.

For the characterization purpose of the one-way shape memory effect (1w-SME) properties depending on the hot classical shape memory cycle, a set of tests were conducted that enabled the verification of the shape memory behavior (SM-behavior) to evaluate the effect of the vulcanized rubber impregnation with fatty acid on its behavior as shape memory smart material, these tests are:

- The quantified shape memory effect test: Used to calculate the shape memory factors, practically, using the self-modified Vernier instrument and Thermal elongation device (Designed, by me and manufactured in cooperation with engineering industrial workshop). These shape memory factors are represented by the Shape fixity ratio, $R_f\%$, Shape recovery ratio, $R_r\%$ and Shape memory index SM-index.
- The visual photography shape memory effect test, using video-image technique.

- Surface-shape memory test, using (Designed, by me and manufactured in cooperation with engineering industrial workshop) surface-shape memory device.
- Differential Scanning Calorimeter (DSC).
- X-ray diffraction (XRD).

In addition Energy dispersive ray spectroscopy (EDS), Field emission scanning electron microscopy (FE-SEM), Fourier transform infrared spectrometry analysis (FT-IR) and cross-link density tests were performed. Also, short-time quasi-static mechanical tests were conducted such as: Tensile strength, surface hardness, and max crushing strength at room temperature. The results have been discussed in detail.

This study showed that the ability of the vulcanized rubber impregnated with fatty acid to temporary fix the applied strain is related to some special phenomena that occur according to the hot thermo-mechanical cycle protocol, such as thermal contraction, elastic retraction, and the permanent plastic strain accumulation. Where these phenomena play a negative role in the process of restricting the mechanically deformed shape during shape programming stage i.e the shape memory effect (SME) property activation stage, in this cycle the real retained applied strain value was (58.7%) instead of (70%) thus negatively affects the retention of the stretching work energy where it decreases from 73.71 KJ/m³ to 61.65KJ/m³. Where this study has clarified the relation of the shape memory performance with the elastic stretching work energy that is restricted from the spontaneous reversal during the SME property activation stage of the shape memory cycle (SMC).

In addition to the previously mentioned, the main factors affecting the shape memory behavior (SM-behavior) were studied, which are: the fatty acid weight percentage, the shape memory cycle number, the applied strain, the cross-link density. It was found that SM-behavior is improved when the weight

percentage of the fatty acid in the vulcanized rubber mass increases, while SM-behavior is weakened with the increasing of both (applied strain, shape memory cycle number, and cross-link density). On the other side, there is the occurrence of the wax blooming phenomenon during the shape memory cycle, SMC. The data of this study also observe an increase in the original shape recovery speed time during the recovery stage of the SMC with the increase in the thermal stimulation temperature where the original shape recovery ratio, R_r , is reached to 99.7%. A slight difference was also noticed in the SM-behavior with the change in the nature of the cooling and heating methods, but this change has a significant impact on the time of the SMC.

Finally, the short-time quasi-static mechanical tests at room temperature, are means of describing the variation in the mechanical properties of vulcanized rubber before and after it is impregnated with fatty acid. In addition to that, by using these conventional tests, the vulcanized rubber impregnated with fatty acid do not show shape memory behavior in spite of its impregnation with the fatty acid, where it behaves similar to a non-smart conventional vulcanized rubber by not showing shape memory behavior; because in these devices there are no exceptional conditions that help in conducting a shape memory cycle to activate and deactivate the SME property, because this property is generally not inherent in the SMP materials.

List of Symbols

No.	Symbols	Description	Unit
1-	$\epsilon_0, \epsilon_1, \epsilon_2, \epsilon_3$	Is the applied strain during the SMC programming step0, step1, step2, step3 sequential.	%
2-	δ_1	Tensile stress.	Pa
3-	ρ_s	Mass density of toluene solvent.	g/cm ³
4-	ρ_r	Mass density of initial dry sample (before the immersion).	
5-	g	Ground acceleration.	m/sec ²
6-	L_o	Initial length.	mm
7-	M	Applied mass.	g
8-	V_R	Volume fraction of the test sample in swollen state.	%
9-	V_s	Molar of toluene solvent	cm ³ /mol
10-	W_d	Weight of sample before immersion in solvent.	g
11-	$W_{D.E}$	Dissipation elastic strain energy.	KJ/m ³
12-	W_{frozen}	The elastic strain energy is recoverable by thermal stimulation.	
13-	W_I	Internal stretching work.	
14-	$W_{plastic}$	Plastic dissipation energy.	
15-	W_s	Weight of sample after immersion in solvent.	g
16-	W_{sp1}	Spontaneous recoverable elastic strain energy.	KJ/m ³
17-	W_{sp2}	Spontaneous recoverable elastic strain energy – reduced after the occurrence of thermal contraction.	
18-	ΔH_m	Latent heat of melting.	J/g
19-	ΔL	Amount of change length.	mm
20-	T_g	Glass transition temperature.	C°
21-	T_m	Melt transition temperature.	

List of Abbreviations

No.	Symbols	Description
1-	CBS	N-cyclohex1-2-benzyhiazde Sulfenamide.
2-	CIE	Crystalline –induced elongation.
3-	DSC	Differential scanning calorimetry analysis.
4-	EAP	Electric – active polymers.
5-	EDS	Energy dispersive X-ray spectroscopy analysis.
6-	F(N)	Stretching force.
7-	FCT	Flat Crush Test.
8-	FE-SEM	Field emission electron microscopy.
9-	FT-IR	Fourier transform infrared spectrometry analysis.
10-	MA	Myristic acid.
11-	PA	Palmitic acid.
12-	phr	Partper hundred rubber.
13-	RB	Natural rubber band.
	Virgin RB	The commercial elastomer product.
14-	RB/PA band SMP	Rubber band/ Palmitic acid shape memory polymer.
15-	RB/SA band SMP	Rubber band/ Stearic acid shape memory polymer.
16-	RSS	Ribbed smoke sheet.
	Virgin RSS	The laboratory elastomer product.
17-	RSS/SA band SMP	Ribbed smoke sheet / Steaic acid blend shape memory polymer.
18-	S	Sulfur.
19-	SA	Steaic acid.
20-	SIC	Strain – induced crystals.
21-	SMAs	Shape memory alloys.
22-	SMCs	Shape memory ceramics
23-	SMG	Shape memory gel.
24-	SMMs	Shape memory materials.
25-	SMH	Shape memory hybrid.
26-	1 Virgin RSS	Labrotary elastomer product at (S=0.75phr).
27-	2 Virgin RSS	Labrotary elastomer product at (S=1phr).
28-	3 Virgin RSS	Labrotary elastomer product at (S=1.25phr).
29-	4 Virgin RSS	Labrotary elastomer product at (S=1.5phr).
30-	5 Virgin RSS	Labrotary elastomer product at (S=2phr).
31-	X	Flory- Huggins polymer- solvent interaction term.
32-	XRD	X-ray diffraction analysis.

No.	Symbols	Description
33-	ZnO	Zinc Oxide.
34-	CPU	Central Processing Unit

List of Acronyms and Shape memory polymer Terminology

No.	Acronyms and Terminology	Meaning
1-	SMPs	Shape-memory polymers: That can change their shape in response to multiple external stimuli.
2-	Hard segment	Stationary phase (Net points).
3-	SME	Shape-memory effect property: That refers to the ability of material to memories its shape.
4-	1W- SME	One – Way shape memory effect: That can change between temporary and original shape many times with the need for more reshaping.
5-	SM-behavior	Shape memory behavior.
6-	SM-index, $R_f\%$ and $R_r\%$	Shape memory index, mechanically deformed shape fixity ratio and permanent original shape recovery ratio respectively: Parameters for evaluating shape memory performance.
7-	Surface –Shape memory test	A test for evaluation the shape memory of the surface of the material.
8-	Programming stage	The shape memory effect property activation stage: It is the stage in which the fixed temporary shape is formed.
9-	Recovery stage	The shape memory effect property deactivation stage: It is the stage makes the materials recovery its original shape.
10-	SMC	Shape memory cycle: It is the cycle in which the shape memory effect property is activated and deactivated.
11-	SM- cycle	Shape memory cycle.
12-	2W-SME	Two –Way shape memory effect property: That refers to that materials can change between temporary and original shape many times without shape need for more reshaping.
13-	SRM	Stimulus – responsive materials.
14-	SCM	Shape change material.
15-	Multiple - SME	Multiple-way shape memory effect: That refers to the ability of materials that exhibit two or more temporary shapes as well as the original shape.
16-	Temporary fixity shape	The shape of the material is mechanically deformed after programming stage.

No.	Acronyms and Terminology	Meaning
17-	Fixity shape	The shape of original material before SMC.
18-	Original shape	Fixity shape.
19-	Recovery shape	The shape material after recovery stage.
20-	Soft segment	Switching phase.
21-	SCPs	Shape changing polymers.
22-	Programmability	It is a term referring to an procedure by the applied of an external stress or force during programming stage.
23-	T_{trans} ($^{\circ}C$)	Thermal transition temperature; Is the inherent temp. Of SMP that permits shape change from the original to temporary shape. This may T_g or T_m .
24-	d_F (mm)	Fixed deformation.
25-	d_{max} (mm)	Maximum deformation.
26-	d_R (mm)	Deformation recovered in a certain cycle .
27-	ϵ_u (%)	Fixed strain after end programming stage.
28-	ϵ_p (%)	Recovery strain after end recovery stage
29-	ϵ_m (%)	Maximum strain during loading.
30-	T_{sm} (sec)	Shape memory cycle time: Refers to the whole necessary time for SMPs temporary shape programming to permanent shape.
31-	SM- polymer	Shape memory polymer.
32-	SMNR	Shape memory natural rubber.
33-	SM- parameters	Shape memory parameters
34-	Dual shape memory testing	It is the test of ability of material to change its original shape to the temporary fixity shape and then return back to its original shape during SMC.
35-	Thermo-mechanical cycle	Shape memory cycle type of Hot-Classical.
36-	Target shape	Fixity temporary shape,
37-	Step0, Step1, Step2, Step3, Step4, Step5	Steps of Hot-Classical SMC, where step0, step1, step2 and step3 during programming stage, while step4 and step5 during recovery stage.
38-	N	Is the shape memory cycle number (N=0,1,2,3...ect.)
39-	SM- recovery stretching strain	Shape memory recovery stretching strain.

No.	Acronyms and Terminology	Meaning
40-	SM-temperature (°C)	Shape memory temperature: Is the transition temperature.
41-	Wax blooming phenomena	The amount of fatty acid that is expelled from the body of SMP sample during SMC.
42-	Wt% difference	It is weight percent difference.
43-	Wt ₀ and Wt _n	Correspond to the sample's initial and nth cycle weight respectively.
44-	Macroscopically demonstration of SME property	The macroscopically demonstration of shape memory effect property by digital imaging or video.
45-	Shape Change Material (SCM)	Molecular structure size / volume change.

Contents

Abstract	i
List of Symbols	iv
List of Abbreviations.....	v
List of Acronyms and Shape memory polymer Terminology	vii
Contents	x
List of Figures	xv
List of Tables.....	xxii
Chapter One:Introduction	
1-1 Introduction.....	1
1-2 Aims of the Study	4
1-3 Strategy of the Study.....	4
Chapter Two:Theoretical Part and Literature Survey	
2-1 Introduction.....	5
2-2 Traditional Materials Classification Systems	5
2-2-1 Metals	5
2-2-2 Ceramics	5
2-2-3 Polymers	5
2-2-4 Composites	6
2-3Classification Systems for Advanced Materials.....	6
2-3-1 Semiconductors	6
2-3-2 Biomaterials.....	7
2-3-3 Materials of Future	7
2-3-3-1 Nano-engineered Materials	7
2-3-3-2 Smart Materials	8
2-4 Types of Smart Materials.....	8
2-4-1Energy-Exchanging Smart Materials	8
2-4-2 Property-Changing Smart Materials.....	9
2-5 Properties of Smart Materials	10

2-5-1 Bionicity	10
2-5-2 Sensor Ability	10
2-5-3 Adaptability	10
2-6 Shape Memory Materials (SMMs)	10
2-6-1 Shape-Memory Alloys (SMAs).....	11
2-6-2 Shape-Memory Polymers (SMPs).....	12
2-6-3 Shape-memory ceramics (SMCs).....	12
2-7 Shape Memory Polymers and Shape Memory Alloys Advantages and Disadvantages Comparison	12
2-8 Shape-Memory Effect (SME) Property	13
2-9 Mechanism of the Shape-Memory Effect (SME) in SMPs and SMAs	15
2-10 Types of Shape Memory Effect (SME) in SMPs	16
2-10-1 One-way Shape Memory Effect (1W-SME).....	16
2-10-2 Two-Way Shape Memory Effect (2W-SME)	16
2-10-3 Multiple-Way Shape Memory Effect (Multiple-SME).....	16
2-11 Activation and Deactivation of SME Property During the Shape Memory Cycle (SMC).....	17
2-12 Thermo-mechanical Cycle.....	19
2-13 Net-Points and Switching Phase in SMP	19
2-13-1 Net-Points	21
2-13-2 Switching Phase	21
2-14 SMP Characteristic Parameters During SM-Cycle	22
2-14-1 Shape Fixity Ratio	22
2-14-2 Shape recovery ratio	22
2-14-3 Recovery Time	23
2-14-4 Shape Memory Cycle Time (t_{sm}).....	23
2-14-5 Shape Memory Index	23
2-15 Structural Categorization of SMPs	23
2-15-1 Thermoplastic Shape Memory Polymers	24

2-15-2 Thermosetting Shape Memory Polymers.....	24
2-15-2-1 Thermosetting Styrene-Based Shape Memory Polymer.....	25
2-15-2-2 Thermosetting Epoxy Shape Memory Polymer (SM-Polymer)	25
2-15-3 Shape Memory Materials of Rubbers.....	26
2-15-3-1 Lightly Cross-Linked Shape Memory Natural Rubber (SMNR).....	27
2-15-3-2 Elastomer/Small Molecule Blend SMPs.....	28
2-16 Fatty Acids	29
2-16-1 Fatty Acids Types.....	29
2-16-1-1 Unsaturated Fatty Acids.....	29
2-16-1-2 Saturated Fatty Acids	30
2-16-2 Properties of fatty acids.....	30
2-17 Application of shape memory materials.....	31
2-18 Literature Survey	35
Chapter Three: Practical Part	
3-1 Introduction.....	43
3-2 Materials in Use:	45
3-2-1 Elastomeric Product (Hard Segment).....	45
3-2-2 Fatty acid (Soft segment)	46
3-3 Laboratory Elastomeric Product Preparation Technique.....	47
3-3-1 Stage of Preparing the Rubber Dough.....	48
3-3-2 Sheets Molding Stage of the Vulcanized Rubber Type (Virgin RSS)...	49
3-4 Shape-Memory Natural Rubber (SMNR) Preparation Technique	50
3-4-1 Preparation of Shape Memory Natural Rubber Type (Rubber Band/Stearic Acid Blend SMP) Sample Code (RB/based SA)	50
3-4-1-1 Stearic Acid (SA) Preparation	50
3-4-1-2 (RB/based SA) Preparation Technique	50
3-4-1-3 Addition Ratio.....	52
3-4-2 Preparation of Shape Memory Natural Rubber Type (Rubber Band/Palmitic Acid Blend SMP) Sample Code (RB/based PA)	52

3-4-3 Preparation of Shape Memory Natural Rubber Type (Virgin RSS/Stearic Acid Blend SMP) Sample Code (RSS/based SA)	53
3-5 Characterization and Test Methods of SMP.....	54
3-5-1 One-Way Shape Memory Test.....	54
3-5-1-1 Quantified Shape-Memory Effect (SME) Test	56
3-5-1-1-1 Air-responsive shape memory effect test.....	56
3-5-1-1-2 The Water-responsive Shape-Memory Effect (SME)Test.....	63
3-5-1-2 Visual Photography (Macroscopic) Shape Memory Effect (SME) Testing	66
3-5-1-3 Surface Shape-Memory Effect (SME) Testing.....	68
3-5-2 Physico -Chemical Characterization Tests.....	70
3-5-2-1 Differential Scanning Calorimetry Analysis (DSC) Test	70
3-5-2-2 X-ray Diffraction (XRD) Test.....	70
3-5-2-3 Fourier transform infra-red (FT-IR) Test.....	70
3-5-2-4 Field Emission-Scanning Electron Microscopy (FE-SEM) Test.....	70
3-5-2-5 Energy dispersive X-ray spectroscopy analysis (EDS) Test	70
3-5-2-6 Determination of the Vulcanized Rubber Cross-Link Density by Solvent Swelling Method	71
3-5-3 Quasi-Static Mechanical Tests at Short Time	72
3-5-3-1 Tensile Strength Test.....	72
3-5-3-3 Flat-Crush Test (FCT).....	72
Chapter Four: Results and Discussion	
4-1 Introduction.....	73
4-2 Analysis of Commercial Natural Rubber Band Swelling in Stearic Acid (SA) Molten.....	73
4-3 Characterization of Commercial Rubber Band Impregnated with Stearic Acid as Shape Memory Smart Material.....	78
4-3-1 DSC Test	82
4-3-2 X-ray Diffraction (XRD) Patterns Examination	85

4-4 The Role of the Melting and Crystallizing of the Stearic Acid Network in Retaining and Releasing the Mechanical Deformation Energy	89
4-5 Demonstration of a Macroscopic Shape-Memory Effect (SME) Property of the Smart Rubber Band	100
4-6 Study of the Surface Shape Memory Effect (SME) of the Smart Rubber Band.....	102
4-7 Study of Factors Affecting the Smart Vulcanized Natural Rubber Shape Memory	103
4-7-1 Study the Effect of Stearic Acid Weight Percentage on the Shape Memory Behavior	103
4-7-2 Studying the Effect of the Imposed Applied Strain on the Behavior of Shape Memory	107
4-7-3 Studying the Effect of Shape Memory Cycle Number on Shape Memory Behavior	109
4-7-4 Study of the Effect of the Fatty Acid Nature on the Shape Memory Behavior	112
4-7-5 Studying the Relation of the Cross- link Density to Shape Memory of the Smart Vulcanized Natural Rubber.	116
4-7-6 Studying the Effect of the Different Nature of the Smart Rubber Material on the Behavior of Shape Memory.	124
4-8 Quasi-static short-time Mechanical Characterization of some Materials under Study Before Undergoing a Shape Memory Cycle.	127
4-9 Factors Affecting Hot Classical Shape Memory Cycle Time.	129
4-9-1 Study the Effect of the Cooling and Heating facility on the Shape Memory Cycle Time Using the Thermal Elongation Device.....	129
4-9-2 Studying the Effect of the Heating and Cooling Method on the Shape Memory Cycle Time Using the Modified Vernier Caliper Tool.....	133
Chapter Five: Conclusions and Recommendations	
5-1 Conclusions:.....	136
5-2 Recommendations.....	138
References	
References: -.....	139

List of Figures

No.	Subject	Page
Chapter One		
1-1	Tetrahedron shape of materials science, the four component of discipline of material science and engineering and their interrelationship.	2
1-2	The increment of the scientific publications numbers growth regarding the topic of shape memory smart polymeric materials in between 1992 to 2014.	3
1-3	The different classes of smart polymeric materials and the percentage of publications of these classes according to the scientific container of publication in Scopus.	
Chapter Two		
2-1	Type of smart materials according the nature of response.	9
2-2	A schematic of tree of shape memory materials (SMMs).	11
2-3	Photographs of the polymeric material showing shape memory effect.	14
2-4	(A) Crystalline structure changing during SME of alloys, (B) mechanism of SME of polymers.	16
2-5	Various shape-memory effect (SME) of SMPs, (a) (1W-SME), (b) (2W-SME) and (c) Multiple-SME.	17
2-6	Shape memory technique includes two stages understood as programming and recovery stages.	18
2-7	SME schematic diagram during a typical thermo-mechanical cycle	19
2-8	Classification of shape changing polymers.	20
2-9	Schematic diagram switching units and net points in a thermally induced SMP.	21
2-10	Schematic diagram of structural categorization of shape memory polymers (SMPs).	24
2-11	General structural formula of the saturated fatty acids.	30
Chapter Three		
3-1	The flowchart of the work steps and its different stages.	44
3-2	(a) and (b), photographic images of the commercial natural rubber bands used in this study (Virgin RB) as a commercial elastomer product, (c) the dimensions of the commercial rubber band.	45
3-3	Schematic of preparing the laboratory elastomeric product type (Virgin RSS).	47
3-4	A photographic image of the vulcanized RSS natural rubber sample with different ratios of the sulfuric cross-linking agent used as a laboratory elastomeric product, denoted by (Virgin RSS).	49

No.	Subject	Page
3-5	Photographic images taken during preparation of RB/based SA, a- preparation of SA for melting process, b-the process of removing the rubber bands after impregnation with SA, c- forming some residues of SA on (RB/based SA) surface, d- scraping process of SA residues off the surface of (RB/based SA), e- Dry the RB/based SA at room temp.	51
3-6	Photographic image of laboratory elastomeric vulcanized rubber after being impregnated with SA molten denoted as (RSS/based SA).	53
3-7	Photographic image of the Self-made shape memory device based on thermal stimulation by hot air.	57
3-8	Is a schematic diagram of the hot-classical shape memory cycle (SMC) based on normal cooling at room temperature ($23\pm 2^{\circ}\text{C}$) for the samples under study.	59
3-9	A photographic image of the self-modified electronic Vernier for being used as a shape-memory instrument based on thermal stimulation by immersing in hot water.	63
3-10	Snapshots taken with the video camera of the fixed temporary shape programming stage steps.	67
3-11	Photographic images of the self- made surface shape memory device based on thermal stimulation with hot water.	68
Chapter Four		
4-1	EDS measurement of commercial natural rubber band.	73
4-2	Swelling behavior of the commercial natural rubber band (RB) in Stearic acid (SA) at (75°C).	74
4-3	FE-SME images at different magnifications for the rubber band sample (RB/ based SA) impregnated with stearic acid for 2hr.	75
4-4	FT-IR spectrum of the rubber band (Virgin RB) and reference spectra for natural rubber and silica.	76
4-5	FT-IR. Spectrum of the stearic acid (SA).	
4-6	The match between FT-IR spectrum of Stearic acid (SA) particles used in this study and the (FT-IR) spectrum of Stearic acid present in the FT-IR device library.	77
4-7	FT-IR spectrum of (RB/ based SA).	
4-8	Matching the Stearic acid (SA) data in the device library (FT-IR) with some peaks of the RB/ based SA spectrum.	78
4-9	The relation of the applied strain during the hot classical shape memory cycle based on normal cooling of the commercial rubber band before and after impregnation Stearic acid (SA) with No. of step.	79

No.	Subject	Page
4-10	(FE-SME) microscope image of the sample surface of type (Virgin RB).	81
4-11	(FE-SME) microscope image of the sample surface of type (RB/based SA).	
4-12	Heating curve taken during DSC test of Virgin RB sample, which was previously subjected to the SME activation stage.	82
4-13	Heating curve of the sample (RB/based SA), which was previously subjected to the SME activation stage.	83
4-14	Heating curve has taken during DSC test for the Stearic acid (SA) sample.	84
4-15	The heating curve taken during DSC test of (RB/based SA) sample after (SME) property deactivation.	85
4-16	The effect of the latent heat of melting, ΔH_m in the SME property state.	
4-17	X-ray diffraction curve of RB/based SA sample of activated SME property	87
4-18	X-ray diffraction curve of RB/based SA sample of deactivated SME property.	
4-19	represents the profile of the hot classical shape memory cycle based on room temperature natural cooling for (RB/based SA).Where (a) shows the temperature relationship, (b) shows the stress relationship, (c) shows the time relationship, and (d) shows the stress relationship, with the number of the programming stage steps of the shape memory cycle followed.	90
4-20	FM-SEM image of the surface of (RB/based SA) that appears in the form of bit layers analogous platelet crystals of SA material coating the rubber band molecules in their crystalline state.	91
4-21	The physical phenomena accompanying the programming stage of the hot classical shape memory cycle of RB/based SA.	92
4-22	The difference in the value of the applied strain that is fixed in step3 from its actual value applied in step1 during (RB/based SA) deformed shape programming stage in the hot classical thermomechanical cycle based on normal cooling at room temperature.	
4-23	The relation of the shape memory recovery strain (retained strain) to the shape memory recovery temperature (SM-temperature).	93
4-24	The analytical framework for the change of molecular architecture configuration for RB/based SA during the hot classical thermomechanical cycle based on normal cooling at room temperature.	94

No.	Subject	Page
4-25	A schematic diagram of the applied strain retention process in the RB/based SA material after completion of the programming stage of the hot classical shape memory cycle.	95
4-26	Schematic diagram of the strain releasing process from the RB/based SA deformed shape into its surrounding medium during the recovery stage of the hot thermomechanical cycle.	96
4-27	Schematic diagram of the practically observed physico-mechanical phenomena during the hot classical shape memory cycle and their relation to the applied elongation work energy meant to be retained. (+) positive role, (-) negative role.	97
4-28	A schematic diagram showing that the stretching work energy is neither consumed nor regenerated during the hot classical shape memory cycle, but is transformed from one form to another.	99
4-29	The relation between the shape memory recovery work energy (SM-recovery work energy) and the shape memory temperature (SM-temperature).	100
4-30	Digital images showing the programming and recovery demonstration of the macroscopic (SME) of (RB/ based SA).	101
4-31	Digital images showing the programming and recovery demonstration of the macroscopic SME of (RB/based SA).	
4-32	Photographic and microscopic images showing the activation and deactivation of surface SME.	102
4-33	The relation of the fixed strain in step3 and the swelling time of (RB based/SA) in the Stearic acid molten.	104
4-34	The relation of the fixed strain in step3 and weight percentage of Stearic acid in the material (RB based/SA).	
4-35	The relation of the shape fixity ratio and swelling time of (RB based/SA) in Stearic acid molten.	
4-36	The relation of the shape fixity ratio with the Stearic acid weight percentage in the (RB/based SA) material.	105
4-37	The relation of non-reversible plastic strain with swelling time of the (RB/based SA) material in Stearic acid molten.	
4-38	The relation of the non-reversible plastic strain to the stearic acid weight percentage in the (RB/based SA) material.	
4-39	The relation of the shape recovery ratio to the swelling time of (RB/based SA) material in stearic acid molten.	106
4-40	The relation of the shape recovery ratio to the weight percentage of Stearic acid in (RB/based SA) material.	
4-41	The relation of the SM- index to the Stearic acid weight percentage in (RB/based SA) material.	107

No.	Subject	Page
4-42	The relation between the tensile strain measured during the shape memory cycle, and the number of steps of the shape memory cycle.	108
4-43	The relation between the tensile strain measured during the shape memory cycle, and the number of steps of the shape memory cycle.	
4-44	The relation between the shape recovery ratio of (RB/based SA) and the strain applied in step1.	
4-45	The relation between the SM-index of (RB/based SA) and the strain applied in step1.	109
4-46	The relation of the stearic acid weight percentage difference with the shape memory cycle number.	110
4-47	The relation of the fixity strain in step3 with the shape memory cycle number.	111
4-48	The relation of the shape fixity ratio of the mechanically deformed shape with the shape memory cycle number.	
4-49	The relation of the permanent plastic strain with the shape memory cycle number.	
4-50	The relation of the shape recovery ratio with the shape memory cycle number.	112
4-51	The relation of the SM-index ($R_f \times R_r$) % to the shape memory cycle number.	
4-52	Effect of the nature of the fatty acid on the swelling percentage of the commercial natural rubber band (Virgin RB) after immersing with this acid.	113
4-53	Effect of the nature of the fatty acid on the fixity strain in step 3 of the deformed shape programming stage.	114
4-54	Effect of the nature of the fatty acid on the shape fixity ratio, R_f (%) of the commercial rubber band deformed shape impregnated with the fatty acid (Code RB/ based fatty acid).	
4-55	Effect of the nature of the fatty acid on the permanent plastic strain formed in the commercial rubber band impregnated with fatty acid (RB/ based fatty acid) after the end of the hot classical shape memory cycle.	
4-56	Effect of the nature of the fatty acid on the shape recovery ratio, R_r (%) of the commercial rubber band impregnated with fatty acid (RB/ based fatty acid).	115
4-57	Effect of the nature of the fatty acid on the SM-index ($R_f \times R_r$)% of the commercial rubber band impregnated with fatty acid (RB/ based fatty acid).	
4-58	The relation between cross-link density and sulfur ratio in Virgin RSS.	116

No.	Subject	Page
4-59	The relation between the weight percentage of Stearic acid (SA) and sulfur ratio in (RSS/based SA).	117
4-60:	The relation between the weight percentage of Stearic acid SA with the cross-link density of (RSS/based SA).	
4-61	The relation between fixed strain and sulfur ratio in (RSS/based SA) after the end of the SME activation stage during the classical hot shape memory cycle based on normal cooling at room temperature.	118
4-62	The relation between the shape fixity ratio and the sulfur ratio in RSS/based SA after the end of the SME property activation stage during the hot classical shape memory cycle based on normal cooling at room temperature.	120
4-63	The relation between the permanent plastic strain and the sulfur ratio in RSS/based SA after the end of the SME property deactivation stage during the hot classical shape memory cycle based on normal cooling at room temperature.	
4-64	The relation between the shape recovery ratio and the sulfur ratio in RSS/based SA after the end of the SME property deactivation stage during the hot classical shape memory cycle based on normal cooling at room temperature.	121
4-65	The relation between SM-index and sulfur ratio of the material RSS/based SA.	122
4-66	The macroscopically demonstration of the shape memory effect (SME) property by digital imaging for the RSS/based SA sample.	123
4-67	The relation between the recovery time and recovery temperature.	
4-68	The relation of the cross link density to the material nature under study.	125
4-69	The relation of the Stearic acid weight percentage (SA wt%) to the material nature under study.	
4-71	The relation of the shape recovery ratio, R_r (%) to the material nature under study.	126
4-72	The relation of the SM-index to the material nature under study.	
4-73	Stress-strain tensile curve for RB without SA (Virgin RB) at room temperature.	128
4-74	Stress-strain tensile curve for (RB based/ SA) at room temperature.	
4-75	The effect of the rubber bands impregnation with Stearic acid on the tensile (stress-strain).	
4-76	Stress-strain tensile curve for (1Rss without SA) (1Virgin RSS) at room temperature.	
4-77	Stress-strain tensile curve for (1Rss based/ SA) at room temperature.	

No.	Subject	Page
4-78	The effect of the 1 Virgin RSS impregnation with Stearic acid on the tensile (stress-strain).	128
4-79	The relation of the Max. crushing strength to the type of sample at room temperature.	129
4-80	The relation of the surface hardness to the type of sample at room temperature.	
4-81	Profile of the classical shape memory cycle temperature using thermal elongation device for the smart rubber under study.	130
4-82	The relation of the shape fixity ratio, $R_f(\%)$ with the type of classical shape memory cycle using Thermal elongation device.	131
4-83	The relation of the shape recovery ratio, $R_r(\%)$ with the type of classical shape memory cycle using Thermal elongation device.	
4-84	Characterization of shape memory behavior during the hot classical shape memory cycle.	132
4-85	The relation of the shape recovery ratio to the original shape memory recovery temperature (SM-recovery temperature).	
4-86	The relation of the shape fixity ratio to device type for SME test.	134
4-87	The relation of the shape recovery ratio to device type for SME test.	

List of Tables

No.	Subject	Page
Chapter Two		
2-1	Properties of shape memory polymers and shape memory alloys.	13
2-2	Constituents to be counted when producing SME natural rubber.	27
2-3	Examples of SMPs application.	32
2-3	(continued).	33
2-4	Examples of shape memory rubber application.	34
Chapter Three		
3-1	The specifications of the materials involved in the vulcanization process of raw rubber (RSS).	46
3-2	Specifications of the natural fatty acids used in this study.	46
3-3	Times of adding the rubber mixture materials.	48
3-4	The materials ratios added to the rubber mixture.	48
3-5	The sample code for different swelling time and type of network sample.	52
3-6	The sample code for different sulfur ratios and type of network sample.	53
3-7	The standard specifications for each of the tests that were conducted in this study.	55
3-8	The water-responsive shape memory effect (SME) test method in images using the developed Vernier.	65
3-9	Determination of the types of the target shape that is previously fixed in the visual demonstration of SME property, with the fixation tools.	66
3-10	Pictures of the surface shape memory effect (SME) test method using ball penetrator.	69
Chapter Four		
4-1	The weight percentage of the commercial natural rubber band components.	73
4-2	X-ray diffraction parameters of the sample RB/based SA of activated and deactivated SME property.	86
4-3	The difference of the shape memory cycle time of (RB/based SA) by different SME property activation and deactivation instruments during the hot classical shape memory cycle.	130
4-4	A comparison between the Thermal elongation device and the modified Vernier caliper tool used in the (SME) property test.	135

1

Chapter One
Introduction

1-1 Introduction

Speaking of the scientific progress and development witnessed by the countries of the world must lead the memory of scientists and engineers to the strenuous efforts that enabled them to overcome the restrictions that were imposed on the concepts and transforming the design into an applied construction that actually exists, especially in the framework of the process and production by focusing on the relation between science and technology. So that, scientists and engineers are not only obliged with implementing the correct solutions to problems, but also with creating radical transformations in the tools and engineering materials resulting from the outputs of human thought represented in innovation and technological creativity that touches all the aspects of the engineering materials science. So, the civilized creativity in materials science throughout history, has led to name the ages by the materials names, such as the stone age, bronze age, and iron age, etc. Where the relationship of materials science and ages was built with the availability of materials in that age [1,2]. Whereas in the stone age, the materials science associated with the materials available in the nature, such as stone, wood, bones, and else of materials used by the ancient man in his daily life. Although, with the approach of the stone age to the end, the materials science history began to develop and modernize itself successively by using gold, silver, copper, and bronze in the daily life mainly; thus entering materials science in the bronze age, and then the iron age by moving to new, advanced and renewable events that occurred with the development of furnaces whose temperature reaches more than 1200°C , which helped a lot in the work of many of metal alloys [2].

In general, all this development led to a real scientific rising in materials science by moving from conventional materials to advanced materials. Examples of that, what have been seen of electronic materials, metallic superconducting materials, modern materials (as ceramics, advanced ceramics, and

superconducting ceramics), semiconductors, polymers, and biodegradable polymeric materials [2].

Due to the entry of oil into industry, the speed of polymeric activity has increased after the setting up of many petrochemical plants in the world. In addition, materials science entered the nanotechnology age, theoretically and practically.

With the activity of studies in the field of internal composition that are related to the properties required in the applications of engineering, industry, agriculture, sport, and in other life fields according to the methodology shown in Figure (1-1), it was possible to obtain new and renewable materials that have exceptional required properties, reaching the smart materials [3,4].

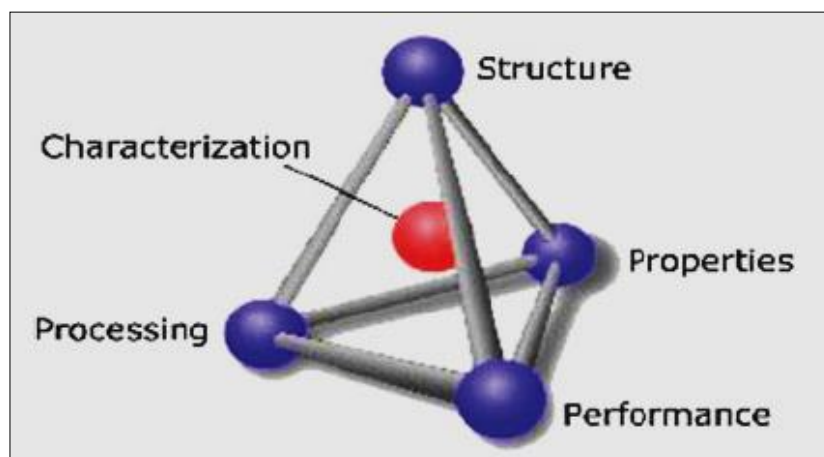


Figure (1-1): Tetrahedron Shape of Materials Science, The Four Component of Discipline of Material Science and Engineering and Their Interrelationship [3,4].

Reaching the shape memory smart materials, where the smart planes, smart textiles, smart homes, and other smart industries refer to the change of the vocabulary of the material world with the emergence of smart materials science, especially based on shape memory polymers. Whereas the past decades have witnessed a tremendous growth in interest in this type of smart materials since the publication of the first scientific articles in the early nineties on these smart polymers. According to one of the statistics carried out by the scientific containers

in Scopus, approximately 6500 scientific articles were published between 1992-2014, which included 6000 scientific work and 500 reviews, as shown in Figure (1-2). Note that publications on this topic are continuous until now (2022) and have not stopped at the limits of the statistics mentioned in Figure (1-2) [5-9].

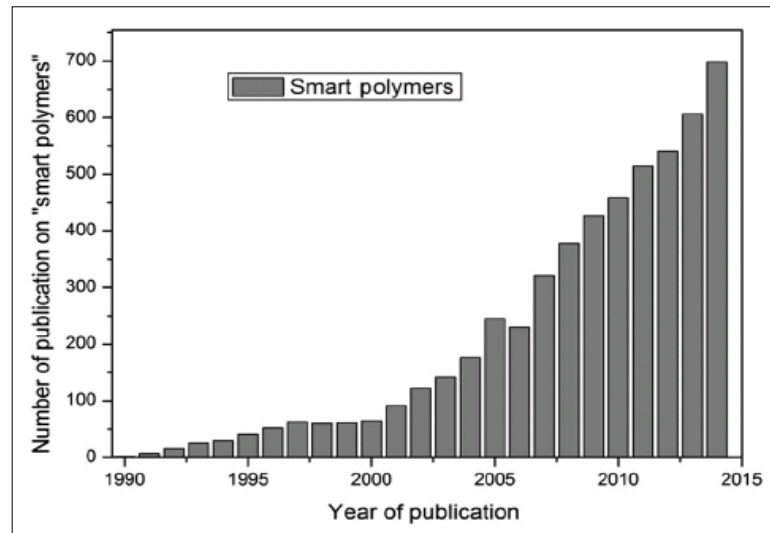


Figure (1-2): The Increment of The Scientific Publications Numbers Growth Regarding The Topic of Shape Memory Smart Polymeric Materials in Between 1992 to 2014 [5].

It is worth noting in this field that the scientific references agree that the science of polymeric smart materials is divided into four main categories: hydrogels, shape memory, self-healing, and smart- packaging, as shown in Figure (1-3) [5].

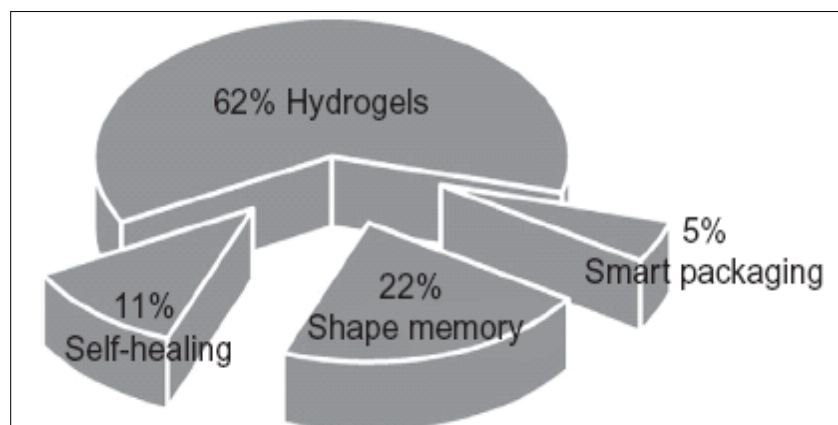


Figure (1-3): The Different Classes of Smart Polymeric Materials and The Percentage of Publications of These Classes According to The Scientific Container of Publication in Scopus [5].

Where these four classes of smart polymeric materials have led humanity to countless pioneering inventions and rapid technological development in the twenty-first century. It is expected globally that this technological growth within the next fifty years will be 4 million times greater than the emergence of this thought [5,6].

I am proud, as an Iraqi woman, to dive into the depths of this choppy sea with its scientific theories and waves, and here I am presenting to you an Iraqi doctor's thesis related to the topic of shape memory smart polymer materials, I hope that I will succeed in this effort, the success is only from God.

1-2 Aims of the Study

Preparation and characterization of polymeric materials with shape memory properties suitable for industrial applications and in the engineering of medical equipment used in the field of cancer diseases.

1-3 Strategy of the Study

The work included finding the latest and best ways to manufacture or prepare smart polymeric materials of type (shape-memory), then executing the flowchart of the operations mentioned in chapter three, by conducting the measurements and tests mentioned in the diagram in Figure (3-1), taking into account that the basis of the work is to activate and deactivate the shape-memory effect SME property, which is according to the protocol of the hot classical shape memory cycle. The study also included studying the factors affecting the process of activating and deactivating the SME property, as well as studying the relation of the shape-memory cycle (SMC) time with the methods of activation and deactivation of the SME property.

Note that this study is being conducted for the first time in the country, as far as we know.



2

Chapter Two
Theoretical Part and
Literature Survey

2-1 Introduction

This chapter begins with an introduction about the advanced and traditional materials classification systems reaching to smart materials, which have been classified and their properties explained. After that, the highlight was on the shape memory polymers, SMPs, in particular, to understand what this science discusses with the term “shape memory” and what are the unique applications offered by SMPs that cannot be obtained from traditional polymers.

2-2 Traditional Materials Classification Systems

Solid materials have been conveniently grouped into basic classifications [2,3,41and43]:-

2-2-1 Metals

This materials group is consisted of single or more of the following elements: Gold, aluminum, nickel, copper, iron, and titanium, in addition to relative small amounts of the elements that are often existed such as: oxygen, nitrogen, and carbon which are non-metallic [2,3 and 41].

2-2-2 Ceramics

They are compounds falling in between nonmetallic and metallic materials; mostly carbides, nitrides, and oxides. Widespread ceramics are represented by silica (silicon dioxide, SiO_2), alumina (aluminum oxide, Al_2O_3), Si_3N_4 (silicon nitride), and SiC (silicon carbide), in addition to minerals of clay (porcelain), glass, cement, etc. which are indicated as traditional ceramics [3,41and43].

2-2-3 Polymers

Polymers are represented by rubber and common plastic materials. Most polymers are in fact organic compounds, their chemical composition mainly consist of hydrogen, carbon, and other elements such as (N, Si, and O). Furthermore, they have very large molecular structures, often chain-like in nature

that have a backbone of carbon atoms. Some of the common and familiar polymers are thermoplastic, thermoset and elastomer [3].

2-2-4 Composites

Composite is a material that consists of two or more of the material classes mentioned in the above sections which are ceramics, metals, and polymers. The composite design purpose is to reach a properties collection that is not offered by the single material alone, as well as to combine the best features of each individual component. Composite types that are existed in big number have different combinations of the material classes, ceramics, metals, and polymers. Fiberglass is considered as one of the most widespread and known composites. It is obtained by embedding small size of glass fibers in polymer (usually polyester or epoxy) [41,42].

2-3 Classification Systems for Advanced Materials

Advanced materials are the materials that used in the applications of high-tech. They are generally traditional materials, their properties are improved and recently developed giving materials of high-performance. Moreover, advanced materials may be metals, polymers, or ceramics, and are typically expensive. They also include biomaterials, semiconductors, and what is known as “the future material”, which is smart and nano-engineered materials, which will be discussed below [2,3 and 41].

2-3-1 Semiconductors

The electrical characteristics of semiconductors fall in between the electrically conductor materials such as metals and metal alloys, and electrically insulator materials such as ceramics and polymers. Moreover, semiconductors electrical properties are sensitive to the impurity atoms at minute-concentrations, that very tiny spatial areas can be employed to control these concentrations. Integrated circuits advent was mainly because of semiconductors, which have

completely made a revolution in electronics, computer industries, and human lives through the last three decades [2,3 and 41].

2-3-2 Biomaterials

When a part of human body is completely harmed, here comes biomaterials that are included in the fabricated component which will be implanted replacing the body damaged part. Toxic substances should not be produced by the biodegradable material, also it should be body tissue-friendly; i.e. should not cause negative effect on the biological system of the body. Biomaterials could be polymers, metals, composites, semiconductors, or ceramics [2,3 and 41].

2-3-3 Materials of Future

2-3-3-1 Nano-engineered Materials

Until recent years, scientists use a certain procedure to comprehend materials physics and chemistry, that procedure includes complex and large structures studying, then investigated about smaller and simpler structures main building blocks. This way at times named “top-down science”, although, with appearing “scanning probe microscopes”, that allowed examining atoms and molecules individually, it has become potential to control and transfer them to compose novel structures. So it became possible to employ simple atomic-level components for designing new materials, meaning “materials by design”. New magnetic, mechanical, electrical, and other characteristics became possible to develop due to this capability of careful atoms arrangement, else, they are not likely to be obtained. This approach is called “bottom-up”; also, these materials properties study is named “nanotechnology”. The prefix “Nano” indicates that these structural entities dimensions are on nanometer order (i.e. equal to 10^{-9} m) like a rule, (<100nm) which nearly equals to the diameters of 500 atoms. Carbon nanotube is an example of this material type[3,4 and 43].

2-3-3-2 Smart Materials

Smart materials (or sometimes named “intelligent”), are a collection of new and modern materials that are being evolved for now and will have an important impact on a large number of technologies. The “smart” adjective means that these materials can sense the environment changes surrounding them, then react to these changes in pre-determined behaviors-traits which can be seen in living organisms. Moreover, the concept “smart”, is being expanded to include advanced systems that composed of materials that are smart and traditional. Smart system (or material) components comprise some sensor type which work on detecting input signal, also an actuator that has the function of responsively and adaptation. Actuators are named according to the change type as shape, mechanical characteristics, natural frequency, or position change in response to the change in magnetic fields, electric fields, and/or temperature [3,4 and 43].

2-4 Types of Smart Materials

Smart materials can be generally classified into two types relying on their functional properties as follows [4,5 and 6]:

2-4-1 Energy-Exchanging Smart Materials

These materials are also called actively smart materials, as these materials have the ability to modify their engineering properties when applying electrical, thermal or magnetic fields; so these materials acquire the ability to convert energy from one form to another. According to that, these smart materials work to convert the energy from one form to another, there are two types of it:

- Irreversible Energy-exchange smart materials.
- Reversible Energy-exchange smart materials.

2-4-2 Property-Changing Smart Materials

This type of smart materials is called “passively smart materials”. They are inactive, despite they are smart materials, which lack the potential ability to transfer energy. These materials change their chemical, mechanical, optical, electrical, magnetic, thermal, and other properties in response to the changing environmental conditions without the need for external control. Figure (2-1) shows the types of smart materials according to the nature of the response.

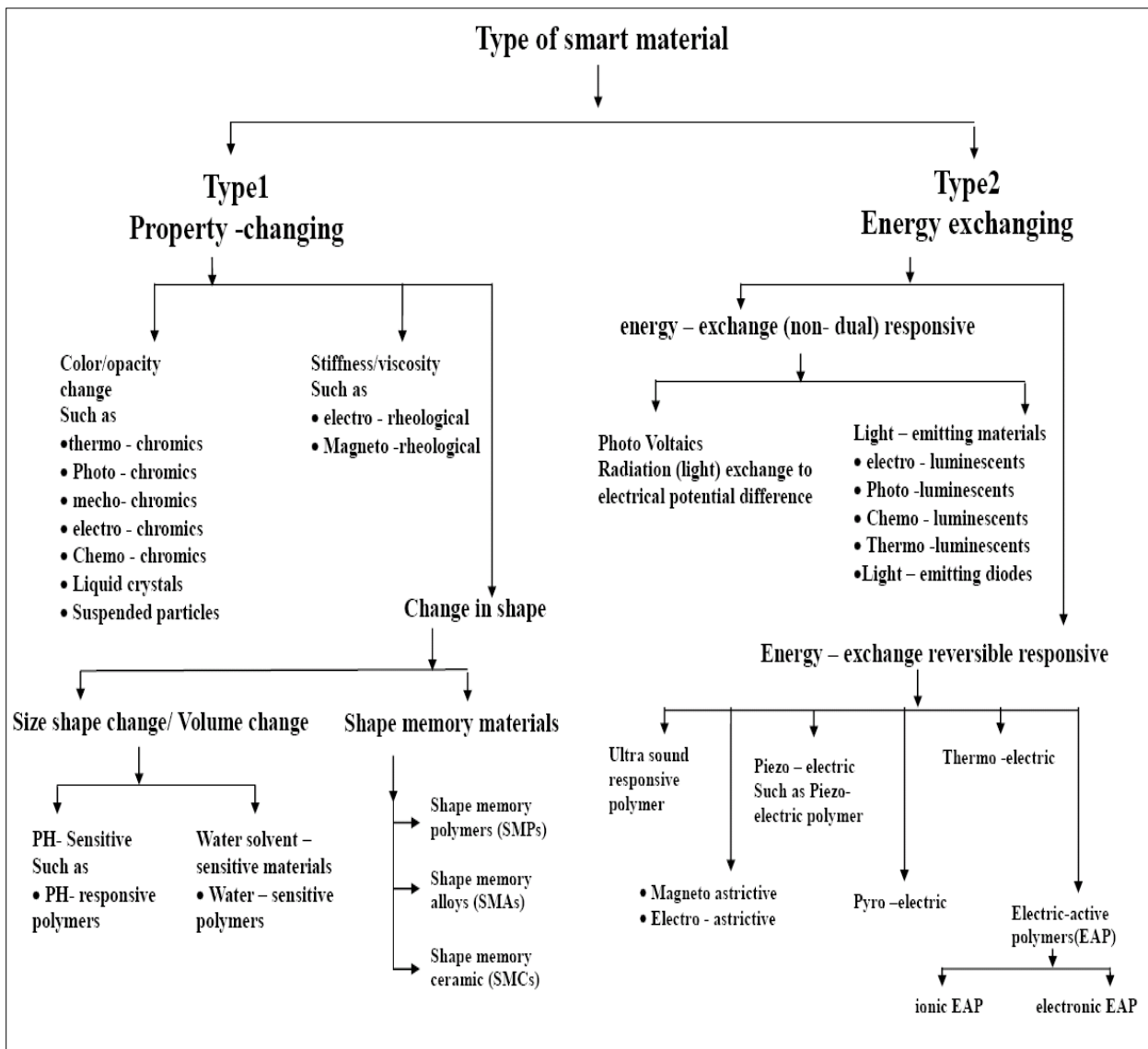


Figure (2-1): Type of Smart Materials According The Nature of Response [4,5 and 6].

2-5 Properties of Smart Materials**2-5-1 Bionicity**

Smart materials, which want to give the original traditional materials human characteristics, are above all characterized by their bionic nature. The basic characteristics of its materials are also based on the adaptive systems created by bionics. Human beings will create and improve intelligent materials based on the laws that have been generalized to biological systems [43].

2-5-2 Sensor Ability

The sensing function is the function of accepting signals from the outside world. In the field of civil engineering, it is possible to establish spatial monitoring of the entire structure. Although smart materials do not have a central system inside them like a conventional CPU, the molecular properties inside them. The recognition of changes in the environment allows this function to be achieved [43].

2-5-3 Adaptability

The most important functional feature we need to introduce smart materials into the civil engineering sector is the ability to adapt. In detail. This means that self-diagnosis and identification can take place during the restoration process. Although the materials do not speak, they can communicate with humans by using special signals that inform the user of their current state [43].

2-6 Shape Memory Materials (SMMs)

Shape memory materials are those type of materials which are able to memorize or retain an obvious (lasting) shape, which can be controlled, stabilized or fixed to a brief and torpid shape under stress and temperature specific states. Then they can return to the initial state, stress free condition under electrical, thermal, or environmental order. This recovery is correlated with the elastic deformation prior to manipulation.

SMMs have stirred unusual attention from scientists and researchers due to their ability to be in two shapes at several circumstances. This property gives SMMs a great potential for plenty of applications as media recorders, sensors, smart devices, and actuators [44].

There are different types of advanced and untraditional SMMs such as the following as illustrated in Figure (2-2) [44,45]: -

- Shape memory alloys (SMAs).
- Shape memory polymers (SMPs).
- Shape memory ceramics (SMCs).

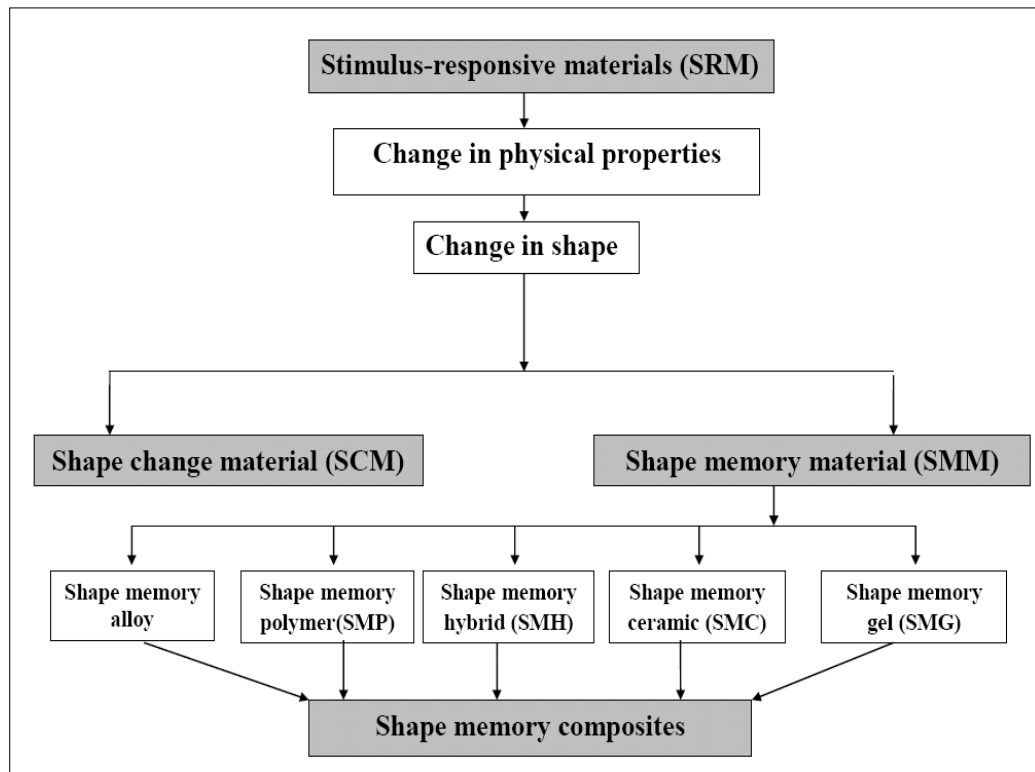


Figure (2-2) A Schematic of Tree of Shape Memory Materials (SMMs)[44,45].

2-6-1 Shape-Memory Alloys (SMAs)

SMAs are a group of metal compounds that experience a shape change in accordance to mechanical or thermal stimuli which are able to be preprogrammed in the material. This is attributed to the two crystallographic phases that this material can be transformed through the transformation (martensitic thermo-

elastic), these phases are “martensite” and “austenite”. That transformation is affected by three parameters; temperature, strain, and stress. The phase “martensite” is easily deformed, and when the stress is absent, martensite is stable at low temperatures. It experiences a change in shape with increasing stress or temperature. Multi variant crystal structure is induced with higher temperatures named “twinned martensite”, while single variant crystal structure is induced at higher stress named “detwinned martensite” [46].

2-6-2 Shape-Memory Polymers (SMPs)

SMPs are materials collection that can change their shape in response to multiple external stimuli e.g., light, solvent vapors, laser heating, heat, leg pressure, moisture, solvents, pH, microwaves, and electricity [46].

2-6-3 Shape-memory ceramics (SMCs)

Ceramic ZrO_2 can undergo a transformation from tetragonal to monoclinic structure, such as the thermal transfer of martensite through the application of stresses, this is called “martensitic ceramics” [3].

2-7 Shape Memory Polymers and Shape Memory Alloys Advantages and Disadvantages Comparison

The comparison of SMPs and SMAs properties shown in Table (2-1) refers to the great number of advantages/disadvantages of these shape memory materials classes [45].

Table (2-1): Properties of Shape Memory Polymers and Shape Memory Alloys [45].

Material Property	Shape Memory Polymers	Shape-Memory Alloys
Density/g cm ⁻³	1	6-7
Extent of deformation (%)	50-600	6
Stress required for deformation (MPa)	1-3	50-200
Stress generated during recovery (MPa)	1-3	150-300
Corrosion performance	Excellent	Excellent
shaping	easy	difficult
At low temperature	rigid	soft
At high temperature	soft	hard
Heat conductivity	Low	High
Biocompatibility and biodegradability	Can be biocompatible and/or biodegradable	Some are biocompatible (i.e. Nitinol), not biodegradable
Processing conditions	<200 °C, low pressure	High temperature (>1000 °C) and high pressure required
cost	Low	high

It can be simply seen that the SMA deformation extent (%) is much lower than that for SMP. Moreover, SMPs are superior to SMAs in many points as , SMAs are heavier, have shaping difficulty, costly, and need higher fabrication temperatures. According to many SMAs disadvantages and limitations, a chance is given to develop other materials specially SMPs materials [45].

2-8 Shape-Memory Effect (SME) Property

The shape memory effect (SME) property refers to the ability of some materials to remember a specific shape on demand, even after very severe deformations [12]; or it is a property that refers to the ability of the material to change its shape under a variety of external stimuli [47]. Also, this property refers to the ability of the material to memories its shape [48], it also means the ability of the material to trap the deformation mechanical energy or back stress in the fixed temporary shape and then release it through morphology changes or changes in the molecular relaxation rate. This property is sometimes known as a phenomenon that expresses a reversible process that allows to store and recover

the deformation mechanical energy during the shape change cycle which is called “shape memory cycle”, SMC.

On the other hand, (SME) property refers to the material ability to change its properties by changing its shape as a behavior response for undergoing heat effects or stimuli; usually these shape changes are reversible [1]. Moreover, SME property indicates the capability of some materials to store a prescribed shape indefinitely and recover it by the specific external triggers such as heat [49].

The SME property expresses the possession of some materials a memory that memorize their permanent original shape [1], it is established that this term refers to the recovery of the original shape or size of the material as a result of heating above a distinct and specific temperature [50]. From what was mentioned, It can be said that the definitions may differ, but the effect has the same result, as shown in Figure (2-3) [51]. This property arises due to morphology and processing conditions, so it is considered an intrinsic property in shape memory materials with all their types [46,50].



Figure (2-3): Photographs of The Polymeric Material Showing Shape Memory Effect [51].

For example, the shape memory behavior of SMPs derives from a association of their deformation history and molecular architecture. Where molecular architecture rely on the polymerization process and composition, that is hard to change at the moment of polymerization process completion, while the deformation history can be practically changed by external forces, which is

termed as "training" or "programming". Under that fact, shape memory is an engineered system characteristic and it is not an intrinsic property in the material.

Shape memory polymers should be trained, educated, or programmed for the SME property demonstration. This is unique for shape memory polymers since traditional polymers as indicated by their name cannot experience physical or mechanical changing without polymer damaging. Therefore, programming provides a solution for engineers, rather than chemists, to change the behavior of polymers at will [1]. Meaning that polymers do not display this effect by themselves [52]. The shape memory effect (SME) is a special mechanical phenomenon usually described by the shape memory cycle (SMC)[53].

2-9 Mechanism of the Shape-Memory Effect (SME) in SMPs and SMAs

In SMAs, shape memory effect depends on the phase transition between the crystalline phases martensite and austenite, see Figure (2-4). While with SMPs, the polymeric chains rearrangement is the responsible for SME property. On the other hand, the changes in shape memory effect of polymers are attributed to the mechanical properties change above and below "temperature of thermal transition". Here, polymers SME has the most concern, specially elastomers. SME property within elastomers is usually joined with other effects, which increase their applications [50].

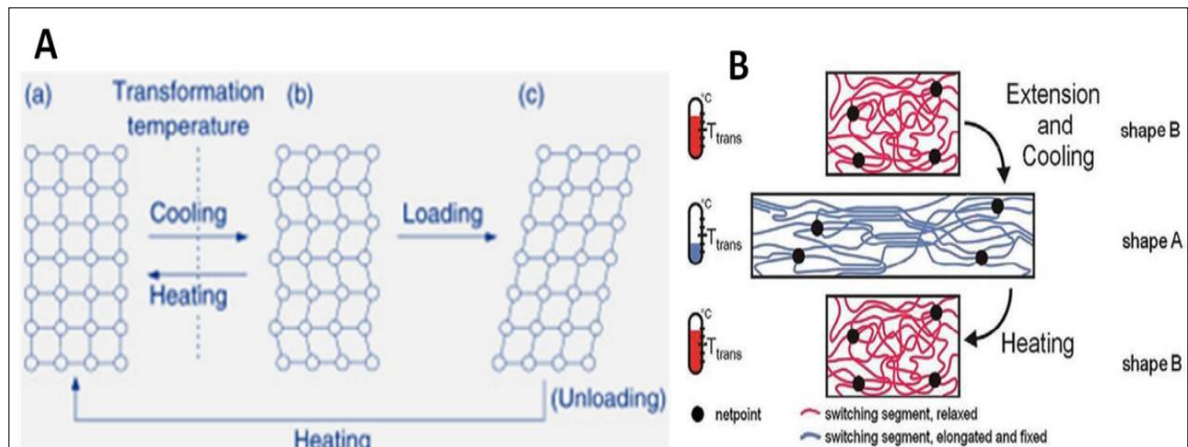


Figure (2-4): (A) Crystalline Structure Changing During SME of Alloys, (B) Mechanism of SME of Polymers [50].

2-10 Types of Shape Memory Effect (SME) in SMPs

2-10-1 One-way Shape Memory Effect (1W-SME)

The shape reversibility is lost in SMP materials, i.e. when the original shape is recovered, in order for the temporary shape to be induced, second step is needed.

2-10-2 Two-Way Shape Memory Effect (2W-SME)

They are materials that can change between temporary and original shape many times without the need for more reshaping. They may also be named “reversible SME”. Regarding the polymers having SME property, they are termed “reversible SMPs”.

2-10-3 Multiple-Way Shape Memory Effect (Multiple-SME)

They are materials that exhibit two or more temporary shapes as well as the original shape. Transformation from one temporary shape to the other is permitted by applying external stimulus, more stimulation allows the material to be back on the original shape [45,54].

The SMPs various shape memory effects, are presented in Figure (2-5) [54].

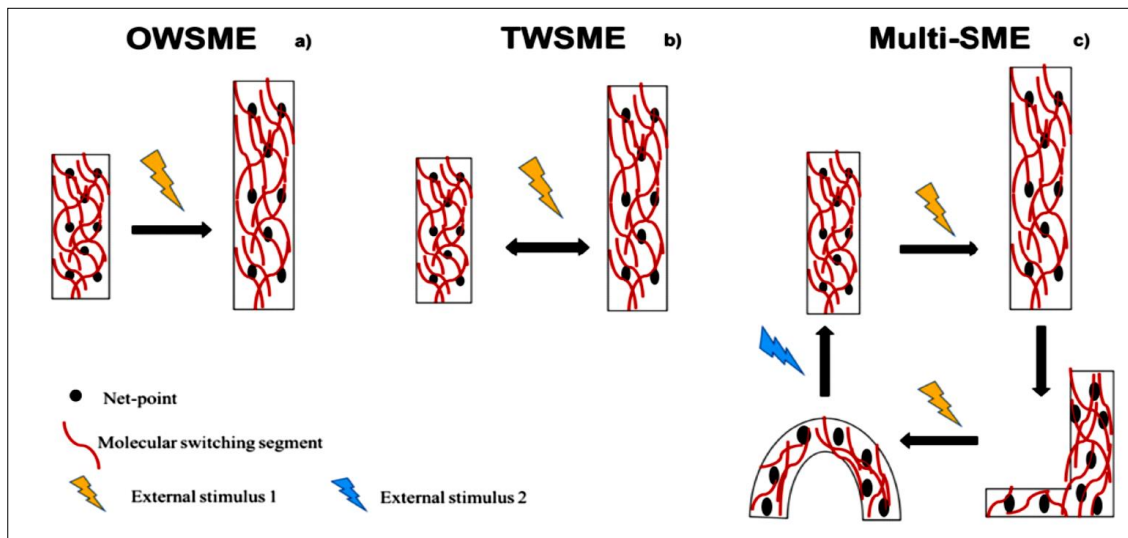


Figure (2-5): Various Shape-Memory Effect (SME) of SMPs, (a) (1W-SME), (b) (2W-SME) and (c) Multiple-SME [54].

2-11 Activation and Deactivation of SME Property During the Shape Memory Cycle (SMC)

The complete process is known to demonstrate the shape memory effect (SME) property by the shape memory cycle, SMC [45,55], where this type of cycles includes two stages, as shown in Figure (2-6):

- Programming stage: It is a process in which the SME property activation is done under different external conditions by allowing the material to be mechanically deformed and fixing that deformation temporarily, where after the end of the programming stage this temporary fixed mechanical deformation is called the programmed shape.

- Recovery stage: A process in which SME property is deactivated when restoring the original external conditions by allowing the temporary fixed shape material to return to its permanent original shape [1,45,52,55 and 56].

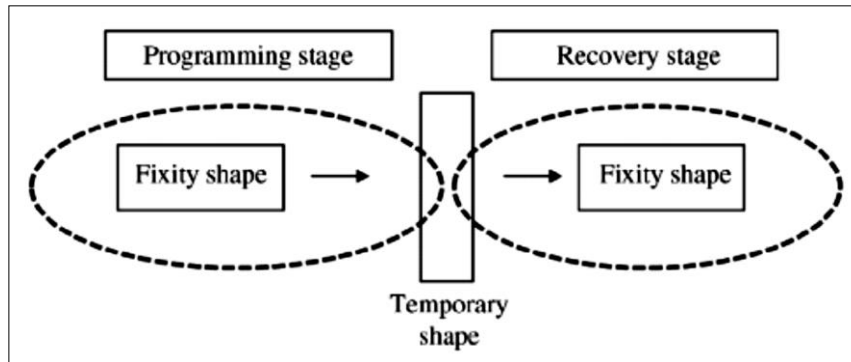


Figure (2-6): Shape Memory Technique Includes Two Stages Understood as Programming and Recovery Stages [51].

In general, there are classifications of the shape memory cycle according to the SME property activation method, which are [1,45,52 and 55]:-

First: Shape memory cycle with cold-programming (SMC-cold programming). In this cycle, the SME property is activated based on stress relaxation.

Second: The classical shape memory cycle with hot-programming, also called “thermo-mechanical cycle”. In this cycle, the SME property is activated based on thermal induction, which is one of the most popular types of cycles used in shape memory elastomer materials [1].

The recover stage may occur in any of these cycles by four methods in order for SMP to recover its original shape, these methods are [55]: -

- Direct or indirect thermal activation.
- Solvents.
- Light (Frequency).
- Mechanically driven.

Thermal activation, whether direct or indirect, is considered as one of the most widely used methods for deactivating SME property during the shape memory cycle.

Finally, in this chapter, the focus will be on the importance of the thermo-mechanical shape memory cycle, for the features achieved by this cycle,

represented by the possibility of fixing a wide range of mechanical deformations during the programming stage.

2-12 Thermo-mechanical Cycle

The SMP usual thermo-mechanical cycle is conducted through the procedure shown below, as illustrated in Figure (2-7):-

- Fabrication of SMP into an original shape.
- Thermal transition temperature (T_{trans}) is determined, the sample is heated above the transition temperature, with no applied stress.
- Next to the programming time, the sample is stressed until it deformed, at this moment the shape memory effect must be studied (ϵ_m).
- Applying stress is continued till cooling down the sample temperature below the transition temperature, fixing the temporary shape, then removing the applied stress. The material ability for fixing the temporary shape can be determined in this step.
- lastly, reheating the polymer above T_{trans} for the initial shape recovery, then determining the material ability for the original shape recovery.

This procedure should be cyclically repeated [45,51].

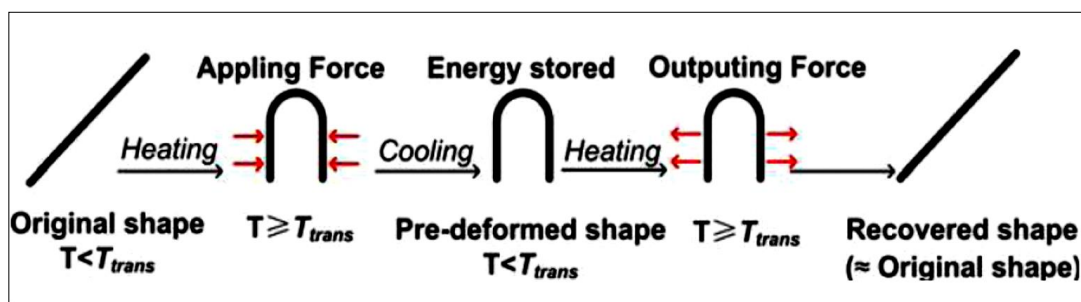


Figure (2-7): SME Schematic Diagram During a Typical Thermo-Mechanical Cycle [45].

2-13 Net-Points and Switching Phase in SMP

The difference between shape memory polymers, SMPs classified in Figure (2-1) and shape changing polymers is what it called “programmability”. Shape changing polymers, SCPs are a class of smart polymers whose their shape change

is limited to their size change as shown in Figure (2-8) by instant and spontaneous way in response to the external stimuli.

While shape memory polymers (SMPs) are characterized by a procedure by which external stress or force is applied during the programming stage of the shape memory cycle, in which the shape shifting pathway is defined. That procedure, which is called programmability, primarily is not related to how the shape memory polymer fabricated or prepared.

Shape memory polymers fall within this distinct class of SCPs, where after the fabrication step, they can be programmed to set the temporary fixation step for the subsequent recovery of the original shape using stimulation (typically heating).

As it is clear, all of the fixation and recovery processes include two main shapes, which are temporary and permanent shapes, all of this is indicated by the phenomenon termed as dual shape memory effect symbolizing for the most usual -known shape memory polymers [57].

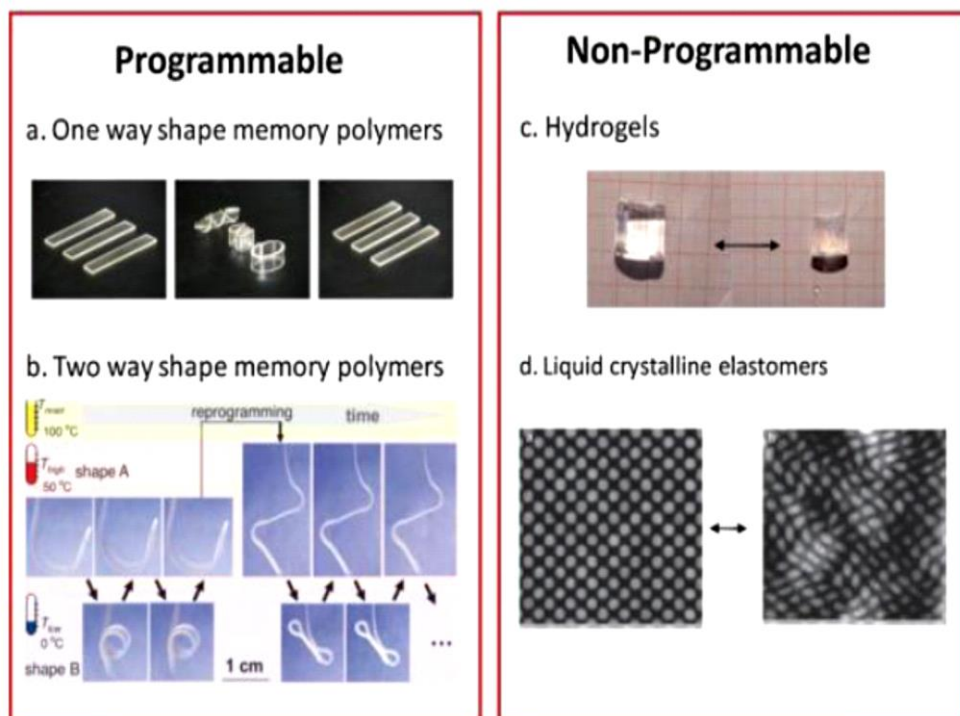


Figure (2-8): Classification of Shape Changing Polymers [57].

For obtaining shape memory effect, the polymer material must have at least two various phases, which are [13]:-

2-13-1 Net-Points

Hard phase (segment), otherwise known as “net points”, it retains the shape memory article permanent shape. At the soft segment transition temperature, this hard phase (segment) does not soften or melt. These net points might be entanglements or local structures characterized by cross-linking and rigidity, they do not disentangle at the temperature of recovery.

2-13-2 Switching Phase

Soft phase (segment), also known as “switch units”. During heating, they softened and have the role of a switch for remembering the article original permanent shape, as shown in Figure (2-9).

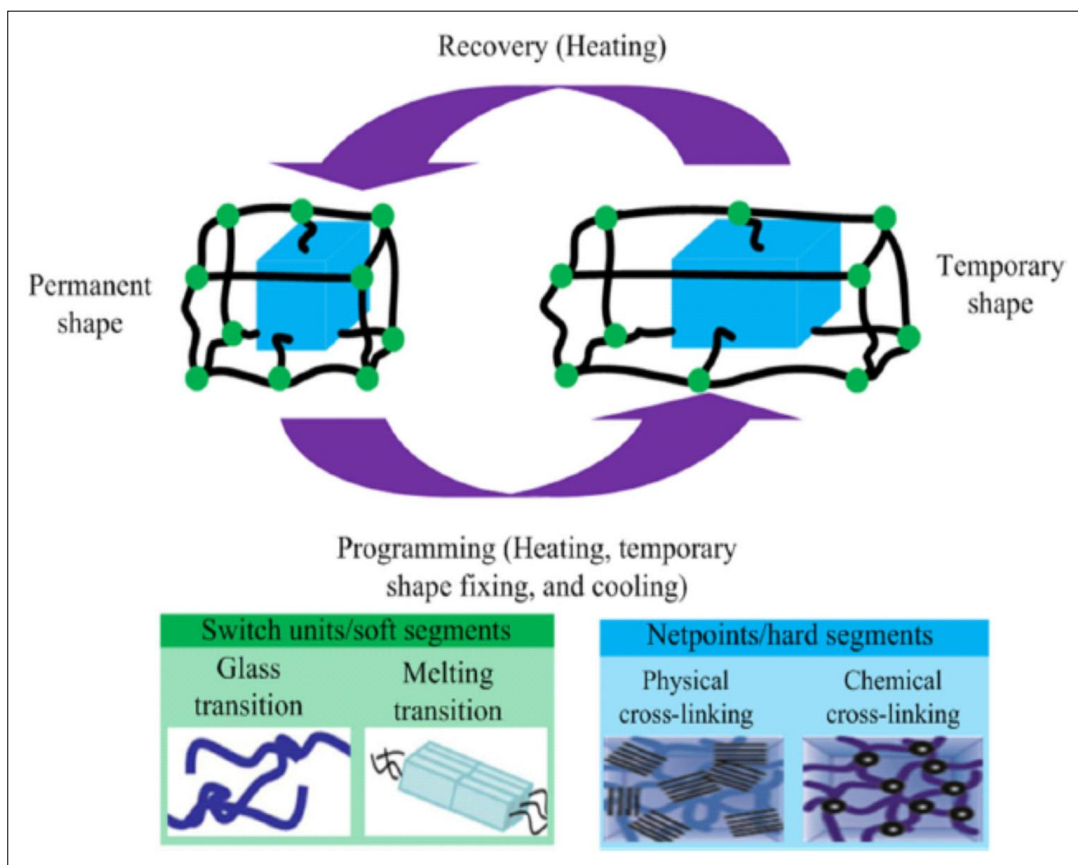


Figure (2-9): Schematic Diagram Switching Units and Net Points in a Thermally Induced SMP [58].

2-14 SMP Characteristic Parameters During SM-Cycle

The shape memory polymer ability is quantified by using two basic parameters which are the “shape fixity ratio” otherwise known as strain fixity ratio, (R_f) and shape recovery ratio, also known as “Strain recovery ratio, (R_r)”, [51,53,59-62].

2-14-1 Shape Fixity Ratio

Shape fixity ratio refer to SMP ability for fixing the strain transmitted into the sample through the step of deformation after succeeding cooling and unloading. Shape fixity ratio, R_f expression is given by [51,53,59-62]:-

$$\text{Shape fixity rate, } R_f = \frac{\text{Fixed deformation, } d_F}{\text{Maximum deformation, } d_{\max}} \dots (2.1)$$

2-14-2 Shape recovery ratio

Shape recovery ratio refers to SMP ability for recovering the accumulated strain through the step of deformation after succeeding cooling and unloading when reheating thermal transition temperature (T_{trans}). It can be defined by two:-

- First way is expressed as [45,50,60 and 62]:-

$$\text{Shape recovery rate, } R_r = \frac{\text{Deformation recovered in a certain cycle, } d_R}{\text{Maximum deformation, } d_{\max}} \times 100\% \dots (2.2)$$

- The second way is expressed as [45,59 and 60]:-

$$\text{Shape recovery rate, } R_r = \frac{\text{Deformation recovered in a certain cycle, } d_R}{\text{Fixed deformation, } d_F} \dots (2.3)$$

R_f and R_r ratios are generally linked with the mechanical deformation and recovery ability of the original shape, they can also be calculated utilizing the following equation [50,61]:-

$$R_f (\%) = \frac{\varepsilon_u}{\varepsilon_m} \times 100, \quad R_r (\%) = \frac{(\varepsilon_m - \varepsilon_p)}{\varepsilon_m} \times 100 \quad \text{Or} \quad R_r (\%) = \frac{\varepsilon_u - \varepsilon_p}{\varepsilon_u} \times 100 \dots (2.4)$$

Where:-

ϵ_m :Maximum strain during loading; ϵ_u : Fixed strain after cooling and removal of load; ϵ_p = Recovered strain after sample reheating.

The parameters R_f and R_r will be mentioned as shape memory cycle steps in chapter (3).

Also, there are main parameters must be counted in the characterization of SMPs, which are[51,59].

2-14-3 Recovery Time

The shape-recovery speed was expressed by the time when SMP reached the maximum recovery ratio.

2-14-4 Shape Memory Cycle Time (t_{sm})

Refers to the whole necessary time for SMPs temporary shape programming to its permanent shape. It is significant for choosing shape memory polymers for certain applications needs. Shape memory cycle time, t_{sm} , relies on the material geometry, characteristics, and experimental circumstances; so that, it must always be reported in the presence of these parameters for suitable selection.

2-14-5 Shape Memory Index

Shape memory effect (SME) can be assessed by the shape memory index (SMI or SM-index), which is a combination of two parameters calculated above and attained by the following equation[61]:-

$$SM\text{-index} = (R_f \times R_r) \times 100\% \dots (2.5)$$

2-15 Structural Categorization of SMPs

More than twenty type of SMPs have been fabricated and researched widely in the last years. SMPs will be classified according to structure as shown in Figure (2-10) [33,45 and 50].

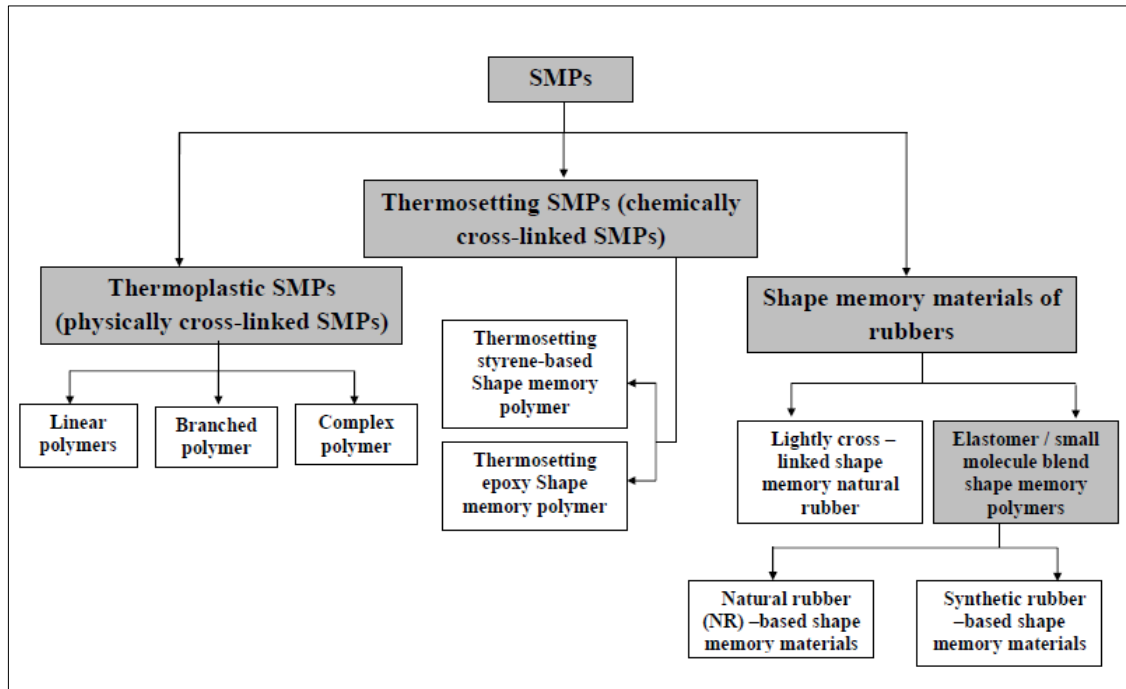


Figure (2-10): Schematic Diagram of Structural Categorization of Shape Memory Polymers (SMPs) [33, 45 and 50].

2-15-1 Thermoplastic Shape Memory Polymers

Thermoplastic shape memory polymers comprise of two separated domains. The first domains are termed as “hard domains” which are linked with the highest temperature of thermal transition. They work as physical net points. In addition, the second domains are termed as “switching segments” which are linked to relatively lower temperatures of thermal transition. They function as molecular switches. Thermoplastics could be more categorized as branched, linear, or complex polymers [45].

2-15-2 Thermosetting Shape Memory Polymers

They are networks that are cross-linked covalently which have structures that are chemically interconnected. These structures determine the shape memory polymers original macroscopic shape. The chemically cross-linked shape memory polymers switching segments are mainly network chains between the net-points. The shape memory switch here is represented by the polymer segment thermal transition.

The two mostly used thermosets as SMPs are [45]: -

2-15-2-1 Thermosetting Styrene-Based Shape Memory Polymer

The SME property is exhibited by the cross-linked structure in the styrene-based SMP. The co-monomers wide availability and the many ways for styrene polymerization have made these important features reachable. Polymerization of styrene could be done through many of methods as free controlled radical, anionic, or cationic polymerization methods. Tunable glass transition temperature (T_g), good SME, and mechanical properties are shown by the styrene-based SMPs when controlling the polymer backbones and cross-link densities. Moreover, styrene based materials exhibit superior shape fixity and recovery ratios, and exhibit good programming characteristics through plenty of shape recovery cycles.

2-15-2-2 Thermosetting Epoxy Shape Memory Polymer (SM-Polymer)

Particularly, it is a thermosetting resin of high performance which has a special thermo-mechanical characteristic along with SME. For shape memory epoxies, " T_g " is the temperature of transformation. Epoxies performance is affected by molecular mobility, cross-link density, and high-chain flexibility. The determination of the epoxies permanent shape is done by the cross-links made throughout the cycle of curing, while their temporary shape is formed as a result of the mechanical deformation applied at T_g on the curing samples. Epoxy shows elasticity at temperature beyond T_g . The conformational changes are allowed to occur because more of mobile polymer chains preserves minimum internal energy and maximum entropy. The fixation of these conformational changes can be done with the subsequent cooling which gives the temporary shape that can be recovered by heating it over again.

2-15-3Shape Memory Materials of Rubbers

The term “rubber materials”, or what are sometimes called “polydiene elastomers”, refers to a group of polymers that exhibit an elastic behavior, where these materials quickly return to their initial dimensions and original shape after the stress is removed. These materials are processed in two stages, in the first stage called “primary processing”, from which a suitable and marketable raw material is obtained, while in the second stage, the raw material is converted into a final product by the process of vulcanization that links the chains of these materials together with three-dimensional bonds called “cross-link”.

Polydiene elastomers can be divided into two types [63-65]:

- The first: natural Rubber (NR)

It is a hydrocarbon polymer (isoprene) polyisoprene with a chemical formula ($\text{CH}_2\text{CCH}_3\text{CH}=\text{CH}_2$), flexible, extracted from the sap of some plants called (*Hevea brasiliensis*). Where raw natural rubber is classified into several types differ from each other by the drying method, percentage of rubber, and color. The most important of these types are:-

- Preserved and concentrated latex.
- Ribbed smoked sheet.
- Pale latex crepe and sole crepe.
- Field coagulum crepe.
- Technically specified rubber.

- The second: Synthetic Rubber

It is obtained by controlling the polymerization process of certain chemicals. There are different types of synthetic rubber, each of which differs from the other according to the different primary chemicals used and which are being polymerized. The most important types of synthetic rubber are the following: -

- Synthetic cis- polyisoprene (PI).
- Styrene-butadiene rubber (SBR).
- Silicone rubber.
- Polyurethane rubber.

In general, the superiority of rubber in many characteristics, the most important of which is that it possesses high flexibility, adhesion, and resistance to tensile stresses, made it an attractive material by entering the manufacture of shape memory smart polymeric materials, by reducing cross-link density or by swelling it with fatty acids or wax [26,27and 33].

2-15-3-1 Lightly Cross-Linked Shape Memory Natural Rubber (SMNR)

Lightly cross-linked SMNR networks possess a cross-linking density less than 0.4%. After releasing the force of stretching, the crystals still present, where they stabilize the network in the very stretched state, reaching 1000% at room temperature. This network recovery could be triggered by heating the network beyond its melting temperature, which is termed as the “trigger temperature”. SMNR trigger temperature can be adjusted in between (20-50)°C. This material is quickly elongated and stays on this shape, without recovering its original shape. A small heat is enough for it to recover its original shape, as the heat of the body. So that, lightly cross-linked NR are programmable under its trigger temperature, also, semi-crystalline polymer stretching gives incomplete recoverability. NR cross-linking inbetween heat and thermoplastics permits crystal formation under strain that can tolerate the network at high elongation temperature. SMNR typical formulation is listed in Table (2-2) [14,50].

Table (2-2): Constituents to be Counted When Producing SME Natural Rubber [50].

Components	Phr
Natural rubber	100
Sulphur	0.2
ZnO	0.15
Zinc diethyldithiocarbamate	0.15

2-15-3-2 Elastomer/Small Molecule Blend SMPs

Conventionally, shape memory polymers are synthesized by chemical or physical cross-linking. These processes incorporate the permanent and reversible networks directly into a single polymer with a wide range of choices of different network formers. However, there is also an alternative method to synthesize shape memory polymers by blending an elastomer and small molecule additive together, a shape memory blend can be acquired. The elastomer will serve as permanent network and small molecule additive will serve as temporary network.

The elastomer-small -molecule blend synthesis is superior in many aspects. Firstly, its process is much easier than that of conventional chemical or physical cross-linking. By simply blending specific elastomer with choice of small molecule, certain shape memory blend can be fabricated. Secondly, in some cases, researchers would use commercial rubbers as elastomers. They are not only cheaper but also offer more varieties. Many commercial rubbers are available that have consistent chemical and physical properties. Some of them have excellent performance when used as elastomer in shape memory blends.

These cross-linked polymers would form permanent network in the blend which gives the material rubbery properties including elasticity. On the other hand, choice of the small molecule form the temporary networks. Their switching behavior according to temperature is the key to the shape memory effect. With different choice of combination of elastomer and small molecule, shape memory of different mechanical properties and switching temperature can be easily fabricated. Since the separation of the synthesis of cross-linked polymer network and reversible network formation makes these two components contribute to the properties of shape memory blend respectively in specific aspects [33].

2-16 Fatty Acids

Fatty acids are of high energy/gram fat (37kJ/g). They play many important roles in metabolism including free fatty acids and those which are a portion of complex lipids. More important, they are main metabolism energy providers, whether transmitted energy as blood lipids (triacylglycerol in lipoproteins), or stored energy as (triacylglycerol in adipose tissue). Fatty acids are major cell membranes constituents of all types such as (phospholipids), and they function signaling molecules as gene regulators (binds to transcription factors). In addition, that, dietary lipids supply polyunsaturated fatty acids (PUFAs) which are precursors of powerful locally acting metabolites, as the eicosanoids. Fatty acids as part of complex lipids, they are necessary for electrical and thermal insulation, and for mechanical protection. Furthermore, free fatty acids and their salts may work as detergents and soaps, attributing to their amphipathic characteristics and micelles formation.

Fatty acids represent 30–35% of total energy intake in many industrial countries and the most important dietary sources of fatty acids are vegetable oils, dairy products, meat products, grain and fatty fish or fish oils [66].

2-16-1 Fatty Acids Types

Fatty acids are carbon chains with a methyl group at one end of the molecule and a carboxyl group at the other. Natural fatty acid may be saturated or unsaturated.

2-16-1-1 Unsaturated Fatty Acids

Monounsaturated fatty acids, MUFAs, possess one (C=C) bond, that may take place in various positions. The length of chain of most familiar MUFAs is (16-22). Their structure is characterized with double bond of cis configuration. For example, Oleic acid (C₁₈H₃₄O₂).

2-16-1-2 Saturated Fatty Acids

Saturated fatty acids, SFAs, are hydrogen-saturated. Most of SFAs have chains with straight hydrocarbon with carbon atoms even number.

According to the length of chain, SFAs are usually divided into subclasses. The common ones contain carbon atoms (12–22) as shown in Figure (2-11):-

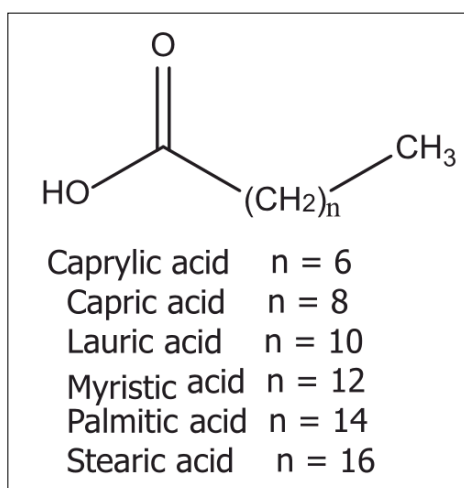


Figure (2-11): General Structural Formula of The Saturated Fatty Acids [67].

The main fatty acids sources are: fatty fish (or fish oil), vegetable oils, meat products, grains, and dairy products.

Palmitic acid is the most mutual saturated fatty acid in plants, animals, and micro-organisms. Stearic acid is a main fatty acid in animals and some types of fungi. It is a minor constituent in most plants. Myristic acid has wide presence, infrequently as a main constituent. Saturated acids of shorter-chain (8-10) carbon atoms are available in coconut triacylglycerol and milk [66].

2-16-2 Properties of fatty acids

- Poorly soluble in water.
- The influence of a fatty acids structure on melting point.
- Saturated fatty acids very stable, unsaturated acids are susceptible to oxidation [67].

2-17 Application of shape memory materials.

Shape memory polymers have made history in succeeding in the commercial field. The applications of SMPs are being developed so fast and got through many industries as SMP aircraft rivets, heat-shrink tubing, and medical implants. In this section it was attempted to show SMPs examples that have witnessed some type of commercial success. This comprises reaching both commercial sales and the use regulatory acceptance needed by law as in biomedical applications. This paragraph is not meant to be intensive summary, but instead a way of exciting the creative process for the designers who are intending to use these unique-functionalized materials for their own application [55]. Table (2-3) clarifies in general some of SMP applications, while Table (2-4) clarifies specifically shape memory rubber applications.

Table (2-3): Examples of SMPs Application.

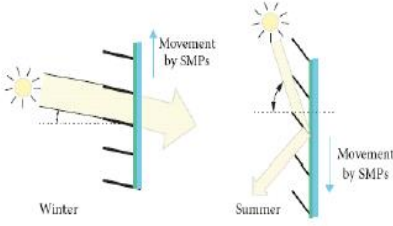
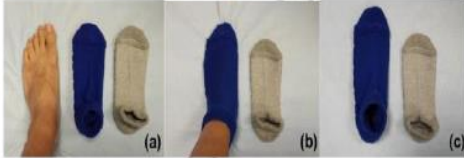
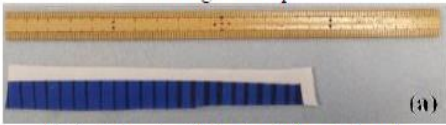
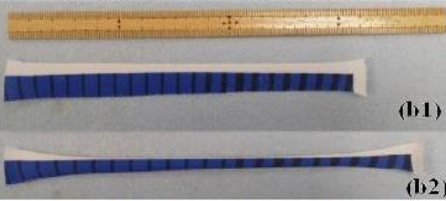
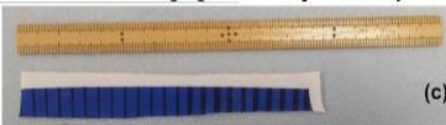
Potential application	Photograph of SMPs in application	Features achieved	Ref.
Deployable architecture (small scale buildings) <ul style="list-style-type: none"> •Retractable house. • Small display areas. •Temporary shelters. •Temporary parking areas. 	 <p>Shape –memory tent</p>	<ul style="list-style-type: none"> •Temporary structure. • Reduce the time required for construction. • Reduce reuse and recycle. • Can be reused for another structures. 	[68]
Building energy savings Movable window blinds	 <p>Window blinds</p>	Can be used in hinges of the blind structures.	[69]
Textile design	Pillow  <p>Shape –memory pillow</p>	Can be adjust its shape to the contour of the neck and shoulder according to body temperature .	[70]
	Sock- shoes Piece without modification (grey) modified piece (blue)  <p>Demonstration of the fitting process of shape memory sock-shoe.</p> <p>a- Original shape. b- During programming process. c- Temporary shape.</p>	Programmable by process:- Heating by hair dryer + wearing.	[71]
	Cloth a- Original shape  <p>(a)</p> b1,2 -After stretching to different length  <p>(b1) (b2)</p> c-After heating again for shape recovery  <p>(c)</p> <p>Shape – memory cloth</p>	Cloth can be programmed at room temperature or body temperature.	

Table (2-3) (Continued).

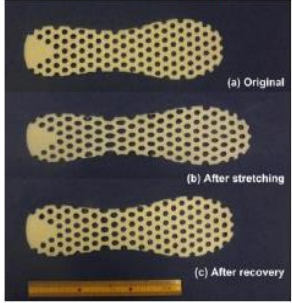
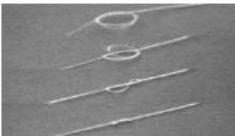
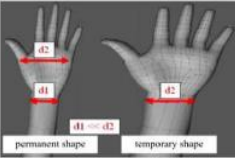
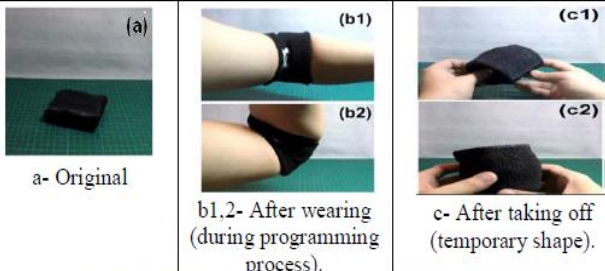
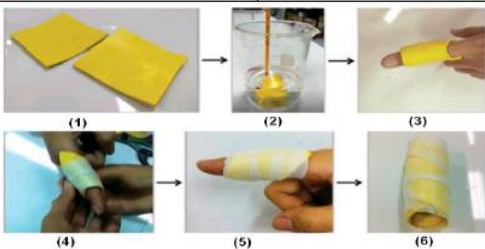
Potential application	Photograph of SMPs in application	Features achieved	Ref.
Slipper shoes manufacturing	<p>Shoe</p>  <p>a- Shape memory shoe. b- Shape memory shoe for 3D printing</p>	Avoid localized over –stretching during wearing many through holes are made to make it more stretchable.	[71]
	<p>Slipper</p>  <p>Shape memory slipper</p>	Perfectly fit the profile of a particular foot for casual wear	
	<p>3D printed insole</p>  <p>Shape memory insole during SMC</p>	The SME in 3D printed insole using flexible.	
Aerospace			[68]
Medical equipment engineering	<p>Cardiovascular devices</p>  <p>Delivery and implantation of the IMPEDE Embolization Plug.</p>	 <p>IMPEDE and IMPEDE-FX Embolization Plugs in their crimped shape and expanded shapes.</p>	[72]
	<p>Degradable sutures</p>  <p>20°C 37°C 41°C</p> <p>The temperature – induced shrinkage of fibber suture</p>	Devalue smart degradable for biomedical application	[73]
	<p>Orthopedic</p>  <p>Shape memory splint</p>		[68]

Table (2-4): Examples of Shape Memory Rubber Application.

Potential application	Photograph of shape memory rubber in application		Features achieved	Ref.															
Medical equipment engineering	Surgical tube	Shape- memory Surgical tube. 	SM- behavior of natural rubber surgical tube swollen with stearic acid,	[68]															
	Medical glove	Shape- memory medical glove 	Medical glove from SMPs in shapes optimized for working and wearing	[74]															
		Shape memory fingerless glove 	It is able to fit the particular shape of a hand in the meantime , provides flexibility and protection by the hand.																
	Elbow hand	 a- Original b1,2- After wearing (during programming process). c- After taking off (temporary shape).	Comfort fitting elbow hand.	[71]															
	Orthopedic	 a- The shape of piece before (top) and after (bottom) fitting (after programming process)  b- After fitting into the position (during programming process).	Halluy valgus correction device to provide comfort fitting and just right for correction.																
Splint tape	 1- Original shape of splint. 2- Splint in warm water (15sec). 3,4- Splint was wrapped around fractured finger and locked. 5,6- Temporary shape.	Shape memory splint programming by warm water.	[38]																
Forensic application	Comparison of imprint prepared from different techniques. <table border="1" data-bbox="574 1780 1077 1993"> <thead> <tr> <th>Object types</th> <th>Marking object</th> <th>Silicone (General grade)</th> <th>Silicone (Forensic grade)</th> <th>SMPs based TPNR</th> </tr> </thead> <tbody> <tr> <td>Cracked object</td> <td></td> <td></td> <td></td> <td></td> </tr> <tr> <td>Bullet marks</td> <td></td> <td></td> <td></td> <td></td> </tr> </tbody> </table>		Object types	Marking object	Silicone (General grade)	Silicone (Forensic grade)	SMPs based TPNR	Cracked object					Bullet marks					Thermo plastic natural rubber (TPNR) shows fine imprint with improved performance and it is easy to handle on compared to the other silicone – based material.	[29]
Object types	Marking object	Silicone (General grade)	Silicone (Forensic grade)	SMPs based TPNR															
Cracked object																			
Bullet marks																			

2-18 Literature Survey

In 1984, the term shape-memory polymer, SMP, formally emerged under the trade name “polynorbonene”, which was referred to by (CDF Chimie) company for describing a novel class of polymeric materials that have the ability to fix the mechanically deformed shape as a temporary shape after removing the applied load. Whereas this shape remains stable until this type of polymer is exposed to a suitable external stimulus that trigger it to recover to its original shape upon demand. While the company (Japan Nippon Zeon) commercialized it, thus a new age has begun in which significant progress was being made on SMP by publishing tens of publications about SMPs, annually [10].

In 1998, F. Li et.al prepared (Maleate polyethylene/nylon6) blend with a weight ratio of nylon6 that ranged between (5-20)%. It was found by differential scanning calorimetry (DSC), scanning electron microscopy (SEM), and dynamic mechanical thermal analysis DMA that this blend exhibits a good shape memory effect (SME) property[11].

In 2002, F. et. al prepared a series of new shape memory polymers (SMPs) by cationic copolymerization, using three types of Soybean oil (SOY), Conjugated Losatsoy (CLS) and Losatsoy oil, (LSS), with Divinylbenzene (DVB), Styrene (ST), and Dicyclopentadiene (DCP). It was shown that the shape memory properties (SM- properties) of these new polymers are closely related with the cross-l density and glass-transition temperature, T_g [12].

In a research published in 2007 by S.Rezanejad, the ability of SMP type (cross-linked low-density polyethylene (XLDPE)) to return from the temporary shape to the permanent original shape was proved by the heating process and that this material often loses SME property with the increase in reinforcement of type micro fillers of weight ratio between (20-30)%, but he also indicated to the possibility of overcoming this disadvantage by using nano clays material with weight ratios ranging between (0-10) wt% [13].

In a study by B. Heuwers and his group in 2012, it was proved that light cross-linked natural rubber (NR, CIS-1,4polyisoprene) exhibits shape memory behavior (SM-behavior) through x-ray diffraction (XRD) and (DSC) tests, after this polymer material was subjected to SME property activation and deactivation process during the shape-memory cycle (SMC) [14].

In 2013, the study conducted by B. Heuwers and his group, recommended the need to reduce the ratio of the sulfur vulcanization agent in between (0.15-0.5) Phr during the vulcanization process of the raw natural rubber type (latex) once and raw rubber of type (standard Malaysian rubber, SMR) again, in order to obtain light cross-linked shape memory natural rubber (SMNR) [15].

In the same year, several studies were conducted, including the following:

- R. Hoehner and his group succeeded in preparing a shape memory polymer (Shape memory polyethylene) by mixing low density polyethylene (LDPE) with dicumyl peroxide (DCP) [16].

- J. Shin showed that adding crystallizing molecules to thermoplastic elastomers leads to the creation of promising functional materials in industry, where this researcher was able to prepare (elastomeric-wax shape memory blend) by making a blend of two materials: styrene-ethylenebutylene-styrene (SEBS) elastomers with microcrystalline wax represented by paraffin wax, hydroxystearic acid (HAS), and finally stearic acid (SA) [17].

In 2014, N. R. Brostowitz and his group prepared shape memory polymer (SMP) by the technique of swelling for a cross linked natural rubber with stearic acid (SA) at a temperature of 75°C. where this type of polymers showed shape memory behavior by the stimulation with water using the developed wrench machine to activate and deactivate the SME property [18].

In 2015, A. Wang and G. Li have prepared shape memory polymer of type (styrene-based shape memory polymer) [19].

In 2016, F. Xi and his group prepared a polymeric material (carboxyl-terminated polybutadiene-polycstyrene-CO-4-vinylpyridine supramolecular thermoplastic elastomers). Where they verified that this material possesses the property of SME using (Vernier caliper and two binder), depending on water stimulation according to the hot classical shape memory cycle [20].

In 2017, L. Xia and his group studied the multiple shape memory effect(multiple-SME) of the shape-memory blend consisted of the simple physical blending process of Trans-1-4-1,3-Polyisoprene (TPI) with low density polyethylene (LDPE) material. Where it was found that the blend ratio of the sample (TPI/ LDPE) that reaches (50/50) gave excellent dual and triple shape memory properties [21].

In the same year, several researches were conducted, including the following:

- J. Sze-Huawee and his group prepared a shape memory natural rubber (SMNR) by swelling process with fatty acid. Where swelling of natural rubber ((Malaysian natural rubber grad L) vulcanized in different proportions from Carbon black-N550) was with Palmitic acid(PA) for a period of (1hr) at a temperature of (75°C).SM-behavior was investigated by DMA test, as well as by SME test using an adjustable spanner instrument developed with hot water-stimulation according to the hot classical shape memory cycle. From these tests, it was found that the weight percentage of Palmitic acid decreases with the increase in the percentage of carbon black, which leads to a decrease in SM-behavior [22].

- X. Chen prepared a Stearic acid/natural rubber bilayer fatty blend using the swelling technique with Stearic acid(SA), by immersing two layers of a rubber product represented by the natural rubber band, attached to each other by a glue substance in the citric acid at a temperature of 80°C for a period of time that reached 4hr. After that, he subjected this prepared material to the hot classical shape memory cycle based on cooling at room temperature 25°C, where the

original shape of the sample, represented by bend-shape, was transformed into a flat-shape during the programming stage of this cycle, then returned to its original bend-shape shape by stimulation with hot water at a temperature of 80°C during the recovery stage. So, it was confirmed that this material possesses SME property that enables it to be described as a shape memory smart material [10].

In the study of the researcher M. Pantoja and his group in 2018, it was shown that the phenomenon of wax blooming occurs with the increase in the number of shape memory cycles and with the change of the fatty acid nature for a shape memory smart rubber prepared from a commercial elastomeric product represented by the natural rubber band impregnated with fatty acid, which includes: Myristic acid (MA), Lauric acid (LA), stearic acid (SA) and, Palmitic acid (PA) [23].

In the same year, several studies were conducted, including:

- R. Abishera prepared the material (shape memory epoxy/carbon nano tube nano composites), where he found that this material shows shape memory behavior(SM- behavior), after being subjected to the shape memory cycle of type(cold-programmed cycle) [24].

- G. Capiel and his group were able to synthesize fatty acid based monomers by adding the fatty acid of type (Oleic) once and (Lauric) again to the material (Glycidylmethacrylate, GMA) in a one-step reaction. Thus the researcher used these monomers in the process of preparing polymeric materials by mixing 50wt% of these monomers with styeneby the polymerization process. It was found that all the polymers obtained from this preparation technique showed the shape memory effect SME property by activating and deactivating it through temperature changes [25].

In 2019, the study conducted by N. M. Setyadewi et.al concluded that the vulcanized natural rubber composite when impregnated with Palmitic acid for a period of 1hr and at a temperature of 75°C, shows the classical shape memory

behavior by stimulation with water, and that this behavior decreases with the increase in the number of shape memory cycles [26].

In the same year, several studies were conducted, including the following:

- N. M. Setyadewi and his group observed the fact of the shape fixity ratio (R_f) decrease and the original shape recovery ratio, (R_r) increase with the increase of vulcanization sulfur ratio of the smart rubber prepared by the technique of swelling with Stearic acid [27].

- L. Xia and his group prepared shape memory blends by the physical blending process between low density polyethylene (LDPE) and natural *Eucommia Ulmoide* gum (EUG). It was clear through shape memory tests that the cross-linked network of LDPE represents the fixed domain in the mixture (LDPE/EUG SMP), while the network of EUG works as the reversible domain [28].

- T. Senqsuk and his group prepared shape memory polymers (SMPs) based thermoplastic natural rubber (TPNR) by the blending technique; by making a blend of natural rubber (NR) in weight percentages ranging between (30-60)% with a thermoplastic material called Block-CO-polymer based polyolefin (BCO). Where they found that increasing the weight percentage of the natural rubber leads to a decrease in the shape memory parameters; where the shape fixity ratio (R_r) reached 70%, while the shape recovery ratio (R_r) reached 60% [29].

- N. M. Setyadewi studied the effect of black carbon types (N220, N330, and N550) on the thermal characterization of shape memory natural rubber (SMNR) prepared by swelling process natural rubber with Stearic acid for a period of (1hr) at a temperature 75°C. It was found that the initial degradation temperature using thermal gravimetric analysis (TGA) test apparatus for the SA (stearic acid)-free vulcanized rubber is higher than that of the shape memory rubber (SMNR); which means thermal stability reduction of the shape memory vulcanized rubber

(SMNR). Moreover, the weight loss for SA-free vulcanized rubber by all types of carbon black is less than for shape memory vulcanized rubber [30].

- W. Wu and his group took the issue of rubber recycling, expressed in their paper as an insurmountable issue. Shape memory rubber was prepared from mixing Carboxylated styrene butadiene (XSBR) with a degradable (Carboxy methyl chitosan (CMCS)) by soaking this smart rubber in water. Smart rubber samples when subjected to the shape memory test, showed that they are distinguished with impressive SM-behavior in a temperature range specified in the study. This makes this material well suited for the smart medical device design for the human body [31].

- Q. Yang and his group studied the one-way shape memory effect (1W-SME) and the two-way shape memory effect (2W-SME) properties of a high-strain shape memory polymer (SMP) prepared from a combination of two substances: (Cis-1,4-Polybutadiene - (CPB-PE) semi crystalline copolymer (CPB-PE)) with 2-ureido-4[1H] pyrimidinone (upy) side groups (UHPB). It was found that the one-way SME property is a function of recrystallization and re-melting of (PE) phase during the programming and recovery stages of the non-reversible shape memory cycle. It was found that the 2W-SME property is a function of crystalline-induced elongation (CIE) and melting-induced contraction (MIC) of the PE phase of the reversible shape memory cycle (SM-cycle) [32].

- L. Zhou prepared shape memory rubber by swelling process of a commercial elastomeric product represented by a rubber band of type (Ethylen propylene Dien monomer (EPDM)) using (Stearic acid, SA) and temperature 75°C for periods of time ranging from (15-300)min. Where he investigated the shape memory behavior (SM-behavior) of this prepared rubber through the quantified shape memory test to practically calculate the shape memory parameters represented by R_f, R_r using a dynamic mechanical analyzer (DMA)

device, as well as through the macroscopic shape memory test using video imaging [33].

In 2020, J. Teng and his group hybridized the matrix represented by (Trans 1,4-polyisoprene (TPI)) using a reinforcing-phase represented by low-cost high density polyethylene (HDPE), to prepare the TPI/HDPE hybrid shape memory polymer. It was found by subjecting this prepared material to a shape memory cycle through the shape memory test, that the shape memory and thermodynamic properties are excellent [34].

In 2021, Y. Ren and his group invented shape-memory polymers of type poly (l-lactide) (PLLA), where they studied the mechanically deformed shape programming and original shape recovery properties of these prepared materials through water-responsive shape-memory. It was possible to measure the shape fixity ratio (R_f), which reached (92%), in addition to measuring the shape recovery ratio (R_r), which reached (94.2%) [35].

In the same year, several studies were conducted, including:

- R. Zhang and his group worked on improving the shape memory parameters represented by R_f and R_r for (Ultra-high-molecular-weight polyethylene (UHMWPE)) using graphene Nano-plates (GNPs) [36].

- C. B. Cooper and his group demonstrated that combining two materials (flexible backbone polypropylene glycol (PPG)) with (methylene bisphenylurea (MPU)) creates a shape memory polymer with one-way shape memory effect (1W-SME) property. In addition to toughness, stretch ability, and high network junction density [37].

- N. Lehman and his group invented a shape memory thermoplastic natural rubber represented by the material (shape memory polymer (SMP) based on thermoplastic natural rubber (TPNR)), which is used in soft-touch applications by combining of polycaprolactone (PCL) and epoxidized natural rubber (ENR). It was

found by the shape-memory test using water-responsive elongation machine according to the hot classical shape memory cycle based on abnormal cooling, that this combination between the two materials mentioned above achieved a significant improvement in the shape memory behavior (SM-behavior) compared to the un-modified natural rubber [38].

In 2022, F. Quadrino and his group manufactured shape-memory epoxy composites by press-molding of the carbon fiber-reinforcement (CFR) pre-impregnated with un-cured epoxy powder, where the number of cardboard fiberslayers ranged between (2-8) and thickness (300um-100um). Optimal adhesion was obtained on the structural and functional levels through tests based on the single thermo-mechanical shape memory cycle and multiple-programming [39].

In the same year, J. M. Yang and his group succeeded in preparing shape-memory composite membranes, by making a blend represented by polycvinylcohol/chitosan/sodium alginate (PCS/SA) in different proportions of (sodium alginate, SA). The physical and chemical properties along with the shape memory properties and mechanism were studied. They noticed that the increase in the weight percentage of sodium alginate causes a decrease in crystallinity and thermal stability, and that the (DMA) test works as a responsive for the shape recovery behavior of these membranes [40].



3

Chapter Three
Practical Part

3-1 Introduction

This chapter includes the practical coverage of the study, it involves six main axes:

- The first axis: shows the raw materials used in preparing the smart shape memory polymer (SMP) materials, with an indication of their general characteristics and properties.
- The second axis: shows the technology used in preparing this type of smart polymers, with a presentation of some photographic images of it.
- The third axis: states the role of the hot-classical shape memory cycle (SMC) by making this type of polymers work as shape memory smart materials by inducing it to activate the shape memory effect (SME) property in the mechanically deformed shape memory programming stage, also, to deactivate the SME property in the original shape memory recovery stage with presenting the illustration chart of this thermo-mechanical cycle.
- The fourth axis: shows how to practically making sure of the shape memory behavior by following two different practical procedures:
First: Shape memory behavior quantified practical measurements are carried out in order to calculate the shape memory factors.
Second: The visual photographic procedure is carried out.
Third: Carrying out some structural and thermal tests.
- The fifth axis includes characterizing and analyzing of some mechanical properties of shape memory polymers before undergoing the shape memory cycle.
- The sixth axis includes the indication of the devices used in the study in terms of their quality, manufacturing point, and photographic images. As shown in Figure (3-1), the work steps and its different stages, starting with the preparation of the raw materials and ending with the measurements for achieving the aim and purpose of the study.

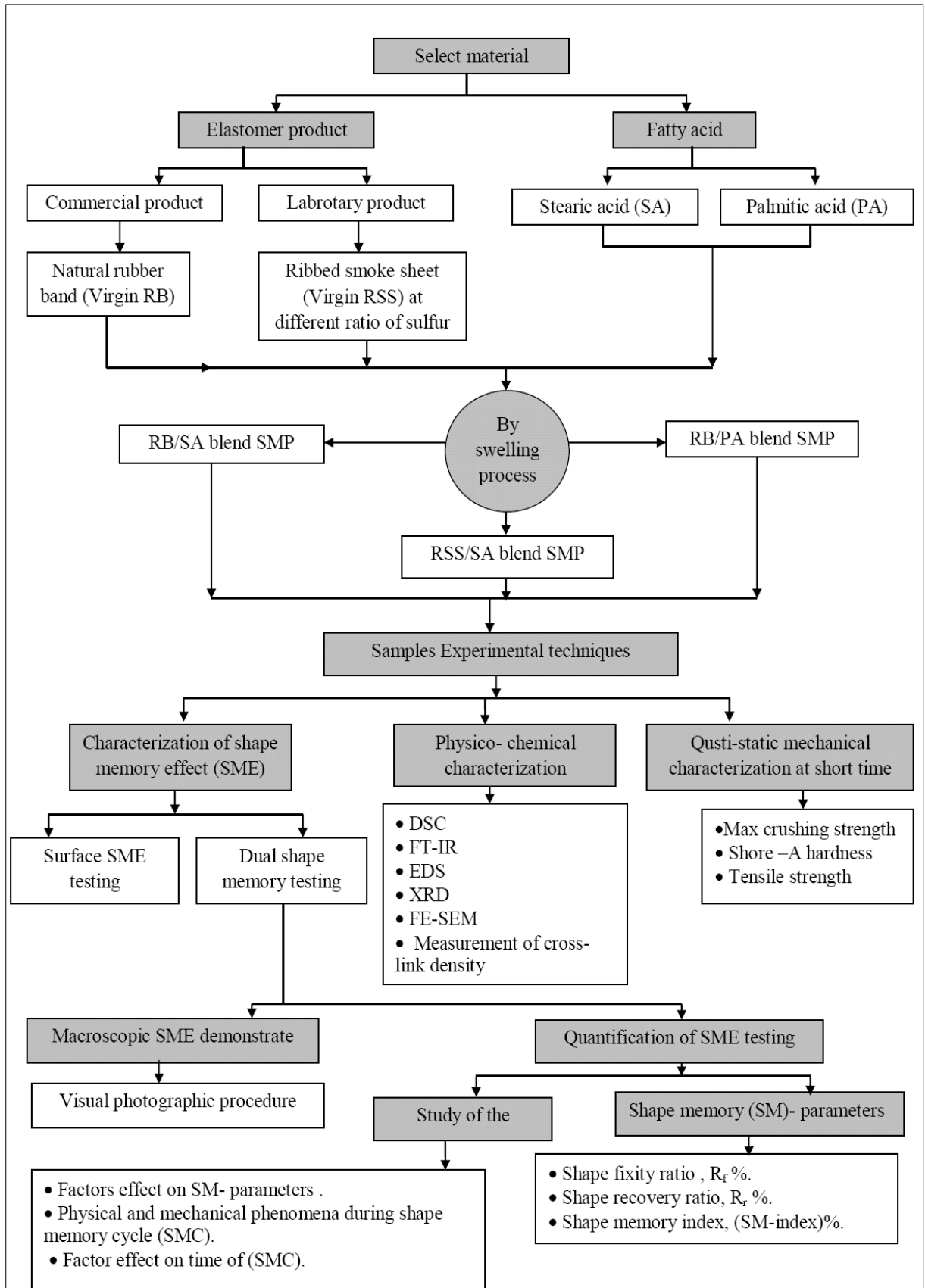


Figure (3-1): The Flowchart of The Work Steps and Its Different Stages.

3-2 Materials in Use:

The materials used in this study are divided into two main parts:

3-2-1 Elastomeric Product (Hard Segment)

Two types of elastomeric products were used as stationary phase or what is also called (hard segment) in preparing the shape-memory polymer (SMP) type elastomer/ small molecule blend SMP. These types are:

First: The Commercial Elastomeric Product

Commercial natural rubber bands type Latex were used as a materials that play the role of the stationary phase in preparing the shape memory polymer material in the form of transparent yellow strips with (flat length=200mm, width=5mm, thickness=1mm), as shown in Figure (3-2) produced by GAO Jixiang Jiao Quan company of Chinese origin, which will be denoted in this study by (Virgin RB).



Figure (3-2): (a) and (b), photographic images of the commercial natural rubber bands used in this study (Virgin RB) as a commercial elastomer product, (c) the dimensions of the commercial rubber band.

Second: The Laboratory Elastomer Product

The laboratory-vulcanized (ribbed smoke sheet (RSS)-5) natural rubber, was used with different percentages of sulfur ranging of (0.75-2) Phr, which will be denoted in this study by (Virgin RSS) as a material that plays the role of a stationary or stable phase in the preparation of the shape memory polymer (SMP) material.

In general, the process of obtaining a laboratory-vulcanized natural rubber required the use of the following raw materials:

- Raw natural rubber type (ribbed smoke sheet (RSS-5) supplied by (Weber & Schaer Since 1844) as a basic material in the rubber mixture.
- The materials involved in the raw rubber vulcanization process(RSS), are shown in Table (3-1).

Table (3-1): The Specifications of The Materials Involved in The Vulcanization Process of Raw Rubber (RSS).

The specifications of the raw materials involved in the vulcanization process of the rubber(RSS)				
Name	Stearic acid (SA)	Zinc oxide	N-cyclohexyl- 2-benzothiazode Sulfonamide (CBS)	Sulfur
Molecular formula	$C_{18}H_{36}O_2$	ZnO	$C_{13}H_{16}N_2S_2$	S
Molecular weight g/mol	284.48	81.39	264.4	32
Color	White	White	Light yellow or light pink powder	Yellow
Shape	Particles	Particles	Particles	Powder
Purity %	95	99.5%	99%	–
Supplier	Himedia .Co. India			Al- Meshrak. Co. Iraq

3-2-2 Fatty acid (Soft segment)

Two types of natural saturated fatty acids produced by Himedia Company of Indian origin, were used. Those fatty acids are represented by Stearic acid and Palmitic acid, as a reversible phase or what is also called the soft segment in the preparation of the shape memory polymer (SMP) material. Table (3-2) reviews the specifications of the natural fatty acids used in this study.

Table (3-2): Specifications of The Natural Fatty Acids Used in This Study.

Type of fatty acid	Molecular formula	Molecular weight , MW (g/mol)	Melting point (°C)	Boiling point (°C)	Density (g/cm ³)	Purity (%)	Shape	Color
Stearic acid (SA)	$C_{18}H_{36}O_2$	284.48	69.3	383	0.941	95	Particles 	White
Palmitic acid (PA)	$C_{16}H_{32}O_2$	256.42	62.9	351.5	0.853	98	Particles 	White

3-3 Laboratory Elastomeric Product Preparation Technique

Figure (3-3) shows that the process of preparing the vulcanized rubber type (Virgin RSS) as a laboratory elastomeric product requires two stages as follows:

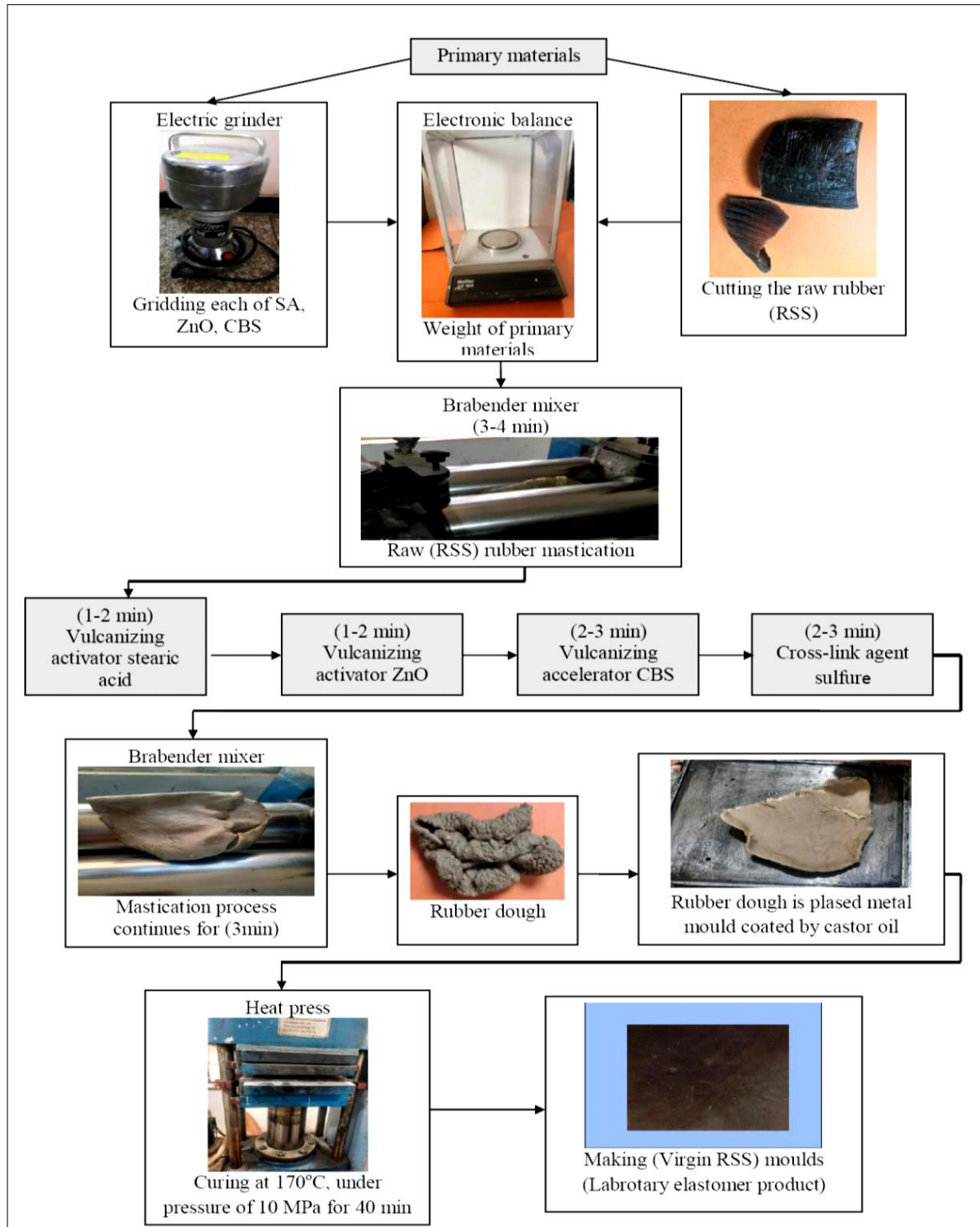


Figure (3-3): Schematic of Preparing The Laboratory Elastomeric Product Type (Virgin RSS).

3-3-1 Stage of Preparing the Rubber Dough

This stage includes four steps:

- Cutting the raw RSS rubber with a scalpel to reach the required quantity.
- Grinding each of SA, ZnO, and CBS separately by electric mill.
- Adding the materials according to the times listed in Table (3-3).

Table (3-3): Times of Adding The Rubber Mixture Materials.

Operation		Time (min)
Mastication of raw natural rubber (RSS)		4
Addition of	Zinc oxide(ZnO)	2
	Stearic acid (SA)	2
	CBS	3
	Sulfur	3

- The Mastication Process of the Rubber Mixture Materials.

The mastication and homogenization of the rubber mixture is carried out by means of a mastication machine by adding the mixture materials, each material separately, by the master batch method according to Table (3-4). In return, this mastication process continues after adding all the vulcanizing agents to the raw rubber for a period of time up to (3min).

Table (3-4): The Materials Ratios Added to The Rubber Mixture.

Materials	Loading (Phr)					Function
	1- Virgin RSS	2- Virgin RSS	3- Virgin RSS	4- Virgin RSS	5- Virgin RSS	
RSS	100	100	100	100	100	Raw elastomeric material
ZnO	3.5	3.5	3.5	3.5	3.5	Activator
SA	1.25	1.25	1.25	1.25	1.25	
CBS	1.25	1.25	1.25	1.25	1.25	Accelerator
Sulfur	0.75	1	1.25	1.5	2	Across link agent sulfur

3-3-2 Sheets Molding Stage of the Vulcanized Rubber Type (Virgin RSS)

After the end of the mastication process, the rubber mass mixture is placed inside a metal mold coated with a non-stick thin layer of castor oil. The mold and mixture are heated without applying load for a period of time reaches (5min) to make sure of the rubber flowing inside the mold; taking care of opening the mold and cover set partially between (2-3) times, to get rid of the air pockets. After that, the pressure of (10MPa) is applied and fixed for (40min) at a temperature of (170°C). Then, the mold is cooled to room temperature (to avoid shrinkage in the sample dimensions) with pressure remaining to maintain the product dimensions.

Thus, vulcanized natural rubber samples were obtained with different ratios of sulfur, with dimensions (13.7×14.2×0.16) cm³, as shown in Figure (3-4):

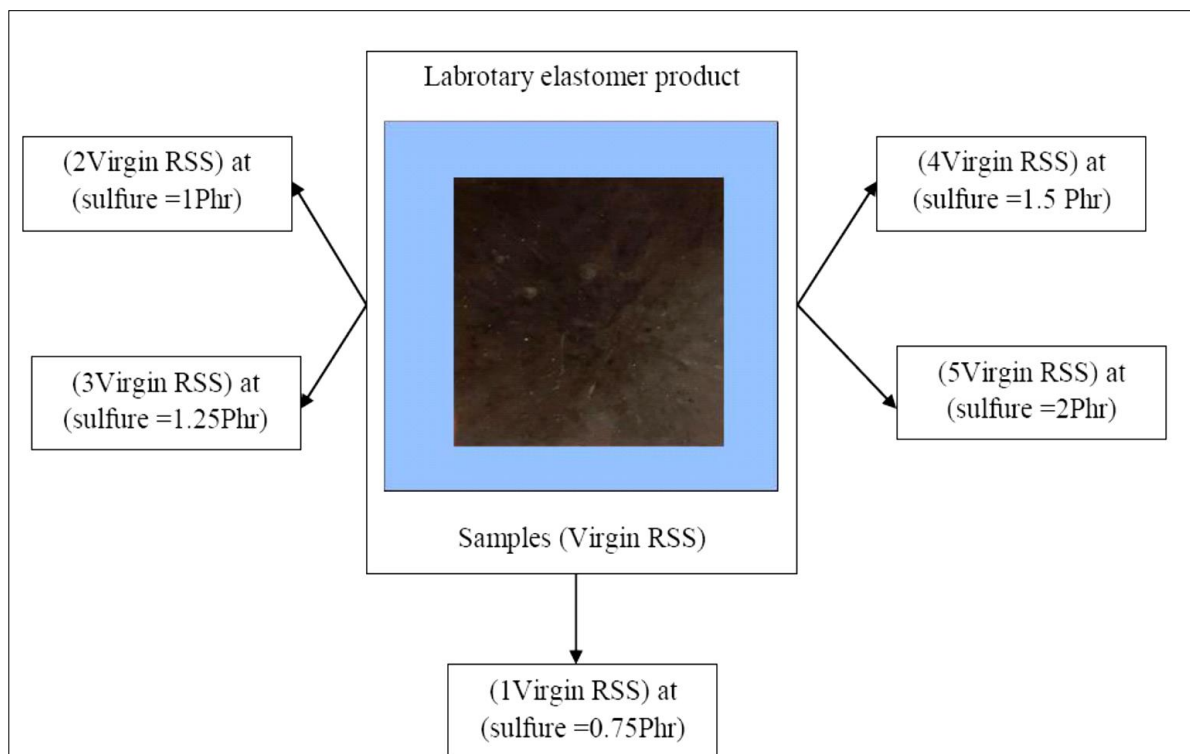


Figure (3-4): A Photographic Image of The Vulcanized RSS Rubber Sample With Different Ratios of The Sulfuric Cross-Linking Agent Used as a Laboratory Elastomeric Product, Denoted by (Virgin RSS).

Then the moldings were cut into strips of (13 cm) length and (0.5 cm) width in order to prepare them for the next step.

3-4 Shape-Memory Natural Rubber (SMNR) Preparation Technique

Elastomer product/small molecule blend SMP technique was used to prepare the shape-memory natural rubber (SMNR) under study; based on the swelling process through impregnation of the commercial and laboratory types of elastomer product with fatty acid according to the references [10,18,22,23,26,27,33and75], as it follows:

3-4-1 Preparation of Shape Memory Natural Rubber Type (Rubber Band/Stearic Acid Blend SMP) Sample Code (RB/based SA)

RB/based SA preparation process comprised three steps:

3-4-1-1 Stearic Acid (SA) Preparation

- Three quarters (375ml) of a 500ml beaker is filled with SA powder. This amount of SA is chosen for being enough for the complete submerging of five under study rubber bands in it in the preparation process next steps.
- SA powder was put on the magnetic stirrer surface at 75°C (which is beyond the melting temperature of SA, that is 69.3°C), see Figure (3-5-a).

3-4-1-2 (RB/based SA) Preparation Technique

Utilizing the swelling technique, RB/based SA is prepared as in the next steps: 1-The electronic balance was used to weigh the under study rubber band. As mentioned earlier, before immersion in the molten of SA, RB weight is denoted by (W_d).

2- The rubber band is fully immersed in SA molten for a pre-determined period of time according Table (3-5) at the temperature (75°C), Figure (3-5-a).

3- RB is taken out of the molten of SA after ending the specified time using stainless steel tongs, as shown in Figure (3-5-b).

4- Immersing the rubber band after impregnating it with SA, directly in isopropyl alcohol for a period of (1min) at room temperature (23 ± 2)°C, in order to free its surface from SA additional layers, as shown in see Figure (3-5-c).

5- The SA-impregnated rubber band (previously denoted as RB/based SA) is stretched in a slight way by hand, then scraping it little a bit to get rid of the remaining layers, see Figure (3-5-d).

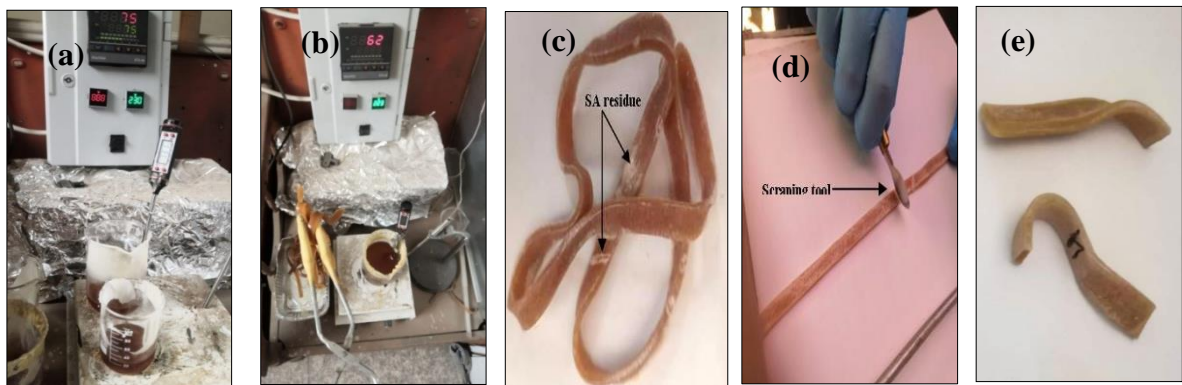


Figure (3-5): Photographic Images Taken During Preparation of RB/based SA, a- Preparation of SA for Melting Process, b-The Process of Removing The Rubber Bands After Impregnation With SA, c- Forming Some Residues of SA on (RB/based SA) Surface, d- Scraping process of SA Residues off The Surface of (RB/based SA), e- Dry The RB/based SA at Room Temp.

6- Instant immersing in (75°C) hot pure water; to eliminate deformations attributed to swelling and stretching (by hand).

7- Leaving the sample to dry for overnight at room temperature (23 ± 2)°C, see Figure (3-5-e).

8- Weighing the rubber band impregnated with SA, so, the W_s reading is recorded. The increase in weight was recorded in the form of the percentage of swelling or absorbency of the rubber band for SA molten (the weight percentage of SA) using equation (3.1), which will be mentioned in paragraph (3-4-1-3).

3-4-1-3 Addition Ratio.

RB/based SA was prepared with a constant value of (SA) weight percentage, using the following equation [10,22,33and75]:-

$$\text{Swelling percentage or Stearic acid ratio(\%)} = \frac{W_s - W_d}{W_d} \times 100\% \dots(3.1)$$

Where:

W_d is the weight of the rubber band before immersion in SA molten (before swelling), measured in (g)units.

W_s is the weight of the rubber band after being immersed in SA molten for a predetermined time, measured in (g)units.

Table (3-5) shows the sample code for different swelling times and type of networks in this type of shape memory rubber samples.

Table (3-5): The Sample Code for Different Swelling Time and Type of Network Sample.

Sample code	Swelling time (min)	Type of network sample	
		Virgin RB	Stearic acid (SA)
RB/based SA	5,10,15,30,40,60,80,100,120,180	Permanent network (hard segment)	Temporary network (soft segment)

3-4-2 Preparation of Shape Memory Natural Rubber Type (Rubber Band/Palmitic Acid Blend SMP) Sample Code (RB/based PA)

This molding included SMNR consisting of a commercial product represented by rubber band impregnated with Palmitic acid (PA), through swelling process for a period of (2hr) at a temperature of (75°C) by following the same previous steps mentioned in the sample preparation section of type (RB/based SA).

3-4-3 Preparation of Shape Memory Natural Rubber Type (Virgin RSS/Stearic Acid Blend SMP) Sample Code (RSS/based SA)

This molding included the SMNR as shown in Figure (3-6), consisting of a laboratory product represented by the natural rubber type RSS, impregnated with Stearic acid (SA) through swelling process for a period of (2hr) at a temperature of 75°C. This type of SMNR can be reached by following the same steps mentioned previously in the sample preparation section of type (RB/based SA).



Figure (3-6): Photographic Image of laboratory Elastomeric Vulcanized Rubber After Being Impregnated With SA Molten Denoted as (RSS/based SA).

Table (3-6) shows the sample code for different percentages of the sulfuric cross-linking factor and the type of networks in this type of shape memory rubber samples.

Table (3-6): The Sample Code for Different Sulfur Ratios and Type of Network Sample.

Sample code	Sulfur ratio Phr	Swelling time (min)	Type of network sample	
			Virgin RB	(SA)
1RSS/ based SA	0.75	120	Permanent network (hard segment)	Temporary network (soft segment)
2RSS/ based SA	1			
3RSS/ based SA	1.25			
4RSS/ based SA	1.5			
5RSS/ based SA	2			

The prepared natural rubber/fatty acid blend shape memory polymer (SMP) is cut into regular samples according to the specifications of the tests that were conducted, as shown in Table (3-7).

3-5 Characterization and Test Methods of SMP.

Nine types of tests were conducted to characterize the materials under study, as shown in Figure (1-3) and table (3-7).

3-5-1 One-Way Shape Memory Test

According to the references [1,10,18,21-23,26-28,75-84], this test is divided into three types through which the verification of the dual shape memory behavior can be made, which are:

First: Quantified shape memory effect (SME) test.

Second: Visual photographic shape-memory effect (SME) test.

Third: Surface shape-memory effect (SME) test.

For the characterization of the shape memory behavior of the prepared materials, these tests require before starting doing them taking into account some conditions that must be worked by and predetermined according to the methodology of the references followed in this study, these conditions are:

1- Using the dual shape thermo-mechanical cycle of hot-classical type, to activated SEM property on two models:

- The first model: It is the dual shape thermomechanical cycle, based on normal cooling.
- The second model: It is the dual –shape thermomechanical cycle based on abnormal cooling.

Table (3-7): The Standard Specifications for Each of The Tests That were Conducted in This Study.

Type of test		Test sample	the conditions	
1-Differential scanning calorimetry analysis (DSC)		5-10mg	—	
2- X-ray diffraction analysis (XRD)		Length =1cm Width=0.5cm	Small flat sample	
3- Energy dispersive X-ray spectroscopy analysis (EDS)		Length =2cm Width=2cm		
4- Field emission scanning electron microscopy (FE-SEM)				
5- Fourier transform infrared spectrometry analysis (FT-IR)		Solid sample: Length =2cm,Width=2cm	—	
		Powder sample: 5-10mg		
6- Optical microscopy		Length =10 cm Width=0.5cm	Rectangular strips	
7- (Quasi-static) mechanical test at short time	Tensile strength		ASTM-D412	—
	Shore-A durometer hardness		ASTM-D4240	—
	Flat crush test (FCT)		Length =1cm Width=0.5cm	Small flat sample
8- Measurement of cross link density		 	ISO 1817	Small rectangular
9- (One-way) shape memory property test	Dual –shape memory (SME) testing	Quantification of (SME) testing	Length =50mm Width=5mm Thickness =1-2mm	Rectangular strips
		Visual photographic (SME) testing	Length =10 -15cm Width=0.5-0.9cm Thickness =0-2cm	
	Surface shape memory effect (SME) testing	Length =10 cm Width=0.5cm		

2- Using the thermal transition temperature (T_{trans}) to move from the original shape of the samples under study to the temporary mechanically deformed shape with a value of up to (75°C), that is, above the melting point of the fatty acid used in preparing shape memory polymeric materials of all kinds of type SMNR in this current study.

3- Prior choosing for the mechanical deformation as a value or as a shape before conducting a shape memory cycle.

3-5-1-1 Quantified Shape-Memory Effect (SME) Test

This test is divided into two parts according to the type of thermo-responsive stimulation used in activating and deactivating the quantified one-way shape memory effect (SME) property according to the references, as follows:

3-5-1-1-1 Air-responsive shape memory effect test.

Thermal elongation device of local origin (Designed, by me and manufactured in cooperation with a local engineering industrial workshop), built according to the standard specifications determined in the reference [85], was used in activating and deactivating(SME) property by the hot-air stimulation. Where, this device is featured by a thermo-chamber with a temperature-controller device that contains a heating element at the back of the chamber; in addition to a water bath with a pump which controls the cooling of the sample by atomization, as shown in Figure (3-7).



Figure (3-7): Photographic Image of The Self-made Thermal Elongation Device Based on Thermal Stimulation by Hot Air.

Test Procedure:

The steps of the dual-shape thermo-mechanical cycle, using the Thermal elongation device, are based on two models:

First model: the dual-shape thermo-mechanical cycle is based on normal cooling at room temperature.

The practical scenario of the hot classical shape memory cycle is based on normal cooling at room temperature ($23\pm 2^{\circ}\text{C}$), as shown in Figure (3-8), which agrees with the research works as it consists of two parts:

1- SME property activation stage (the deformed shape programming stage) for the material under study. It consists of three steps:

- The test sample heating process in step0: Heating the test sample under study at room temperature to 75°C (above the melting point of all types of fatty acid used in this study), gradually, for a period of (11min); to ensure the occurrence of the thermal equilibrium.
- The process of applying a tensile load in step1: applying a tensile load to one end of the sample causes the strain to be fixed during the activation stage, that was previously determined.

- Cooling process with tensile load applying in step2: Cooling the sample by turning off the thermal heating system used in this study with opening the heating chamber door, and leaving the sample at room temperature for a period of (30 minutes) under tension; to allow the fatty acid to solidify while taking into account the continuation of the loading process, then taking the elongation reading which represents the value of the change in length (ΔL) in step2.

- The process of removing the applied load in step3: Removing the applied load off the material, then leaving it for 10min. After that, the reading of the elongation scale was recorded, which represents the value of the change in length (ΔL) in step3.

2- SME property deactivation stage (permanent original shape memory recovery stage). It consists of two steps:

- Reheating the test sample in step4: Reheating the test sample from room temperature to 75°C, with recording the elongation reading, which represents the change in length (ΔL) in step4 at the end of the recovery process.

- Leaving the sample after the end of the recovery process to cool down to room temperature.

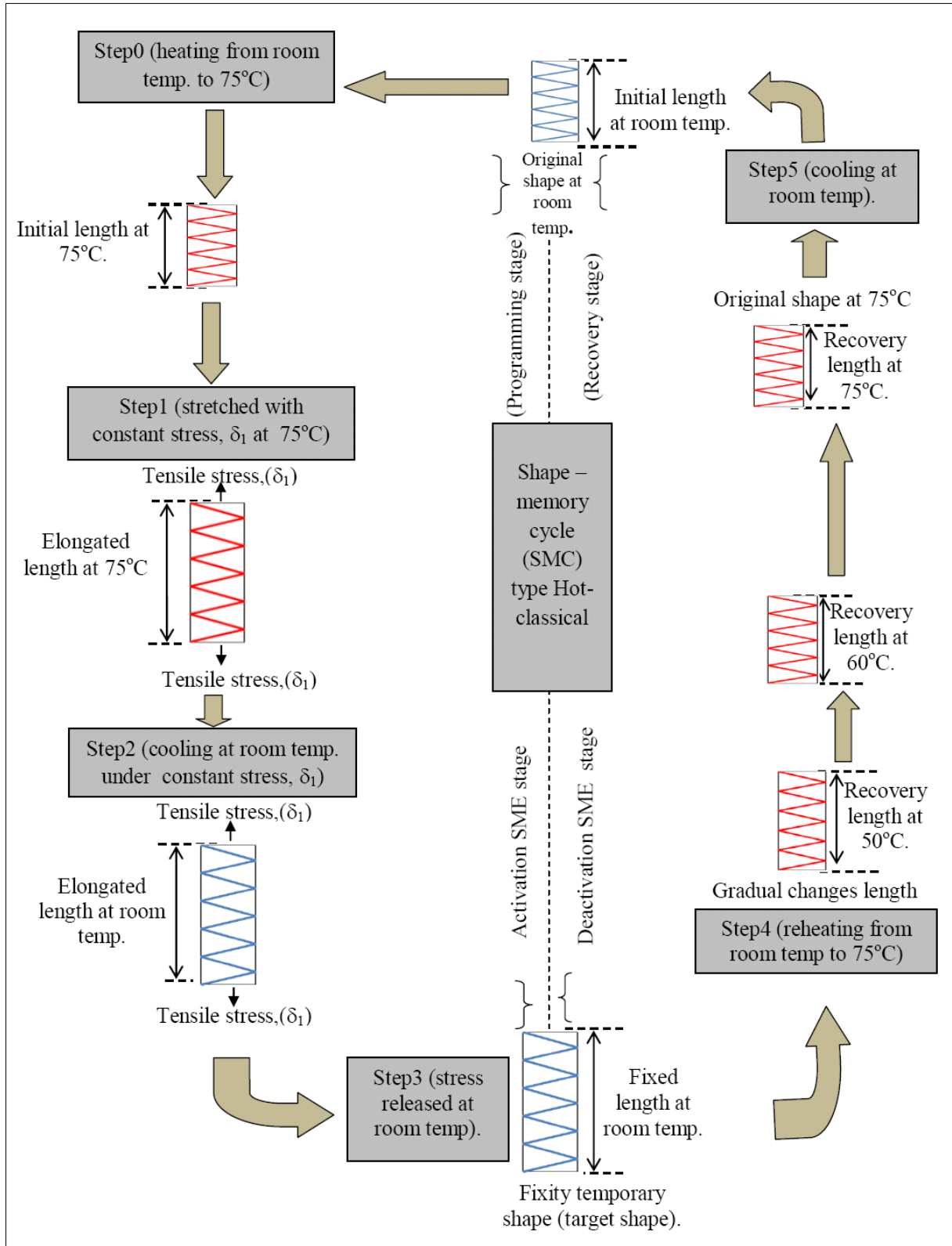


Figure (3-8): Is a Schematic Diagram of The Hot-Classical Shape Memory Cycle (SMC) Based on Normal Cooling at Room Temperature ($23\pm 2^\circ\text{C}$) for The Samples Under Study.

Depending on the results obtained from each step of the hot classical shape memory cycle steps followed in this study, SME property can be described by calculating the shape memory factors represented by the following:

1- Calculation of the mechanically deformed shape fixity ratio during the SME property activation stage (the deformed shape programming stage) according to the following equation [10,18,22,23,26,27,38,75-77]: -

$$R_f(N) = \frac{\varepsilon_3(N)}{\varepsilon_1(N)} \dots (3.2)$$

where:

$R_f(N)$: is the mechanically deformed shape fixity ratio.

N : Is the shape memory cycle number, which takes the values $N = 0, 1, 2, 3$, etc., for experiments with only single SMC, $N=0$.

$\varepsilon_1(N)$: is the applied strain during the shape memory cycle programming stage in step1, which is called “loaded strain”, calculated according to the following equation:

$$\varepsilon_1 = \frac{\Delta L \text{ at step1}}{L_0} \times 100\% \dots (3.3)$$

Where:

$\Delta L \text{ at step1}$: It is the amount of change in length representing the dial gauge reading at step1 after applying the tensile load, measured in (mm)units.

L_0 : is the distance between the two loading points measured in (mm), which represents the initial length of the sample that is fixed tightly in between the grips of the SME test before starting with the shape memory cycle, which represents the initial clamp gap.

ε_1 : is generally predetermined as one of the conditions to be worked by before the start of the shape memory cycle.

$\varepsilon_3(N)$: It is the value of the applied strain after the process of removing the applied load in step3, which is called the fixed strain or unload strain for the cycle number (N), which is given by the equation:

$$\varepsilon_3(N) = \frac{\Delta L \text{ at step3}}{L_0} \times 100\% \dots(3.4)$$

$\Delta L \text{ at step3}$: It is the amount of change in length representing the dial gauge reading at step3, measured in (mm)units.

2- Calculation of the permanent original shape recovery ratio during the SME property deactivation stage (the recovery stage) according to the following equation [10,18,22,23,26,27,38,75-77]: -

$$R_r(N) = \frac{\varepsilon_3(N) - \varepsilon_4(N)}{\varepsilon_3(N) - \varepsilon_0(N)} \times 100\% \dots(3.5)$$

$R_r(N)$: is the shape recovery ratio for the cycle number (N).

where:

$\varepsilon_4(N)$: It is the value of the (irreversible permanent) or (residual) strain in step4 of cycle number (N) after reheating the sample to the pre-determined thermal transition temperature (T_{trans}) temperature, which is (75°C), as one of the conditions to be worked by before starting with the shape memory cycle (SMC) based on the thermal specifications of the temporary network in the prepared shape memory polymeric material, it is given by the equation:

$$\varepsilon_4(N) = \frac{\Delta L \text{ at step4}}{L_0} \times 100\% \dots(3.6)$$

$\Delta L \text{ at step4}$: It is the amount of change in length representing the dial gauge reading at step4, measured in (mm)units.

3- Calculation of the shape-memory index (SM-index), according to the following equation [86]:

$$SM - index (\%) = R_f \times R_r \dots(3.7)$$

4- Calculation of the mechanical work energy consumed by specimen deformation during the followed thermomechanical cycle, according to the references [15,55-59,74 and 85]:-

- Calculation of the internal stretching work energy consumed in deforming the sample during the SME property activation stage (the deformed shape programming stage) according to its steps, as follows:

a- Calculation of the internal stretching work energy in step1.

$$W_I(at\ step1) = \delta_1 \times \varepsilon_1 \ (KJ / m^3) \dots(3.8)$$

Where:-

δ_1 : is the applied stretching stress, which can also be denoted by ($\delta_{applied}$) in step1, which is given by the following equation:

$$\delta_1 = \frac{F}{A} = \frac{M \times g}{A} \ (Pa) \dots(3.9)$$

Where:

(F): is the stretching force (N).

(M): is the applied mass (g).

(g): is the ground acceleration (9.8m/sec²).

b- Calculation of the internal stretching work in step2.

$$W_I(at\ step2) = \delta_1 \times \varepsilon_2 \ (KJ / m^3) \dots(3.10)$$

c- Calculation of the internal stretching work in step3.

$$W_I(at\ step3) = \delta_1 \times \varepsilon_3 \ (KJ / m^3) \dots(3.11)$$

- Calculation of the internal stretching work in step4 of the recovery stage.

$$W_I(at\ step4) = \delta_1 \times \varepsilon_4 \ (KJ / m^3) \dots(3.12)$$

5- Calculation of the storing or retaining efficiency of the elastic strain energy [15].

$$\eta = \frac{W_i \text{ at step3}}{W_i \text{ at step1}} \dots(3.13)$$

Second model: The dual-shape thermo-mechanical cycle based on abnormal cooling using the Thermal elongation device shown in Figure (3-7).

In this model, the same practical scenario of the shape memory cycle mentioned in the first model, is followed, except that in (step2) of the programming stage in this second model, the process of cooling is conducted using iced water until the sample temperature reaches 10°C.

3-5-1-1-2 The Water-responsive Shape-Memory Effect (SME) Test

In this current study, the Chinese-origin digital Vernier was self-modified and turned into a stretching instrument upon request, to activate and deactivate SME property of the materials under study, as shown in Figure (3-9). It was similar to the method that created by Brostowitz and his group after the development of (wrench) [18] which was adopted by many researchers in the SMP field [20,22,26,27,29,38 and 75].



Figure (3-9): A Photographic Image of The Self-Modified Electronic Vernier for Being Used as a Shape-Memory Instrument Based on Thermal Stimulation by Immersing in Hot Water.

Test procedure:

The protocol of the hot classical shape memory cycle based on stimulation with hot water, as shown in Table (3-8), which includes the following:

1- Length of (10mm) was marked at two sides of the center of rectangular strip by two distance lines as initial length, L_0 .

2- The specimen was clamped in outside the jaws of Vernier caliper.

3- Programming the deformed shape (target shape) according to the following steps:

- Step0: The marked rectangular strip sample was immersed in hot water at 75°C for (30sec) before stretching.

- Step1: The marked distance on the specimen was elongated to the desired length, L_1 at 75°C for (10sec).

- Step2: The elongated specimen was cooled in iced water ($10\pm 1^\circ\text{C}$) for (30sec) under load.

- Step3: The stretched specimen is removed out of the modified Vernier jaws (removing the external force), then the fixed length of the fixed specimen is measured after leaving it for 60sec to relax at room temperature ($23\pm 2^\circ\text{C}$).

Where the length L_3 , which includes (the distance between the two lines) is measured by means of a ruler or a Vernier.

4- The stage of the original shape recovery according to the following step:

- Step4: The fixed sample is reheated to the recovery temperature to recover its original shape, which is done by re-immersing it again in the water bath at 75°C for 30sec. Then the marked distance (the distance between the two lines) is measured, which represents " L_4 " in this step. Where L_4 , is measured by means of a ruler or a Vernier.

From the obtained results, the shape memory factors are calculated according to the previously mentioned equations.

Table (3-8): The Water-responsive Shape Memory Effect (SME) Test Method in Images Using The Developed Vernier.

Test protocol		Photos	
1- Drawing two distance lines			
2- Clamped on modified Vernier			
3-Programming stage of Hot-classical (SMC)	Step0		
	Sample immersion in hot water for (30sec)		
	Step1		
	Sample stretching in hot water.		
Step2			
Stretched sample in cold water for (30sec).			
Step3		Fixed sample 	
Stretched sample remove from jaws of Vernier at room temp.			
4- Recovery stage Hot-classical (SMC)	Step4		Recover sample 
	Fixed sample reheating by immersion in hot water.		

3-5-1-2 Visual Photography (Macroscopic) Shape Memory Effect (SME) Testing

This type of the macroscopic SME property demonstration test requires the use of a video camera to record images for the fixed temporary shape that represents the target shape to be formed in the fixed temporary shape programming stage (SME property activation stage). Moreover, recording the original shape recovery process in the recovery stage (SME property deactivation stage) of the hot classical shape memory cycle based on the thermal stimulation with hot water.

- Test procedure:

1- The original and the target shapes were determined before the start of the shape memory cycle, as shown in Table (3-9).

Table (3-9): Determination of The Types of The Target Shape That is Previously Fixed in the Visual Demonstration of SME Property, With The Fixation Tools.

Shape of test sample	Name of sample shape in (SMC)	No. of step in (SMC)	Work tools		
Straight - shape	Original - shape	Step0	<ul style="list-style-type: none"> • Hot-water bath. • Cold cushion pack/ • Target-shape fixation tools are: 		
Long strip - shape	Fixed temporary shape (Target shape) or (Deformed shape)	Step3	<ul style="list-style-type: none"> 1-Long-strips shape holding with hands. 2- Holding the spiral shape with pliers or index finger 3- Holding U-shape with laboratory pipette 		
Spiral - shape			  		
U- shape					

2-Taking snapshots with the video camera for the test sample with the original shape represented by the straight-shape, after undergoing the steps of the programming stage shown in Figure (3-10), to reach the fixed temporary shape or called the target shape (deformed shape).

3- Taking snapshots with the video camera for the programmed test sample of the fixed temporary shape, while it is recovering its original shape during the reheating process in the recovery stage of the water-responsive hot classical shape memory cycle.

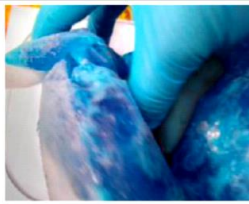
Type of (target –shape)	<u>Step1:</u> Heating by hot water bath at 75°C and applied force load for (30sec).		<u>Step2:</u> Cooling by cold cushion pack under load for (30sec).		<u>Step3:</u> Load removed
Long-strip shape					
Spiral- shape					
					
U- shape					

Figure (3-10): Snapshots Taken With The Video Camera of The Fixed Temporary Shape Programming Stage Steps.

3-5-1-3 Surface Shape-Memory Effect (SME) Testing

Surface shape memory device of local origin (Designed, by me and manufactured in cooperation with a local engineering industrial workshop) was used to activate and deactivate the surface-SME property. Its idea is based on using a ball penetrator with a diameter of (11.7 mm) of ceramic material, according to the references [79,81], where this penetrator is fixed by a holder and it is affected by a compressive load, as shown in Figure (3-11).

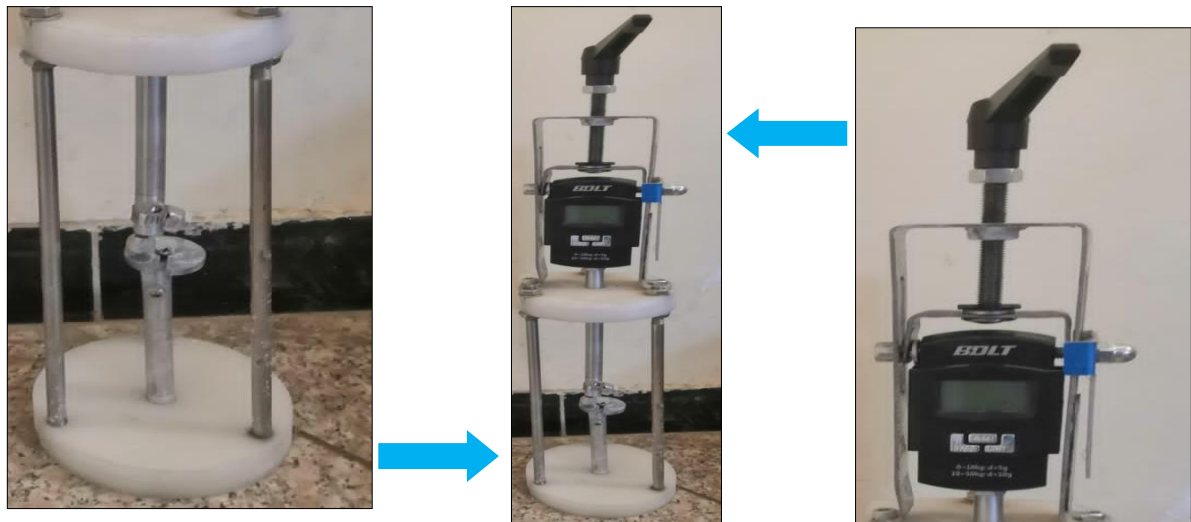


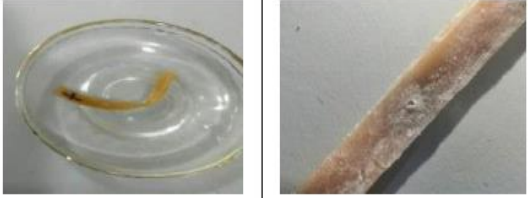
Figure (3-11): Photographic Images of The Self- Made Surface Shape Memory Device Based on Thermal Stimulation With Hot Water.

Test Procedure:

- 1- The test sample is put in the surface-SME device specified place, then making the ball penetrator touches the sample surface with a fixing load of (0.05 kg).
- 2- Determining the compressive load value to be applied to form the fixed temporary shape of the surface before starting with the hot classical shape memory cycle based on thermal stimulation with hot water.
- 3- Taking snapshots with the video camera and optical microscope for the sample surface after undergoing the programming stage, as shown in Table (3-10).
- 4- Taking snapshots with the video camera and optical microscope for the programmed test sample surface while it is recovering its original surface shape

by reheating it with hot water at a temperature of 75°C, for a period of (30sec) in the followed shape memory cycle recovery stage.

Table (3-10): Pictures of The Surface Shape Memory Effect (SME) Test Method Using Ball Penetrator.

Test protocol	Photos	
<p>1- Programming stage</p>	<p>Step0 Sample was immersed in hot water at 75°C for (30sec).</p>	
	<p>Step1 Applied constant load using ball indicator at 75°C for (10sec).</p>	
	<p>Step2 Cooling at room temp, under load for (30min).</p>	
	<p>Step3 Fixed sample remove from Surface – SME device.</p>	 <p style="text-align: center;">Fixed shape</p>
<p>2- Recovery stage</p>	<p>Step4 Fixed sample reheating by immersion in hot water at 75°C.</p>	

3-5-2 Physico -Chemical Characterization Tests

3-5-2-1 Differential Scanning Calorimetry Analysis (DSC) Test

The French origin (DSC) device was used with a heating rate of (10°C/min), calibrated using a standard indium specimen, as shown in Table (3-7), in studying the relation of the latent heat of fusion, ΔH_m for the samples subjected to this test, with the SME property condition, whether it is activated or deactivated.

3-5-2-2 X-ray Diffraction (XRD) Test

The Japanese origin (XRD) device, which is shown in Table (3-7) (Cu-BF target, scanning step 50°/min, current (1.5A), and input voltage 220V/50Hz), was used to obtain the x-ray diffraction patterns of the samples subjected to this test, to study the effect of SME property activation and deactivation on x-ray diffraction parameters.

3-5-2-3 Fourier transform infra-red (FT-IR) Test

The German (FT-IR) spectrometer, which is shown in Table (3-7), was used to prove that there was no chemical reaction between the vulcanized rubber samples and the fatty acid after the impregnation process.

3-5-2-4 Field Emission-Scanning Electron Microscopy (FE-SEM) Test

The Dutch-origin (FE-SEM) device, which is shown in Table (3-7), was used to study the samples surface subjected to this test, after coating them with a layer of gold using the sputter coater system.

3-5-2-5 Energy dispersive X-ray spectroscopy analysis (EDS) Test

The elemental chemical composition of sample was investigated by the energy dispersive x-ray spectroscopy system (Oxford instruments X-Max EDS, UK). The test sample stage with conductive paste, and the applied voltage was 20 KV as shown in Table (3-7).

3-5-2-6 Determination of the Vulcanized Rubber Cross-Link Density by Solvent Swelling Method

This is the simplest and most common technique for measuring the cross-link density of vulcanized rubber according to the references [21,84,87-89].

-Test procedure:

- 1- Measuring the mass of the test samples before immersion in toluene, using an electronic balance sensing readings of four decimal places.
- 2- Submerge the test samples in plastic bottles containing toluene, as shown in Table (3-7), in a dark place at room temperature ($23\pm 2^\circ\text{C}$) for 7 days.
- 3- Taking the test samples off the bottles after the end of the specified immersion time, then drying them using filter paper, then quickly measuring the mass of these samples.
- 4- Calculating the volume fraction value for the rubber samples while they are in swollen state from the following equation [21,84,87-89].

$$V_R = \frac{1}{1 + \frac{\rho_r + (W_s - W_d)}{\rho_s W_d}} \dots(3-14)$$

Where:

V_R is the volume fraction of the test sample in swollen state.

ρ_s is the mass density of toluene solvent (0.867 g/cm^3).

ρ_r is the mass density of the initial dry sample (before the immersion).

W_s is the weight of swollen test sample after (7days).

W_d is the weight of initial dried test sample (before the immersion).

- 5- Calculating the cross-link density using Flory –Rehner equation [89]:

$$V_e = -\left[\ln(1 - V_R) + V_R + V_R^2\right] / 2V_S(V_R^{1/3} - \frac{1}{2}V_R) \dots(3.15)$$

Where:

V_S is the molar of toluene solvent ($106.83 \text{ cm}^3/\text{mol}$).

X is Flory –Huggins polymer - solvent interaction term. The value of this parameter depends on the type of polymer and the type of solvent such as for natural rubber – toluene. The value of (X) can be calculated by following equation [89]:

$$X = 0.44 + 0.18 V_R \dots (3.16)$$

3-5-3 Quasi-Static Mechanical Tests at Short Time

3-5-3-1 Tensile Strength Test

The Tensile testing machine of type (HSOKT), British origin, with operability (50KN) and operating voltage (220V/50Hz), as shown in Table (3-7), was used to measure the tensile strength at room temperature ($23 \pm 2^\circ\text{C}$).

3-5-3-2 Hardness Test

The manual durometer hardness type Shore-A of Chinese origin was used to conduct the hardness test for the samples subjected to this test at room temperature ($23 \pm 2^\circ\text{C}$). This test is done by the point penetrator indenting the surface of these samples under the influence a certain load leads to giving a reading that represents a measure of the surface indentation of the material, as shown in Table (3-7).

3-5-3-3 Flat-Crush Test (FCT)

A Spanish-origin crush tester device was used to measure the crush resistance at room temperature ($23 \pm 2^\circ\text{C}$) for the samples subjected to this test , as shown in Table (3.7).



4

Chapter Four
Results and Discussion

4-1 Introduction

This chapter includes all the results obtained in the current study, with their discussion and interpretation. They are illustrated in graphical Figures for each case and for all shape-memory tests subjected to the hot classical shape memory cycle, structural tests, and Quasi-static mechanical tests based on short loading at room temperature. In addition to presenting and interpreting the results of the role of time of shape memory cycle in determining the shape memory polymer appropriate type for a particular application.

4-2 Analysis of Commercial Natural Rubber Band Swelling in Stearic Acid (SA) Molten

It is clear from the results of energy-dispersive- x-ray spectroscopy (EDS) as shown in Figure (4-1) and Table (4-1) that the natural commercial rubber band is one of the chlorinated vulcanized rubber products.

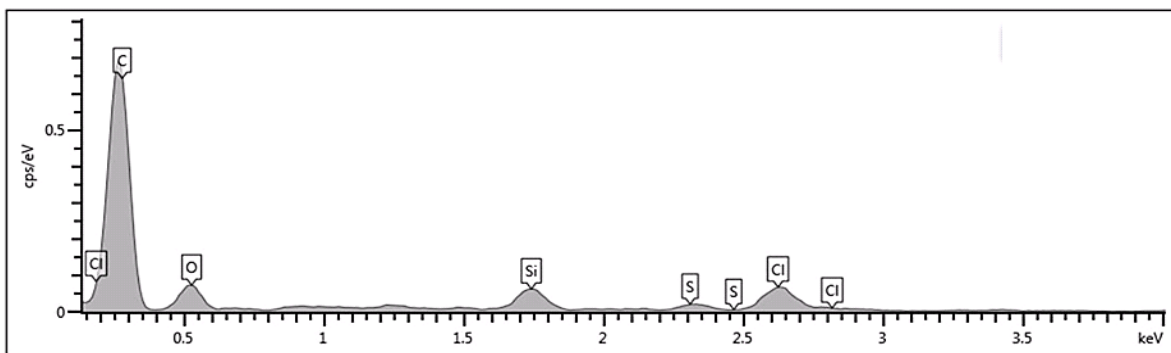


Figure (4-1): EDS Measurement of Commercial Natural Rubber Band.

Table (4-1): The Weight Percentage of The Commercial Natural Rubber Band Components.

Element	Wt%	Wt% Sigma
C	78.74	1.86
O	8.51	1.40
Si	3.49	0.60
S	1.80	0.53
Cl	7.47	1.06
Total:	100.00	

Figure (4-2) represents the swelling behavior of the rubber band (Code Virgin RB) in stearic acid (SA) molten at 75°C (above its melting point which is 69.3°C).

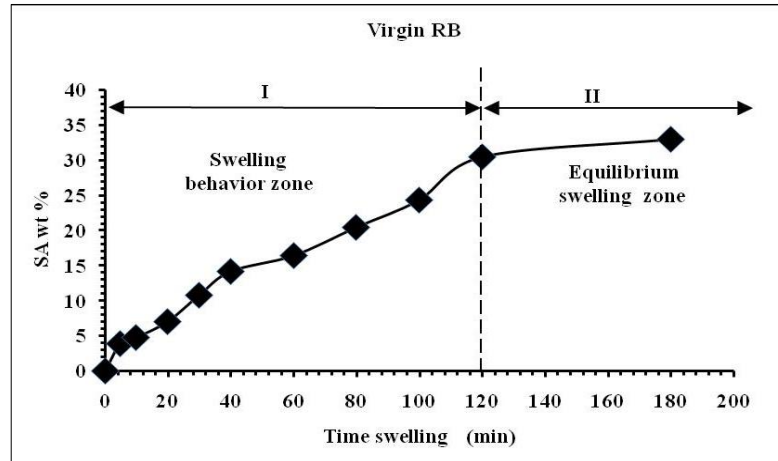


Figure (4-2): Swelling Behavior of The Commercial Natural Rubber Band (RB) in Stearic Acid (SA) at (75°C).

Generally, the (SA wt%-time swelling) curve represented in Figure (4-2) can be divided into two zones according to the swelling behavior or sometimes called the diffusion behavior as follows: -

1-The swelling behavior zone: This is a region that represents the diffusion behavior of monotonic increase during swelling duration of (0-2)hr, due to the transition of Stearic acid (SA) molten molecules from the high to low concentration area by penetrating the rubber molecules by the impregnation process.

2- Saturation limit or equilibrium swelling behavior zone: it represents the zone in which SA begins to accumulate in clear form to the naked eye, On the surface of the rubber sample whenever it heads toward the peak during a swelling duration of more than (120min). These results that were reached are in agreement with the findings of the references [10,18,23,33].

On the other hand, Figure (4-3) shows images taken by field emission scanning electron microscope, (FE-SEM) of the surface of the commercial rubber band (RB) sample after impregnating it with Stearic acid for a period of 2hr.,

which is denoted as (RB/ based SA), that is a continuous network consisting of analogous platelet network that encapsulates the rubber molecules with a percolated layer, which gradually grows until it reaches the peak stage, this result is consistent with the findings of the reference [18].

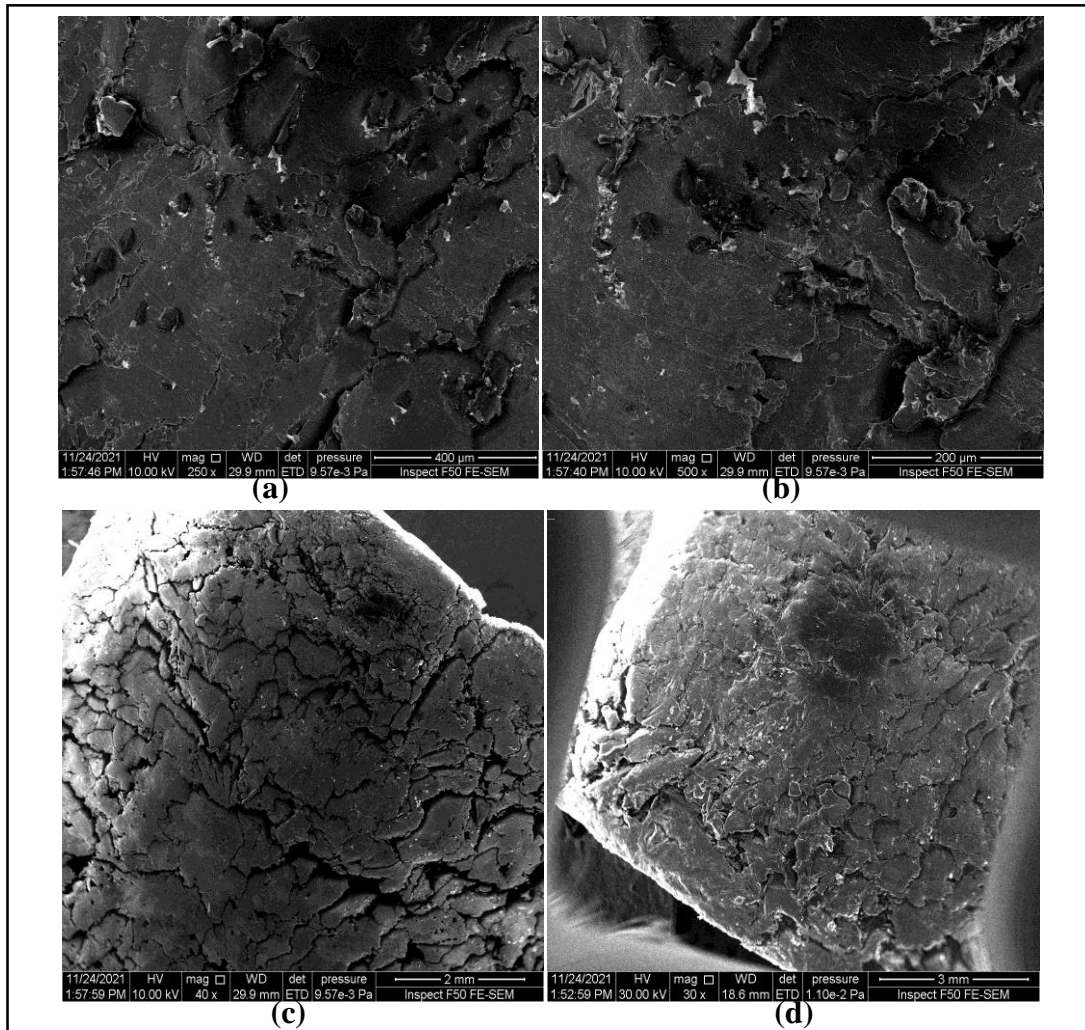


Figure (4-3): (a,b,c,d) Represent FE-SME Images at Different Magnifications for The Rubber Band Sample (RB/ based SA) Impregnated With Stearic Acid for 2hr.

Figure (4-4) indicates the FT-IR spectrum of the commercial rubber band non-impregnated with stearic acid (SA), which was denoted by (Virgin RB) in this study. The peaks appeared at $(3411.77) \text{ cm}^{-1}$, $(2959.31) \text{ cm}^{-1}$, $(2917.98) \text{ cm}^{-1}$, and $(2849.72) \text{ cm}^{-1}$; which are attributed to the natural rubber. The peaks $(1093.65) \text{ cm}^{-1}$ and $(1016.28) \text{ cm}^{-1}$, are attributed to silica. This is consistent with the findings of researcher Nicole and his group [18].

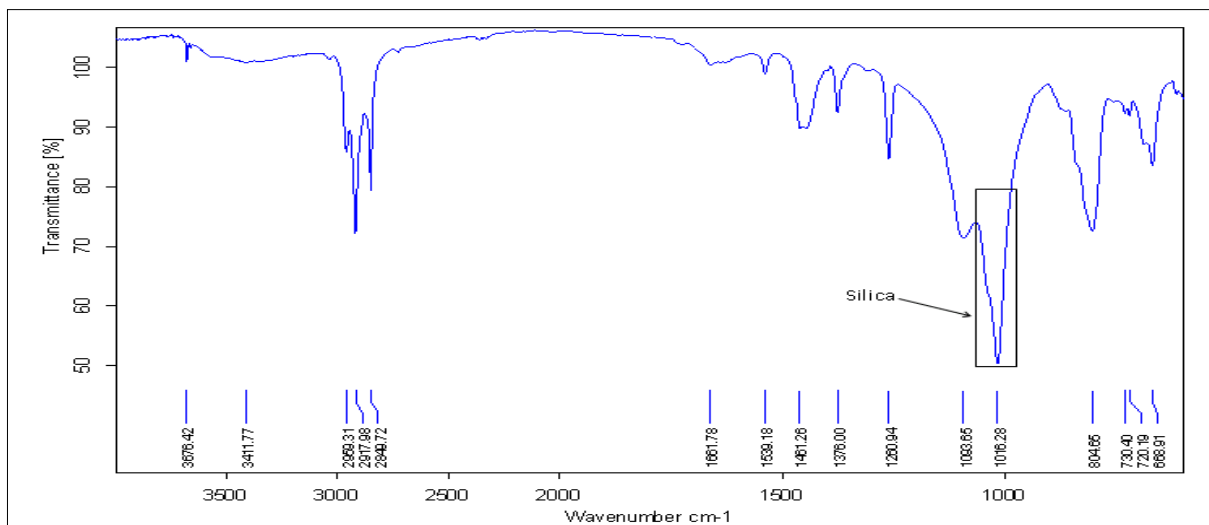


Figure (4-4): FT-IR Spectrum of The Rubber Band (Virgin RB) and Reference Spectra for Natural Rubber and Silica.

Figure (4-5) indicates that the Fourier transform infrared (FT-IR) spectra of Stearic acid (SA) particles, which shows main peaks at (1698.97) cm⁻¹, (2849.80) cm⁻¹, and (2914.75) cm⁻¹; which are consistent with the data of the stearic acid (SA) material present in the FTIR device library according to the Vesta software, as shown in Figure (4-6).

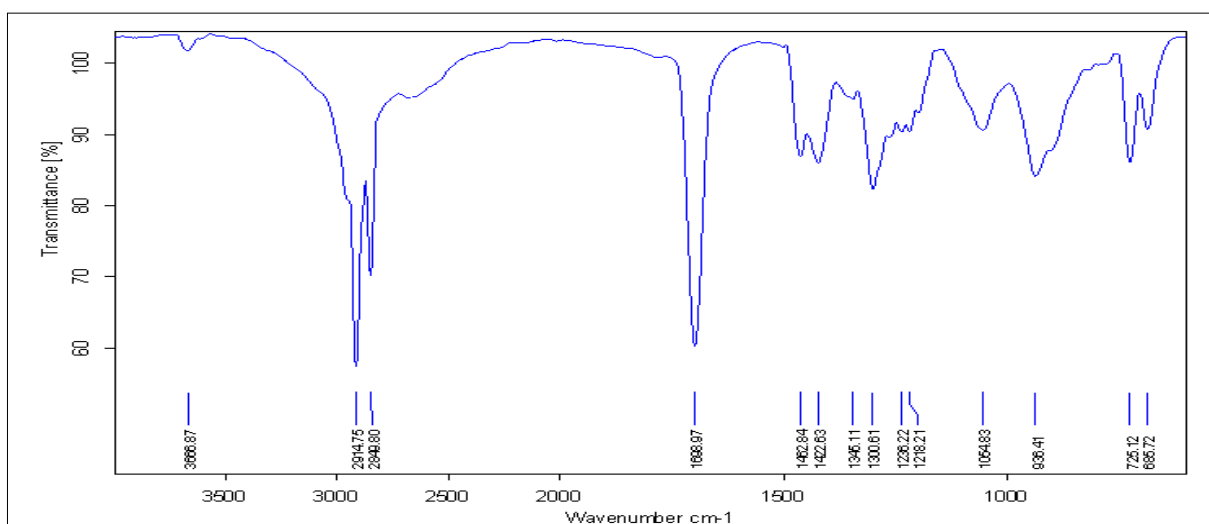


Figure (4-5): FT-IR. Spectrum of The Stearic Acid (SA).

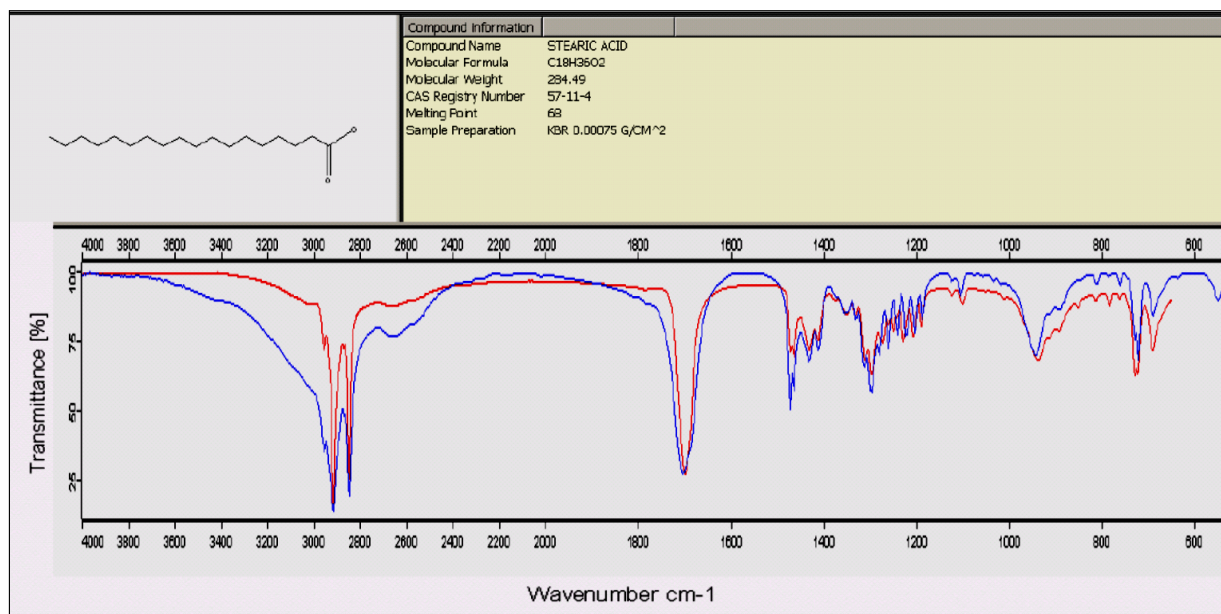


Figure (4-6): The Match Between FT-IR Spectrum of Stearic Acid (SA) Particles Used in This Study and The (FT-IR) Spectrum of Stearic Acid Present in The FT-IR Device Library.

While Figure (4-7) indicates the results of the Fourier transform spectrum of the rubber band material after impregnation with the material (SA), (Code RB/ based SA), for a period of 2hr., where it shows a peak at $(2915.93) \text{ cm}^{-1}$ attributed to (SA), also a peak at $(1111.69) \text{ cm}^{-1}$ attributed to silica.

As for Figure (4-8), it indicates that some of the (RB/ based SA) peaks match the data of the device library (FT-IR) represented by the data of Stearic acid only; because the device library does not contain data on the rubber band material (Virgin RB).

In general, the presence of peaks expressing SA, natural rubber, and silica, each separately, is the best evidence that the process of impregnating the rubber band with stearic acid was a physical process represented by the diffusion of Stearic acid between the rubber band chains, this result agrees with the reference [18].

(swelling time=2hr), has caused retention of (58.7%) of the applied strain, which is 70% in this current study.

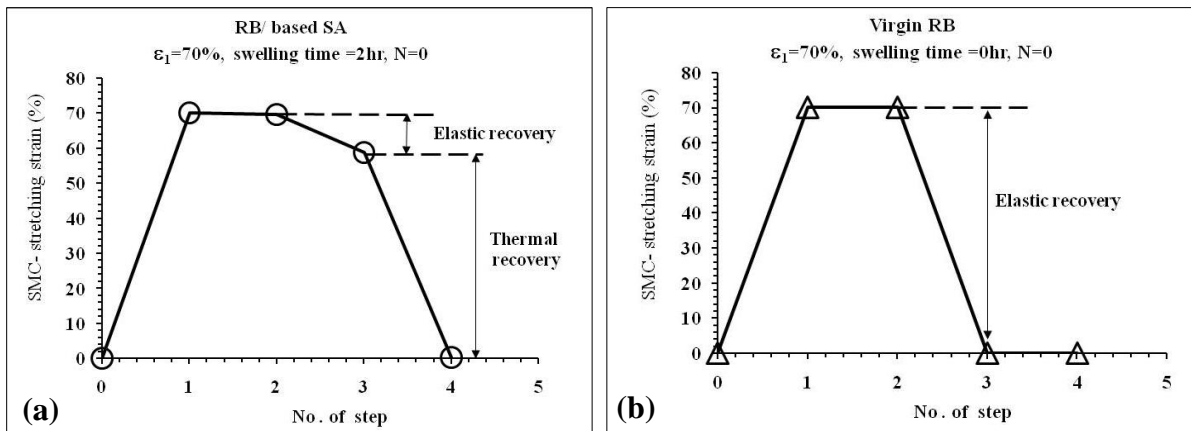


Figure (4-9): The Relation of The Applied Strain during The Hot Classical Shape Memory Cycle Based on Normal Cooling of The Commercial Rubber Band Before and After Impregnation Stearic Acid (SA) with No. of step.

After removing the load applied in step3, which represents the last step in the shape memory effect (SME) property activation stage, also called the mechanical-deformed shape programming stage during the hot classical shape memory cycle(the first part of the cycle) to temporarily keep this mechanical deformation after removing the applied load as mentioned previously (which is called as the temporary fixity strain),where the shape fixity ratio, R_f is 83.8%. So that, this material will not return to its permanent original shape, which it was in before the shape memory effect (SME) property activation unless this property is deactivated by completing the second part of the followed shape memory cycle represented by the recovery stage of the permanent original shape before the mechanical deformation occurrence, in which the material (RB/based SA) is required to be reheated above the melting point of stearic acid, SA which is 75°C for this type). As the heating temperature rises little by little, the strain formed previously according to the programming stage, will also be released little by little accordingly with this temperature increase in step4, until the original shape recovery ratio, R_r , is reached, which is estimated by 99.7%. So that, no matter the

time the sample (the sample impregnated with SA, which was denoted in this study by (RB/based SA) was left in under the influence of the reheating stage, R_r will not raise more than it reached; because the original shape recovery ratio depends on the material nature, the applied strain, and the type of the shape memory cycle. While the shape fixity ratio, R_f was equal to zero for the commercial rubber band free of Stearic acid (SA) with swelling time =0 hr (which was denoted in this study as Virgin RB) after undergoing an (SME) property activation stage (the mechanically deformed shape programming) (Figure 4-9-b); since Virgin RB showed a complete disappearance in mechanical deformation, where the value of the applied strain in step3 was equal to Zero, after removing the applied stress in step3 of the programming stage. These results are in agreement with the scientific research [10,23,75].

Thus, Virgin RB is considered as a traditional polymeric material, since it did not achieve the two aims together of the shape memory cycle correspondingly, as it follows:

- High performance in retaining the temporary mechanical deformation by the (SME) property activation.
- High performance in recovering the original shape before the mechanical deformation occurs during the (SME) property deactivation stage. This agrees with the reference [1,85,90].

Although, this rubber band can be easily converted from a traditional polymer material to a shape memory polymer if it was combined between the natural (Virgin RB) rubber elastic network with the reversible switching network of Stearic acid (SA) that can melt and crystallize by changing temperatures with each other. As in the aforementioned (RB/based SA) sample, through the impregnation process, whereby this impregnation process results in physical net points. With this physical blending, the virgin (RB) rubber band is coated with

Stearic acid, and this is shown by the microscopic images taken by the scanning electron microscope Figures (4-10) and (4-11).

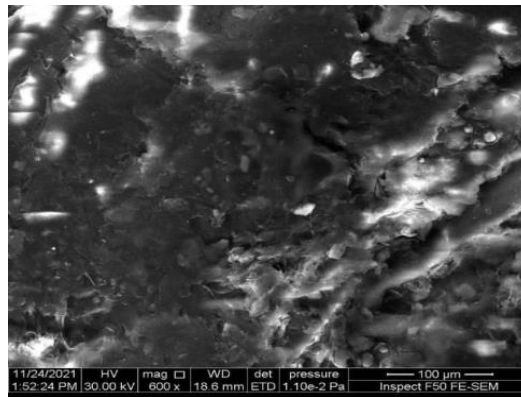


Figure (4-10): (FE-SME) Microscope Image of The Sample Surface of Type (Virgin RB).

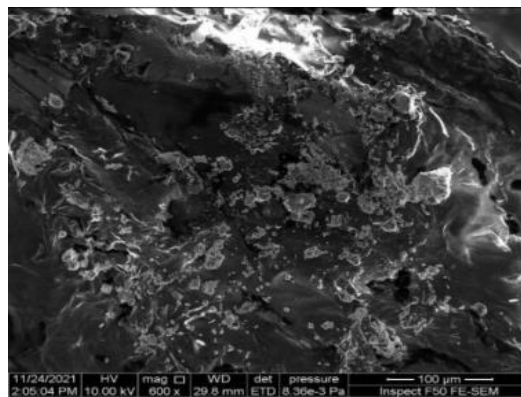


Figure (4-11): (FE-SME) Microscope Image of The Sample Surface of Type (RB/based SA).

Figure (4-10) shows that surface of the rubber band sample that is not impregnated with (SA) material (represented by Virgin RB), appears as flat. While the microscopic image (Figure 4-11) of the same rubber band surface, but after impregnation with Stearic acid, showed high crystal formation. Where the rubber band impregnation with (SA) causes the growth of analogous platelet crystals on the rubber band surface, this, in turn, leads to impeding the rubber segments movement, which leads to the rubber band showing the shape memory effect after undergoing a shape memory cycle, this agrees with what the researcher found [18,22 and 75].

Thus, the reversible switching phase in this study is represented by SA material. As mentioned previously, SA has the role-play of the lock in the elastic rubber band network, which allows of this rubber band through the shape memory cycle to lock and cancel the strain-induced crystals (SIC) by melting and crystallization SA network.

Generally, this difference in thermomechanical behavior between (Virgin RB) and (RB/based SA) occurred during the shape memory cycle, can be explained from the perspective of differential scanning calorimetry (DSC) as well as from the perspective of x-ray diffraction (XRD) as follows:

4-3-1 DSC Test

The method of thermal analysis for this test depends on the physical or chemical changes that occur to the material as a result of the temperature change that is usually accompanied by the emission or absorption of thermal energy.

Accordingly, samples were prepared for the DSC test of these materials under study represented by (Virgin RB) and (RB/based SA) after they were subjected to the (SME) property activation and deactivation stage; in order to observe the success indications of these materials in their characterization as shape memory smart materials, by identifying some of the information taken from the heating curves of the DSC test for these materials Figures (4-12) and (4-13).

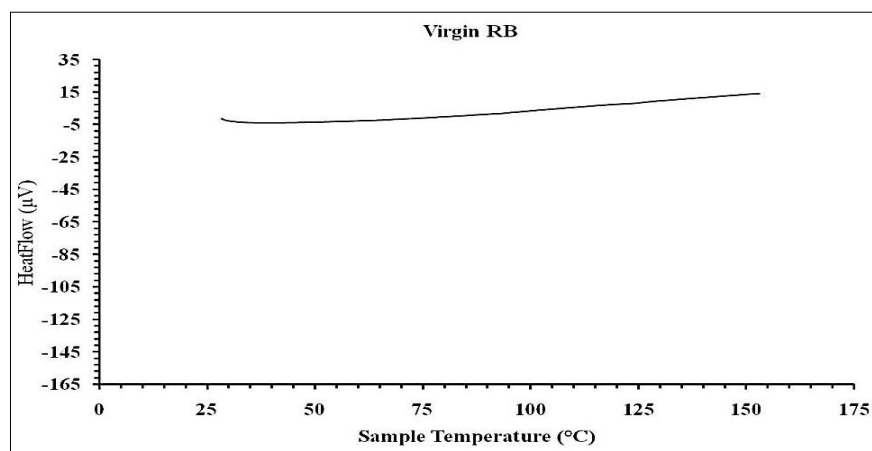


Figure (4-12): Heating Curve Taken During DSC Test of Virgin RB Sample, Which was Previously Subjected to The SME Activation Stage.

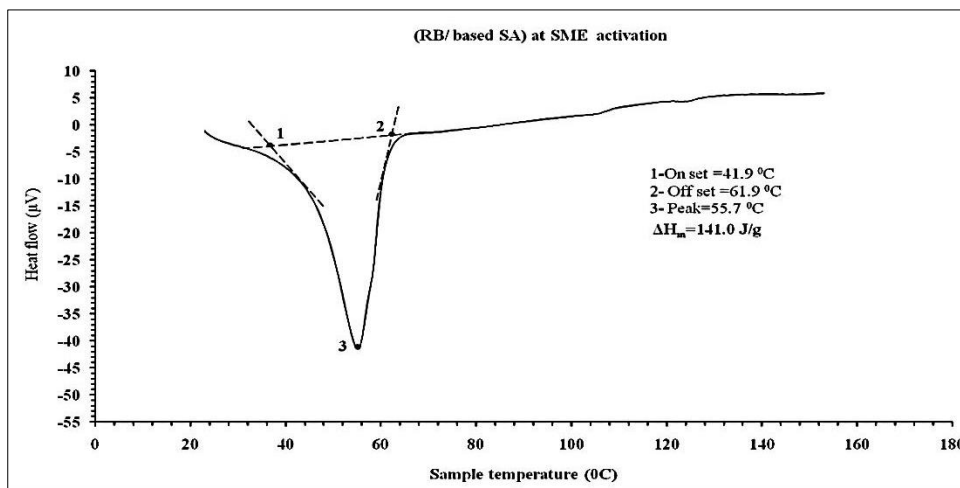


Figure (4-13): Heating Curve of The Sample (RB/based SA), Which was Previously Subjected to The SME Activation Stage.

In general, Figure (4-13) of the sample (RB/based SA) is distinguished from Figure (4-12) of the sample (Virgin RB) in that, it contains one endothermic peak, which puts it in the rank of materials that undergo a phase change during the thermal range extending from 41.9 $^{\circ}\text{C}$ to 61.9 $^{\circ}\text{C}$, which requires the absorption of thermal energy of 141.1 J/g for this thermal event to occur. While the sample (Virgin RB) falls under the character of thermally stable materials within the thermal range from 23 $^{\circ}\text{C}$ to 152 $^{\circ}\text{C}$; because no absorbent peak appears on its heating curve, and these indicators refer that the absorbent peak belongs to the Stearic acid (SA) material that coats the structure of the rubber band. The melting temperature of the Stearic acid (SA) after penetration into the structure of the rubber band decreases from its original value Figure (4-14). This decrease is attributed to the fact that the continuous phase in RB/based SA is rubber band, this is consistent with the findings of the scientific research [14,20,38,75 and 86].

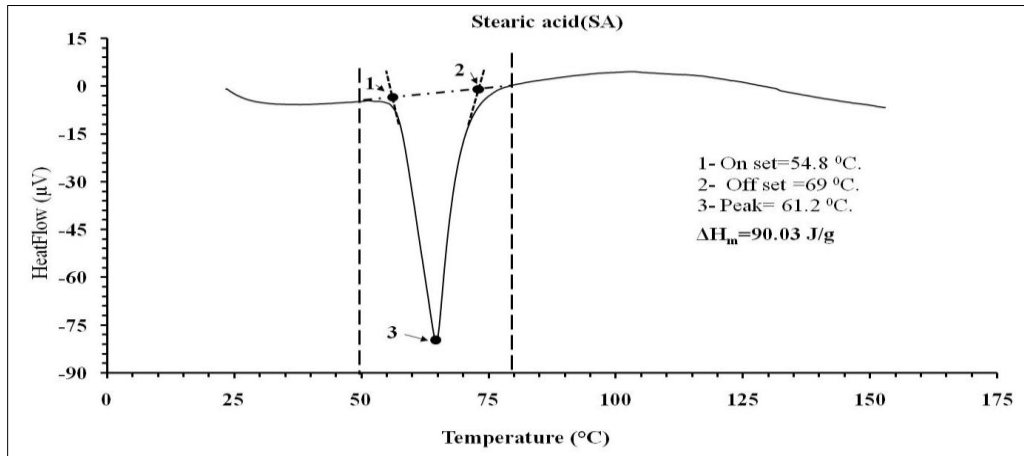


Figure (4-14): Heating Curve Has Taken During DSC Test for The Stearic Acid (SA) Sample.

Anyway, the Virgin RB sample DSC curve with this stable characteristic refers to no occurrence for any restriction process for the strain-induced crystals after removing the applied load in step3, and that this material does not have the ability to restrict the mechanically deformed elastically network during the first part of the shape memory cycle; thus, it is not considered as a shape memory smart material.

So that, the direct responsible for restricting the strain-induced crystals is the presence of Stearic acid (SA), so, it was found that the heat fusion, ΔH_f required for the phase change in RB/based SA material after SME property activation is more than it is in the case of deactivating the SME property, which is shown in Figures (4-13),(4-15) and (4-16). Where this increase in the heat fusion, ΔH_f is attributed to melting of SA crystals in addition to the removal of restricted strain-induced crystals (SIC), where there is a direct relation between the heat fusion and the degree of crystallinity, and these results are consistent with the findings of the researchers (Y.Y.Kow) et al. [75], and (F.Xie) et al. [20].

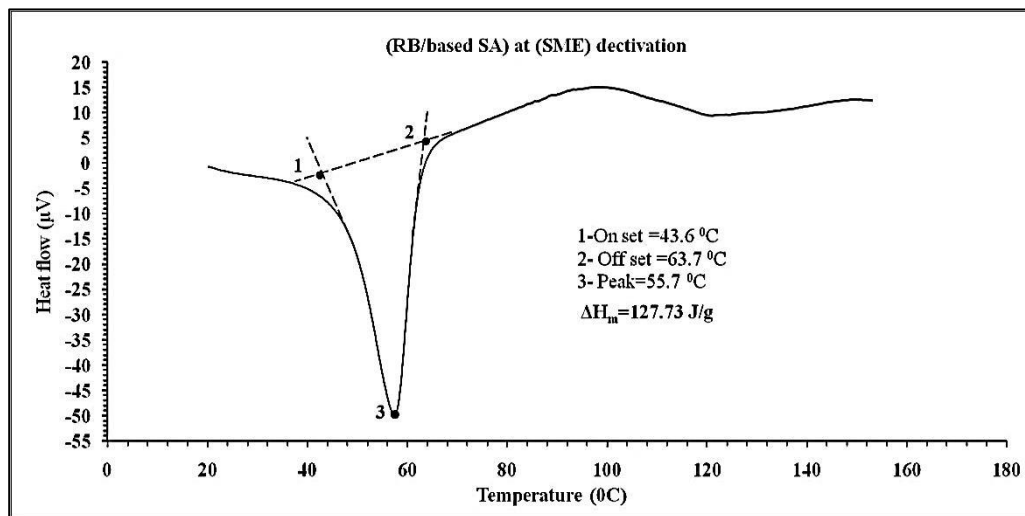


Figure (4-15): The Heating Curve Taken During DSC Test of (RB/based SA) Sample After (SME) Property Deactivation.

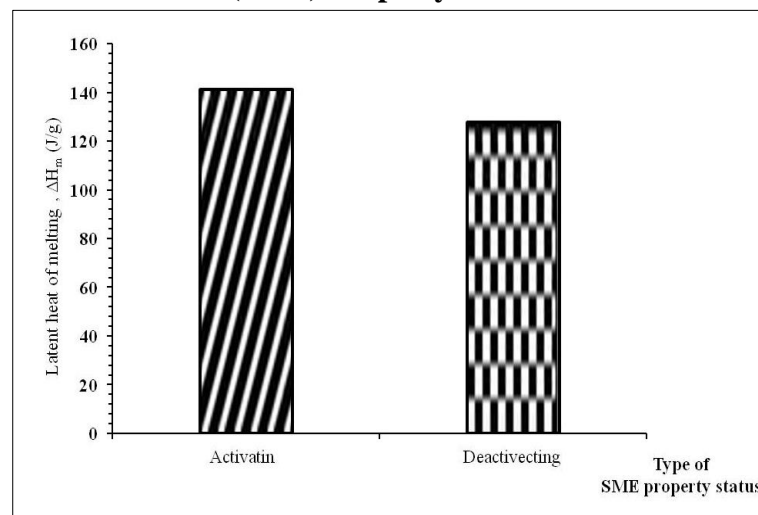


Figure (4-16): The Effect of The Latent Heat of Melting, ΔH_m in The SME Property State.

4-3-2 X-ray Diffraction (XRD) Patterns Examination

The results of XRD examination in Table (4-2) obtained from the diffraction patterns shown in Figures (4-17) and (4-18) using the Williamson-Hall and Debye-Scherrer equations according to the Vesta software program, showed that the degree of crystallinity of the RB/based SA that subjected to a SME property activation stage during the hot classical shape memory cycle, is of higher value than that of the sample but after being subjected to the SME property

deactivation stage. Therefore, the important question here: is the degree of crystallinity of the (RB/based SA) sample after being subjected to the deactivation stage (i.e. removing the mechanical deformation), an indication of the disappearance of the strain-induced crystal layers? The answer immediately, yes. The common phenomenon that occurs to natural rubber is the entangling of this rubber type elastic networks with each other to undergo the crystallization process, by forming the aforementioned strain-induced crystal layers during mechanical deformation, which quickly disappear after removing the applied load by the reaction force of the natural rubber network sulfur bonding entangling (cross-linking), which leads to its return to the equilibrium shape. That what was happened to the non-impregnated with SA Virgin RB sample, this means that SA in the rubber band impregnated with it has played the role of a lock that can be closed on the mechanically deformed shape by the aforementioned SME property activation stage, also to be opened by SME property deactivation stage This agrees with the reference [14]. Thus, RB/based SA material of activated SME property is characterized by two types of crystallization sources, which are:

- Strain-induced crystals restricted by SA network freezing during the SME property activation stage.
- Bi- crystalline layers of Stearic acid (SA) network.

Table (4-2): X-ray Diffraction Parameters of The Sample RB/based SA of Activated and Deactivated SME Property.

Type of SME property status	Lattice parameters						Unit – cell volume (\AA^3)	Degree of crystallinity (%)	Crystallite size (nm)	Dislocation density	Micro-strain	Type of unit cell
	a	b	c	Alpha (α)	Beta (β)	Gama (γ)						
Activation	16.1512	4.3389	11.5146	90°	99.368°	90°	796.11	67	19.712	0.25735_4	0.09164_2	Monoclinic $a \neq b \neq c \neq \alpha = \gamma = 90^\circ$ $\beta \neq 120^\circ$
Deactivation	7.24931	11.08430	8.16133	$90^\circ.0000$	109.0862°	90.0000°	619.740951	47	39.849	0.0629	0.006165	

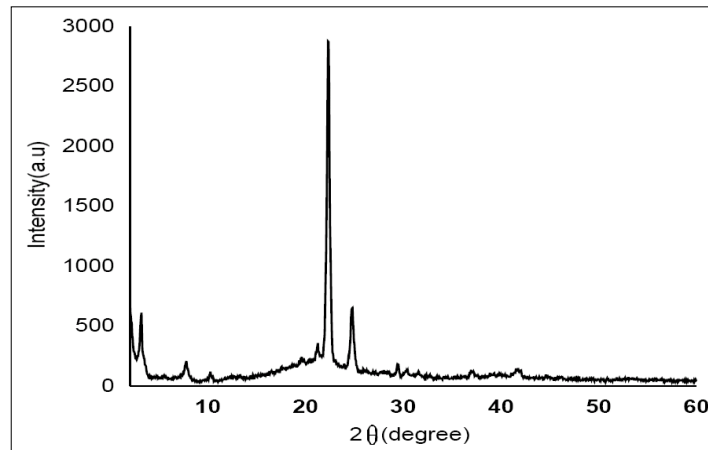


Figure (4-17): X-ray Diffraction Curve of RB/based SA Sample of Activated SME Property.

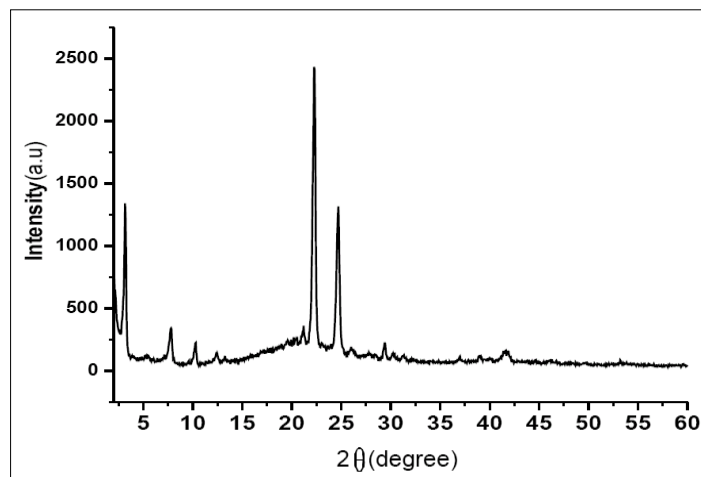


Figure (4-18): X-ray Diffraction Curve of RB/based SA Sample of Deactivated SME Property.

These crystallization sources work side by side in increasing the x-ray diffraction during the XRD examination. This diffraction increase is translated into an increase in the degree of crystallinity from the data of the Figure (4-17), if it was compared to the x-ray diffraction when the strain-induced crystals disappear after the SME property deactivation stage, Figure (4-18). As shown by the results of XRD examination, as shown in Table (4-2), the RB/based SA sample of activated SME property has the same unit-cell type after SME deactivation, where there is no difference in both stages, the composition of the unit cell is of a monoclinic type ($\alpha \neq b \neq c$, $\alpha = \gamma = 90^\circ$, and $\beta \neq 120^\circ$), but the difference was clear in

some results of the XRD examination that confirm the aforementioned facts about the formation of strain-induced crystals during the SME property activation stage and their disappearance during the SME property deactivation stage, which are:-

- The unit-cell size of the sample after the SME property activation stage is greater than the unit cell size of the sample after the SME property deactivation stage.
- The degree of crystallinity of the sample after the SME property activation stage is greater than the degree of its crystallinity after the SME property deactivation stage.
- Crystallite size of the sample after the SME property activation stage is less than the crystal size in the sample after the SME property deactivation stage.

Moreover, among the data of the XRD examination is the determination of the value of dislocations density and micro-strain as shown in Table (4-2), which indicate the presence of non-reversible permanent deformations in the (RB/based SA) body. Where the dislocations density and micro-strain in the sample after the SME property deactivation stage is less than they were after the SME property activation stage, and this result is consistent with the fact shown by Figure (4-9) from the accumulation of part of the applied strain in the form of non-reversible, permanent, plastic strain in step4 of the hot classical shape memory cycle. Generally, these results agree with the findings of the scientific research [14,16].

4-4 The Role of the Melting and Crystallizing of the Stearic Acid Network in Retaining and Releasing the Mechanical Deformation Energy

From the Figure (4-19), several points can be summarized:

- As it showed by Figure (4-19-a), applying stretching stress of the value (105.3KPa) in (step1) easily formed a strain estimated by 70% when heating the (RB/based SA) sample in (step0) to a temperature (75°C) which is higher than SA melting point, that is 69.3°C, as shown in Figures(4-19-b) and (4-19-d). This attributed to the change of the SA network from crystalline to molten state in the sample body, this result is in agreement with the references [10,18,22].
- As shown in the Figures from (4-19-a) to (4-9-d) the temperature decrease of the mechanical deformed (RB/based SA) material from 75°C to room temperature, under the conditions of the continuous application of the stretching load in (step2), that leads to the transformation of the SA from the molten to the crystalline state in the body of (RB/based SA). Thus the crystallization of the SA network leads to the freeze of the deformed configuration of the (RB/based SA) who is still under the influence of the applied load. As agrees with the reference [18,23,75 and 85].

As referred by the references [74,85], maintenance process of the SMP in a mechanical deformation state, necessitates maintaining two thirds (2/3) of the stored applied load Accordingly, for the mechanical deformation residue in step3 after the removal of the applied load, (70.2KPa) must be maintained of (105.3KPa) as the stored applied stress in the sample body, for restricting the rubber band cross-linking entropic recovery force.

So that, at the hot classical cycle, SA network crystallization and melting factors are correlated with the (RB/based SA) temperature, where the reversible phase is represented by SA network. Whereas the factor of the entropic recovery

force of the RB network (which indicates to the RB/based SA stable phase) is correlated with SA weight percentage, also with the SM cycle protocol used in this work. This agrees with the references [18,23,75,85].

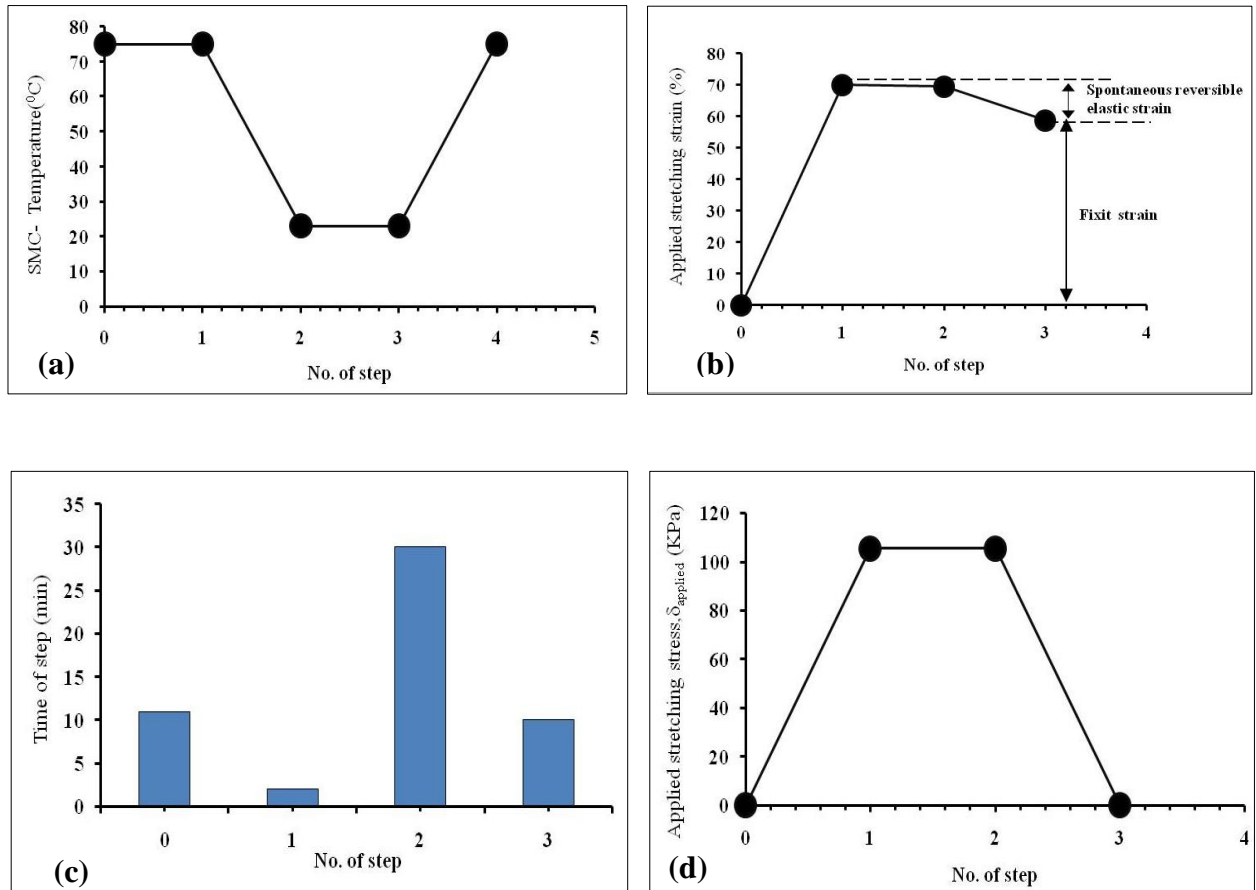


Figure (4-19): Represents the Profile of The Hot Classical Shape Memory Cycle Based on Room Temperature Natural Cooling for (RB/based SA). Where (a) Shows The Temperature Relationship, (b) Shows The Stress Relationship, (c) Shows The Time Relationship, and (d) Shows The Stress Relationship, With The Number of The Programming Stage Steps of The Shape Memory Cycle Followed.

Figure (4-20) shows FE-SEM characterization image of Stearic acid (SA) after freezing, where it is representing the natural rubber particles coated by bi-layers analogous platelet crystals, this agrees with the references [10,18,23,26,75 and 85].

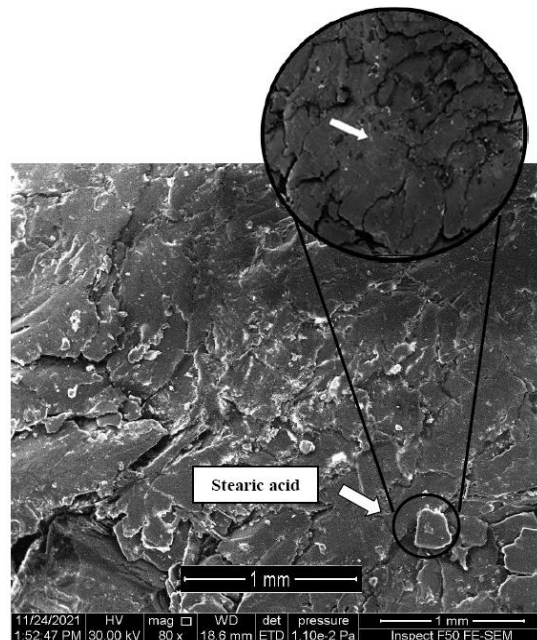


Figure (4-20): FM-SEM Image of The Surface of (RB/based SA) That Appears in The Form of Bit Layers' Analogous Platelet Crystals of SA Material Coating the Rubber Band Molecules in Their Crystalline State.

As shown earlier in Figures (4-19-a) and (4-19-b), it can be noticed during the process of transition from step1 to step2, the domination of the temperature change view from 75°C to room temperature. This ending to a part loss of the applied internal stretching work energy (W_I), because of the occurrence of the thermal contraction phenomenon, as clear in Figure (4-21). On the other side, the emergence of the elastic contraction phenomenon (as indicated by Figure (4-21)) through the process of transition from step2 to step3 is attributed to the Stearic acid weight percentage utilized in the (RB/based SA) preparation, which reached (30.4%) when swelling time was (2hr). The occurrence of these phenomena do not permit the completion of the entropic recovery force movement restriction, this result is in agreement with references [10,26,59,85 and 90].

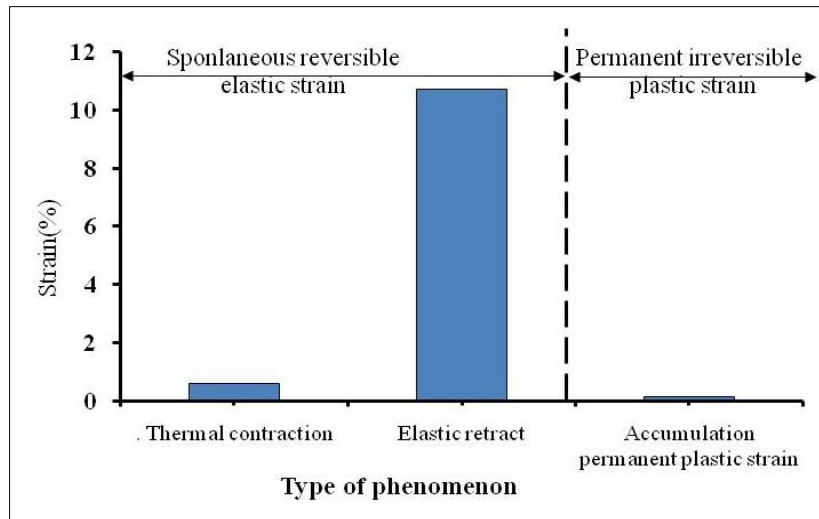


Figure (4-21): The Physical Phenomena Accompanying The Programming Stage of The Hot Classical Shape Memory Cycle of RB/based SA.

So that, the way for the applied strain (meant to be fixed) decreasing is briefed in releasing a part of the strain which is represented as spontaneous elastic strain in addition to the non-desired physico-mechanical phenomena through the deformed shape programming stage of the hot classical cycle (activation of the SME property). Consequently, in this cycle the real retained applied strain value was (58.7%) instead of (70%), as shown in Figure (4-22).

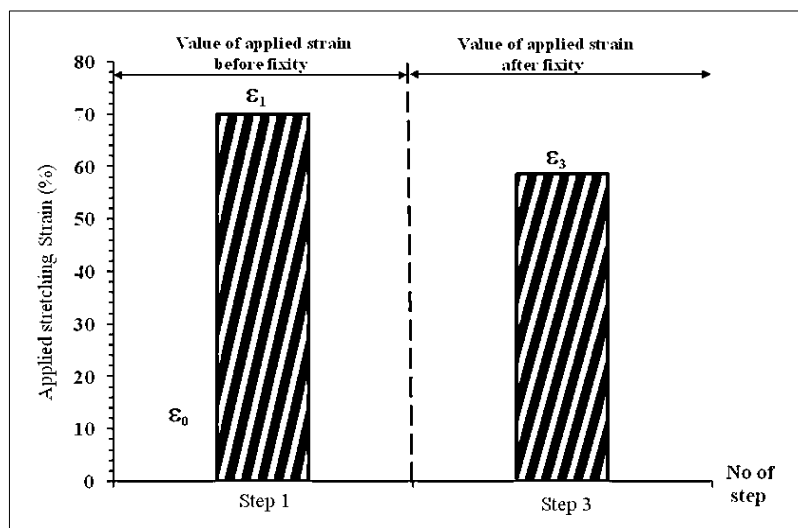


Figure (4-22): The Difference in The Value of The Applied Strain That is Fixed in Step3 From its Actual Value Applied in Step1 During (RB/based SA) Deformed Shape Programming Stage in The Hot Classical Thermomechanical Cycle Based on Normal Cooling at Room Temperature.

Contrariwise, the fixity of this strain in the deformed shape, which named “fixed temporary shape”, may last forever except when the Stearic acid network is stimulated to move from crystalline to molten state. Figure (4-23) shows the moment after (RB/based SA) gradual reheating, starting from room temperature and ending to 75°C again. The fixed strain will fade gradually through the stage of recovery as a result of SA network re-melting which permits for the network of the mechanically deformed rubber band to be back to its original molecular architecture con Figure ration that was in before deformation nearly by a ratio equal to ($R_r=99.7\%$). This is attributed to the material tendency to pile up the non-reversible permanent plastic strain in its body during the deformation stage in step1, as seen before in Figure (4-21).

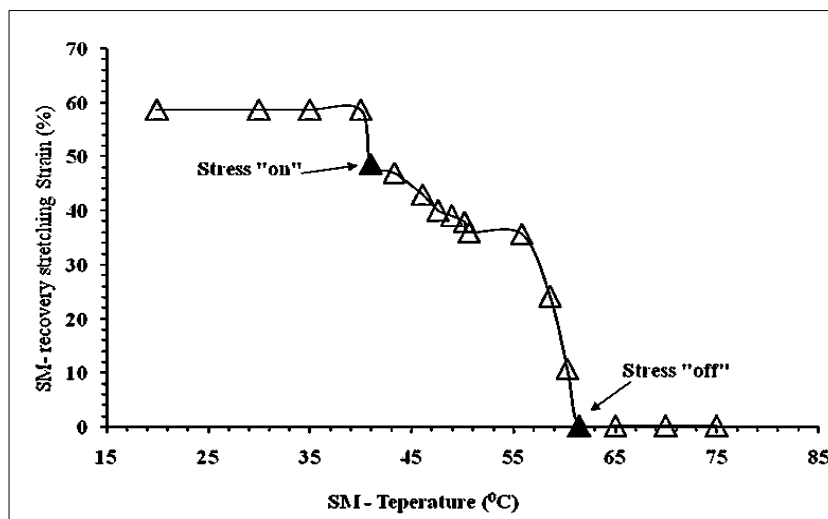


Figure (4-23): The Relation of The Shape Memory Recovery Strain (Retained Strain) to The Shape Memory Recovery Temperature (SM-Temperature).

Figure (4-24) refers to the (RB/based SA) molecular architecture con Figure ration accompanied by photographs of it prior to the mechanically deformed shape programming having the shape denoted by “shape A”, and after the programming stage in step3 taking the shape denoted by “shape B” after removing the load. The sample is back to its original form (shape A) during

reheating in (step 4) with slight difference because of the occurrence of the non-reversible permanent plastic deformation.

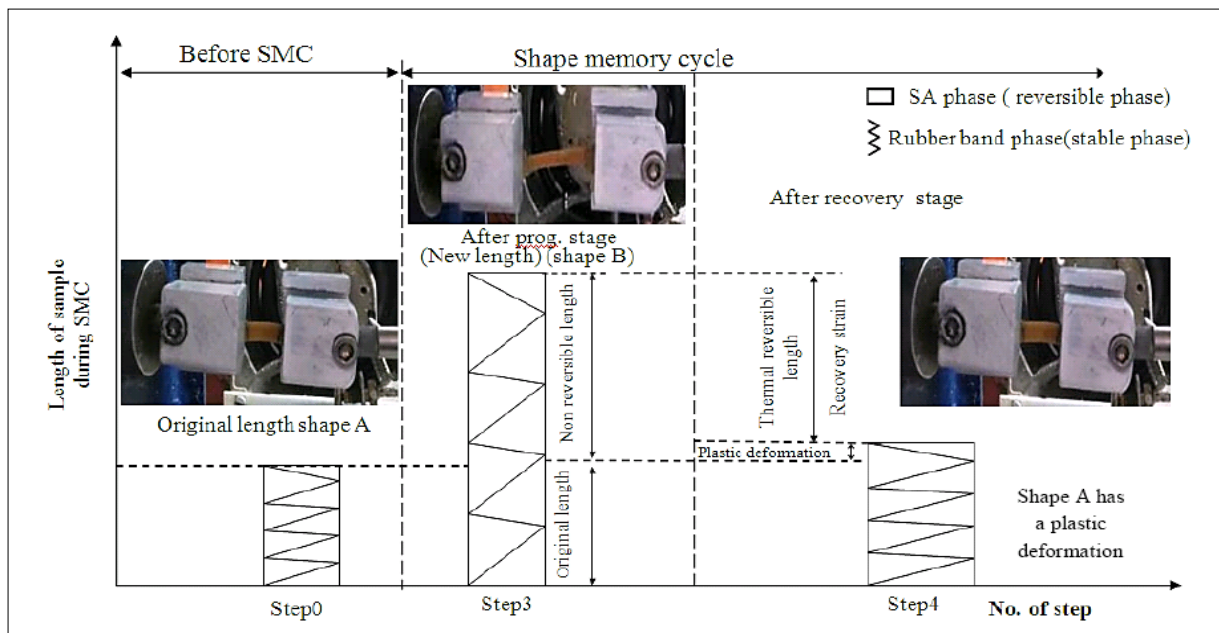


Figure (4-24): The Analytical Framework for The Change of Molecular Architecture Con Figure Ration for RB/based SA During the Hot Classical Thermomechanical Cycle Based on Normal Cooling at Room Temperature.

Mostly, the SME property is evidenced by forming the “shape B” in (step3) after removing the load, after that the sample returned to its initial shape “shape A” in (step4) but with slight difference.

Therefore, it can be indicated that the applied strain can be divided into three classes in step1 during the shape memory cycle as the following:

The first class: it is named as the “frozen elastic deformation “that can be reversed by thermal stimulation to the SA freezing phenomenon on the network of the mechanically deformed rubber band.

The second class: it is named as the “elastic deformation” that reversed spontaneously, attributing to the phenomena “elastic retraction “and “thermal contraction”.

The third class: it relies on the material nature, denoted as “non-reversible permanent plastic deformation” because of the plastic strain accumulation. It can be seen from Figure (4-25), the frozen elastic strain is the cause for continuing the (RB/based SA) material temporarily deformed shape after the applied load removal. By this strain formation, the first purpose of the SMC (shape memory cycle) is reached. On the other hand, the second purpose of SMC is reached by one of the external stimulating methods such as hot air as it is followed in the present study the elastic strain releasing through untying the freezing of the entropic recovery force by the ridding process of the stored tensile stress (the material here becomes in state of stretching), this process is accomplished by the melting of the Stearic acid crystals, by so, the material has recovered its original shape, this is shown by Figure (4-26).

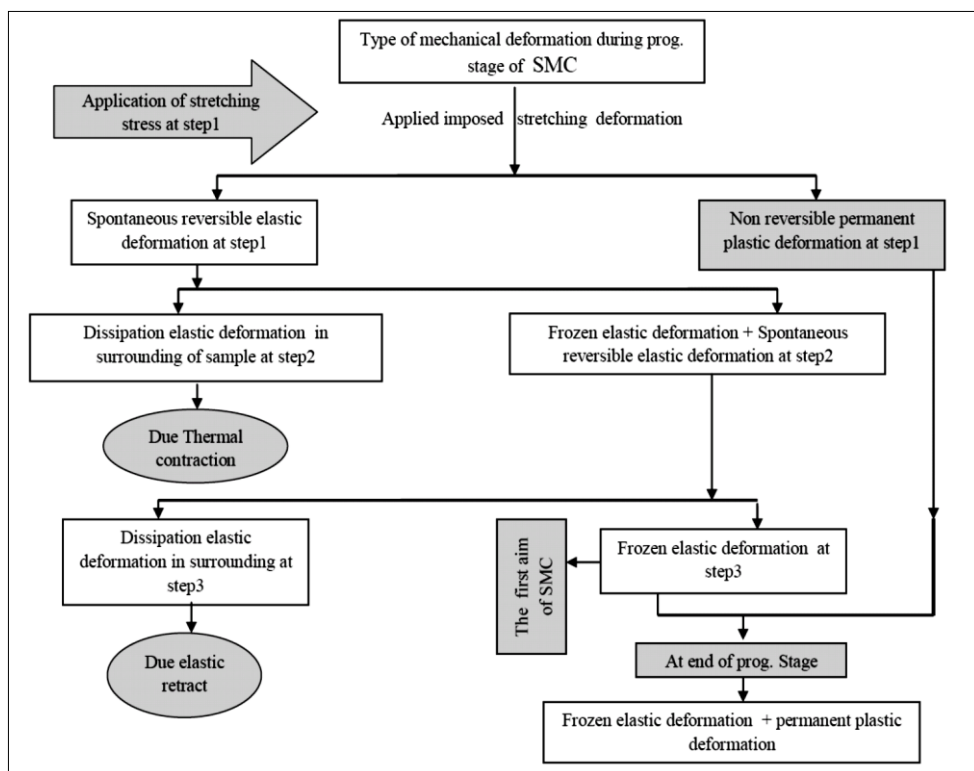


Figure (4-25): A Schematic Diagram of The Applied Strain Retention Process in The RB/based SA Material After Completion of The Programming Stage of The Hot Classical Shape Memory Cycle.

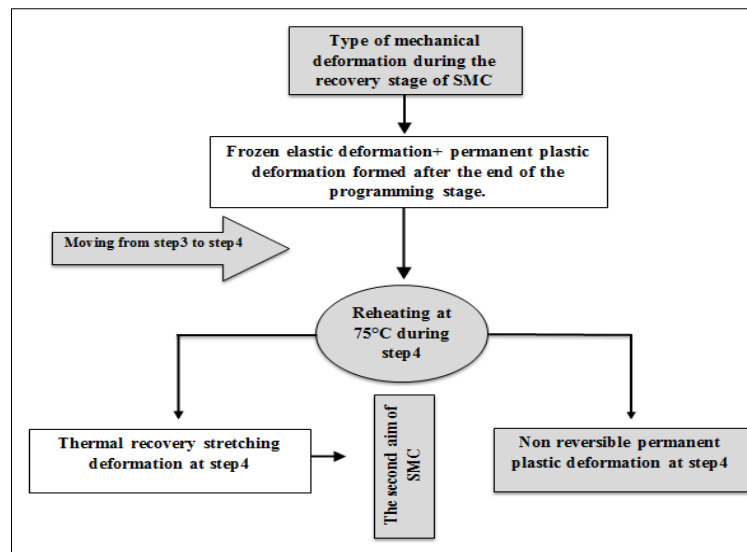


Figure (4-26): Schematic Diagram of The Strain Releasing Process From The RB/based SA Deformed Shape into Its Surrounding Medium During The Recovery Stage of The Hot Thermomechanical Cycle.

This agrees with the results of Ingrid and others, which clarify that the SM material shape recovery and fixity are controlled by the strain that depends on strain relaxation, thermal contraction, and spontaneous elastic recovery [59].

So that, Figure (4-27) demonstrates that the main condition for a material to have the property of continuing on a temporary mechanical deformation state and recovering its original shape again (the shape it was on prior to the mechanical deformation) is its capability to store and release the elastic elongation work energy through thermal stimulation. Where it is a positive relation between the elongation work energy, applied in (step1) (wanted to be fixed in the temporarily deformed shape) and the elastic elongation work energy frozen as a result of the freezing of (SA). Nevertheless, the practical achievement of the classical SMC in applied elongation work energy storing as spontaneous non-reversible storing still not reaching the goal, because of the physico-mechanical phenomena resulted with the hot classical SMC, which have negative relation with the applied elongation work energy [15,55 and 59].

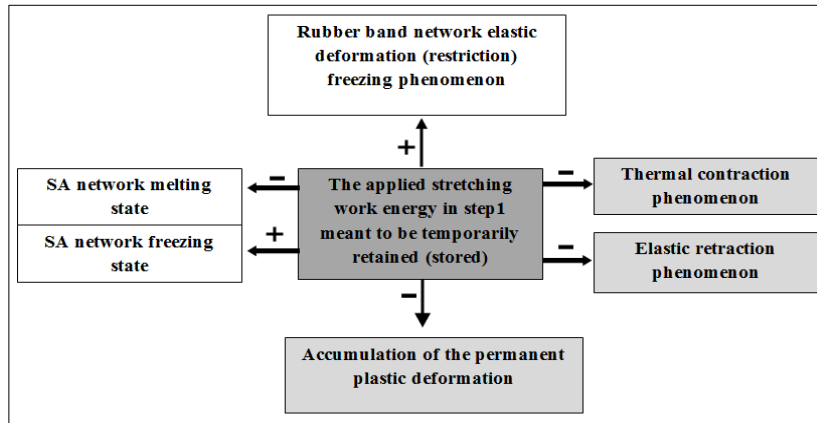


Figure (4-27): Schematic Diagram of The Practically Observed Physico-Mechanical Phenomena During The Hot Classical Shape Memory Cycle and Their Relation to The Applied Elongation Work Energy Meant to be Retained. (+) Positive Role, (-) Negative Role.

Figure (4-28) shows that the elastic retraction, thermal contraction, and permanent plastic strain accumulation phenomena are practically classified from this current study as the phenomena that reduce the applied stretching energy meant to be temporarily retained from (73.71 KJ/m^3) to (61.65 KJ/m^3) and efficiency of elastic strain energy $\eta=83.6\%$. Also, the applied stretching energy of the quantity (12.06 KJ/m^3) , is considered as not temporary restricted according to the hot classical shape memory cycle steps. This part of the stretching work energy is lost as dissipated energy in the (RB/Based SA) structure as an irreversible permanent plastic deformation and as the energy dissipated to the surrounding medium of this material. Figure (4-28) shows that the applied mechanical work energy can be divided into several sections according to its images in the followed thermomechanical cycle, as follows:

1- Elastic strain energy lost by the spontaneous reverse in the surrounding medium, $W_{D,E}$ by [15,55 and 59]:

- **Thermal contraction**

$$W_{D,E} (\text{due thermal contraction}) = \delta_1 \times (\varepsilon_1 - \varepsilon_3) (\text{KJ/m}^3) \dots (4.1)$$

- **Elastic retraction**

$$W_{D,E}(\text{due elastic retraction}) = \delta_1 \times (\varepsilon_2 - \varepsilon_3) (\text{KJ} / \text{m}^3) \dots (4.2)$$

2-The internal energy consumed by the sample deformation is [15,55 and 59]:

- Plastic dissipation energy, $W_{hardening}$ by the plastic strain.

$$W_{plastic} = \delta_1 \times \varepsilon_4 (\text{KJ} / \text{m}^3) \dots (4.3)$$

ε_4 : Non-reversible permanent strain at deformation temp (residual strain).

- The elastic strain energy is recoverable by the thermal stimulation (frozen elastic strain, W_{frozen}).

$$W_{frozen} = \delta_1 (\varepsilon_3 - \varepsilon_4) (\text{KJ} / \text{m}^3) \dots (4.4)$$

ε_4 : is the recovery strain at a particular temperature.

This means that each step of the shape memory cycle steps is one of the applications of the energy conservation law. The first step includes the energy consumed by the sample deformation, W_I , which is:

$$W_I = W_{plastic} + W_{sp1} \dots (4.5)$$

W_{sp1} : is the spontaneous recoverable elastic strain energy. This internal energy, W_I became in the second step of the cycle (which includes the cooling process) as follows:

$$W_I = W_{plastic} + W_{sp2} + W_{D,E}(\text{due thermal contraction}) \dots (4.6)$$

W_{sp2} ; is the spontaneous reversible elastic strain energy-reduced after the occurrence of the thermal contraction.

In step3 (which includes the applied load removal), the internal energy consumed by the deformation is:

$$W_I = W_{plastic} + W_{frozen} + W_{D,E}(\text{due elastic retract}) \dots (4.7)$$

While in the last step of the shape memory cycle (which includes reheating the material to the deformation temperature (75°C), the internal energy consumed by the sample deformation at the deformation temperature is:

$$W_I = W_{plastic} \dots (4.8)$$

While the frozen elastic energy is transformed to a thermally recovered energy (SM-recovery elastic energy), that means the shape memory effect property is based on the frozen elastic strain energy, W_{frozen} , this agrees with the references[15,26,45].

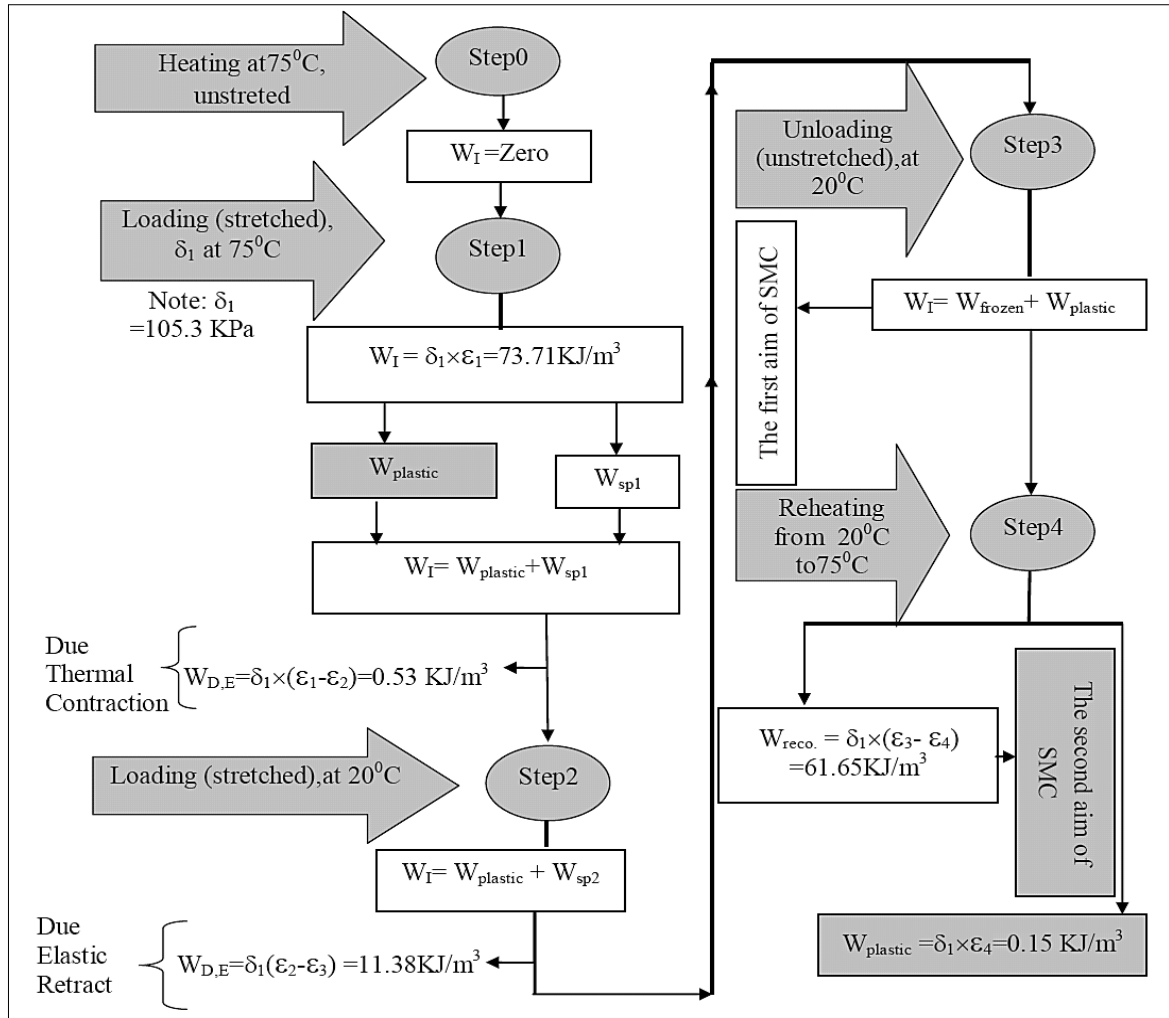


Figure (4-28): A Schematic Diagram Showing That The Stretching Work Energy is Neither Consumed Nor Regenerated During The Hot Classical Shape Memory Cycle, but is Transformed From One Form to Another.

Generally, the elastic stretching work energy that is restricted from spontaneous releasing (frozen elastic stretching work energy) will not be released from the RB/based SA material to its surrounding medium unless it is under temperature-controlled conditions.

Figure (4-29) shows that the first region of the shape memory recovery work energy curve (SM-recovery work energy) and shape memory recovery temperature (SM-temperature) has no change in the restricted elastic stretching work energy value. Also, the fixity continues until reaching the temperature of 41°C , where at this temperature, (RB/based SA) got rid of about (10.6 KJ/m^3) but it still retains (51.2 KJ/m^3) , When the temperature increasing continues, the material continues in ridding of the stored energy which causes to return it back to its original shape little by little until reaching to the second region end and as for the third region it represents a stage in which recovery steps.

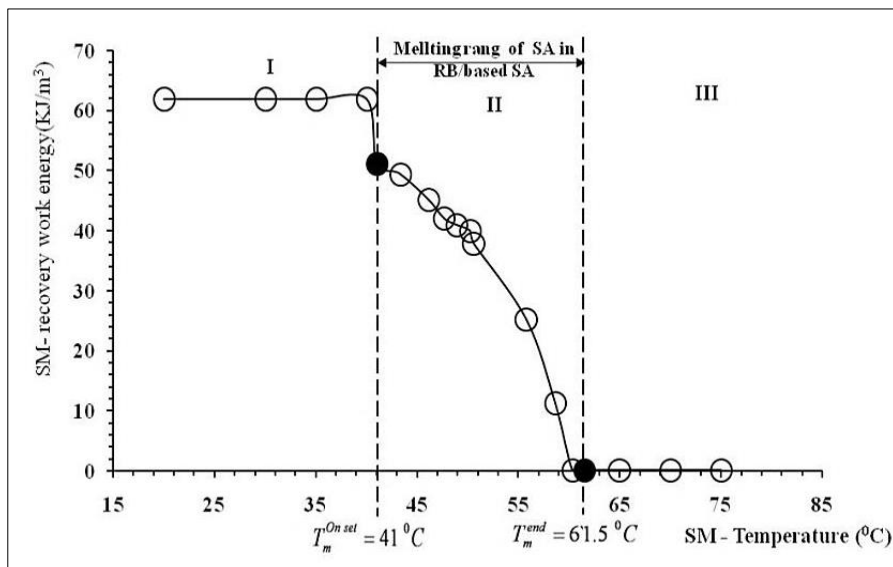


Figure (4-29): The Relation Between The Shape Memory Recovery Work Energy (SM-Recovery Work Energy) and The Shape Memory Temperature (SM-Temperature).

4-5 Demonstration of a Macroscopic Shape-Memory Effect (SME)

Property of the Smart Rubber Band

Figures (4-30) and (4-31) show how to macroscopically demonstrate by digital photography (videography) the SME property, that depends on photographic documentation of the original shape change of (RB/ based SA) impregnated for 2hrs with Stearic acid, represented by a straight-shape to a new shapes represented by long-strip shape, spiral-shape, and L-shape again by

the SME property activation process (programming stage) and returning to the initial shape by SME property deactivation process (the recovery stage).

Before the start of SMC		After the prog. Stage is over		During recovery Stage				After the recovery Stage is over	
Original permanent shape		Temporary shape		Stimulus	Recovery process			Recovered permanent shape	
Straight -shape		Spiral- Shape		Reheat in water at 75°C					
		t = 0s			t = 0s	t = 4s	t = 9s	t = 30s	
	Long strip -shape								
			t = 0s		t = 0s	t = 5s	t = 9s	t = 30s	

Figure (4-30): Digital Images Showing The Programming and Recovery Demonstration of The Macroscopic (SME) of (RB/ based SA).

Before classical shape – memory cycle type Hot		After the prog. Stage is over		During recovery stage		After recovery stage is over	
Original permanent shape		Temporary shape		Stimulus	Recovery process		Recovery permanent shape
L- Shape		U-Shape		Reheat in water at 75°C			
					t=5 s	t=10 s	t=30 s

Figure (4-31): Digital Images Showing The Programming and Recovery Demonstration of The Macroscopic SME of (RB/based SA).

4-6 Study of the Surface Shape Memory Effect (SME) of the Smart Rubber Band

Figure (4-32) shows the surface shape memory effect (SME) for a sample of rubber band impregnated with Stearic acid (RB/based SA) for a period of 2hr., by forming a temporary surface circular trace with a diameter of (8mm) with an irregularly dimensional hole in the center of this trace which showed by the macroscopic and microscopic images after the end of SME activation stage.

Figure (4-32) also shows that during the SME property deactivation stage, the circular trace disappears as it appears macroscopically. While the hole has gradually decreased in size with the increase in the recovery time from 0s to 30s, but it did not disappear completely after the completion of the SME property deactivation stage. As a result of the effect of surface shape memory effect property deactivation stage, by applying pressure up to (11.33 Kg) through the small contact area, it causes the formation of an elastic deformation followed by a permanent plastic deformation represented by the hole in the sample body (RB/based SA) that is not reversible by thermal stimulation during the SME property deactivation stage; because it is a rupture.

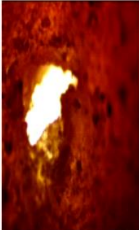
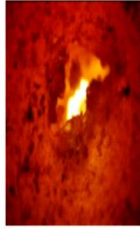
	Before the start of SMC	After the surface shape memory effect (SME) activation		Stimulus	During surface shape memory effect deactivation		After surface (SME) deactivation is over	
	Original permanent Surface shape	Temporary Surface spherical indentation			Recovery process		Recovered permanent surface shape memory	
		Macroscopic	Digital optical microscope		Macroscopic	Digital optical microscope	Macroscopic	Digital optical microscope
Surface without spherical indentation				Reheat up in water at 75°C				
		t = 0s	t = 0s			t = 15s		t = 30s

Figure (4-32): Photographic and Microscopic Images Showing The Activation and Deactivation of Surface SME.

4-7 Study of Factors Affecting the Smart Vulcanized Natural Rubber Shape Memory

4-7-1 Study the Effect of Stearic Acid Weight Percentage on the Shape Memory Behavior

Figures (4-33) to (4-36) showed an increment in both; the fixed strain (the restricted strain in the mechanically deformed shape) and the mechanically deformed shape fixity ratio for (RB/based SA) with an increment in the weight percentage of Stearic acid (SA wt%) after the completion of the (SME) property activation stage of the hot classical shape memory cycle. Furthermore, the results clarified in the Figures (4-37) and (4-40) have shown an increment in the non-reversible plastic strain accumulation, and a decrease in the original shape recovery ratio. Also, there was an increment in the swelling time as well as the Stearic acid percentage after the end of the shape memory cycle recovery stage.

The reason for that is that the increase in the period of the rubber band immersion in Stearic acid molten leads to increase the Stearic acid percentage in the commercial rubber band body, thus resulting in an increase in the switching phase that is responsible for retaining the elastic deformation. With switching phase increase, the elastic retraction phenomena decreases, which leads to an increase in the number of retained elastic effective chains. At the same time, an increase in the (SAwt%) percentage leads to an increase in the non-reversible plastic strain accumulation; due to a decrease in the recovery driving force or what is called the recovery entropic force, this is consistent with the references [10,33,75].

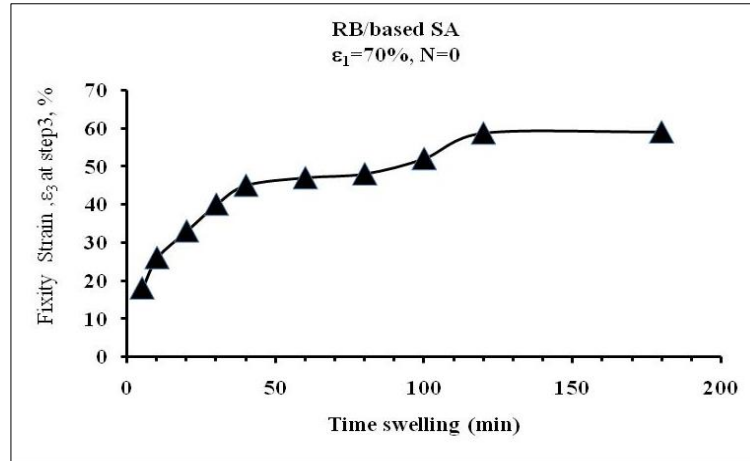


Figure (4-33): The Relation of The Fixed Strain in Step3 and The Swelling Time of (RB based/SA) in The Stearic Acid Molten.

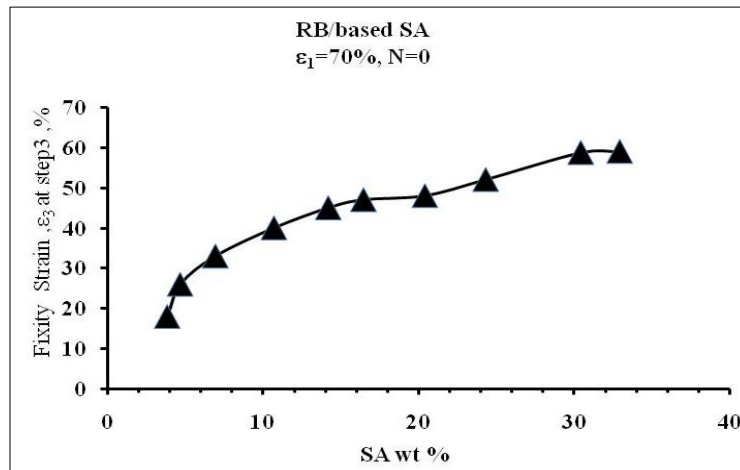


Figure (4-34): The Relation of The Fixed Strain in Step3 and Weight Percentage of Stearic Acid in The Material (RB based/SA).

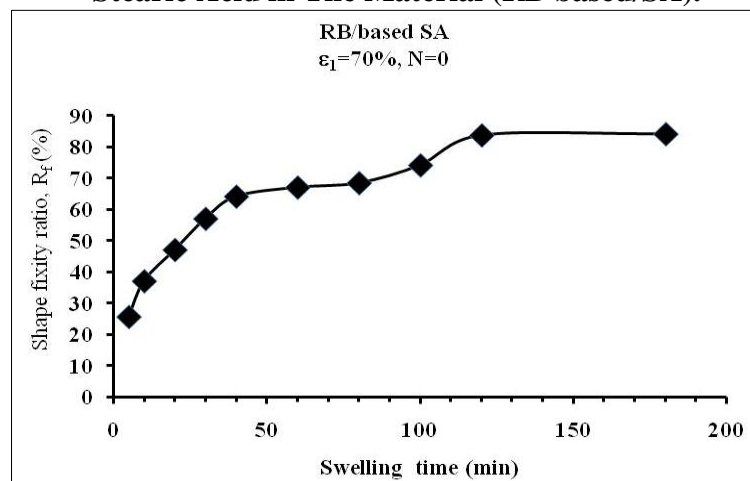


Figure (4-35): The Relation of The Shape Fixity Ratio and Swelling Time of (RB based/SA) in Stearic Acid Molten.

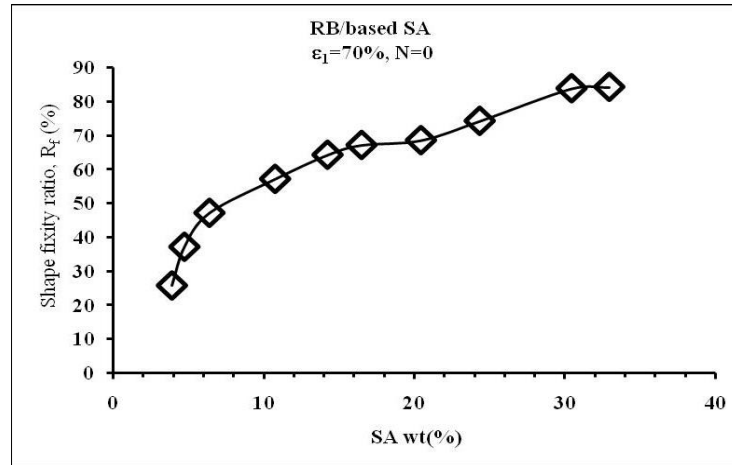


Figure (4-36): The Relation of The Shape Fixity Ratio With the Stearic Acid Weight Percentage in The (RB/based SA) Material.

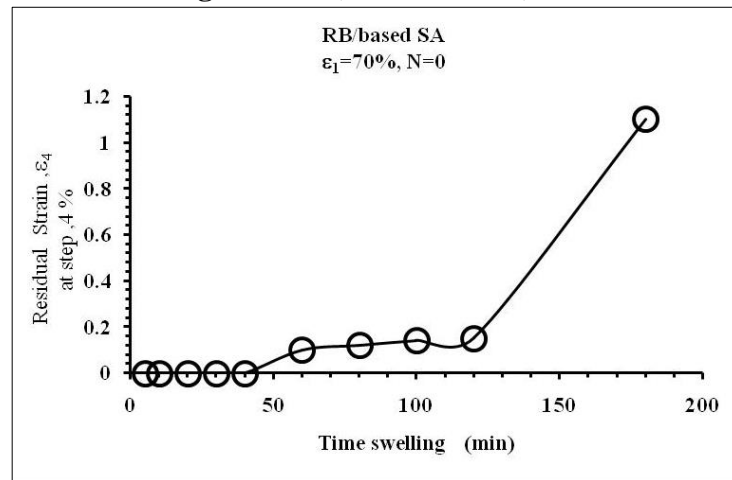


Figure (4-37): The Relation of Non-Reversible Plastic Strain With Swelling Time of The (RB/based SA) Material in Stearic Acid Molten.

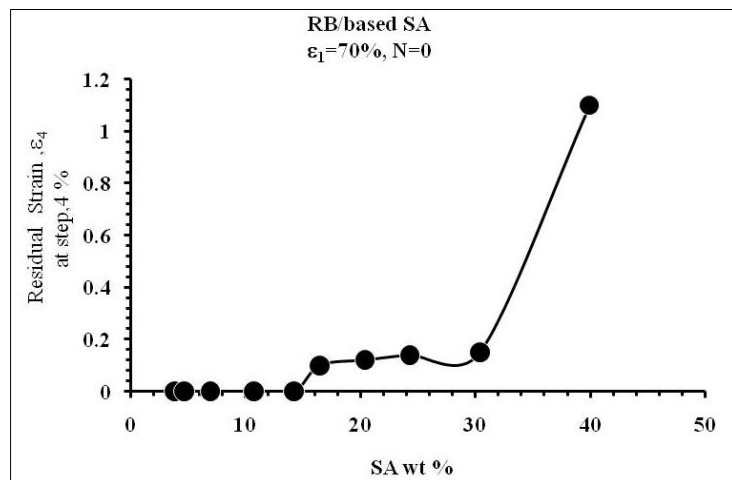


Figure (4-38): The Relation of The Non-Reversible Plastic Strain to The Stearic Acid Weight Percentage in The (RB/based SA) Material.

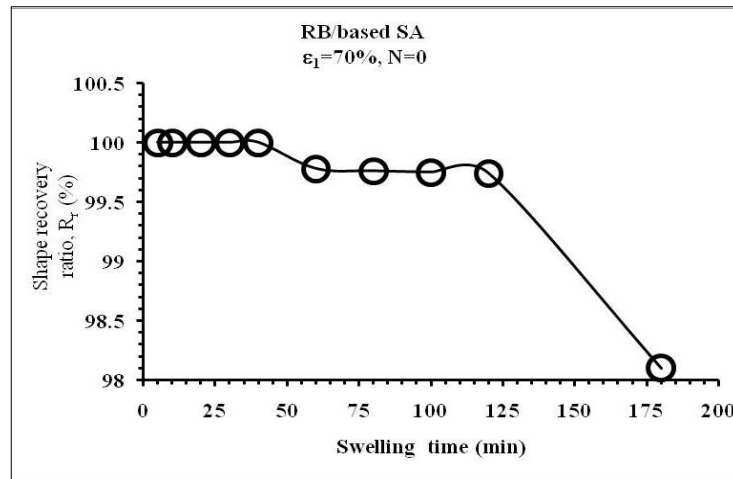


Figure (4-39): The Relation of The Shape Recovery Ratio to The Swelling Time of (RB/based SA) Material in Stearic Acid Molten.

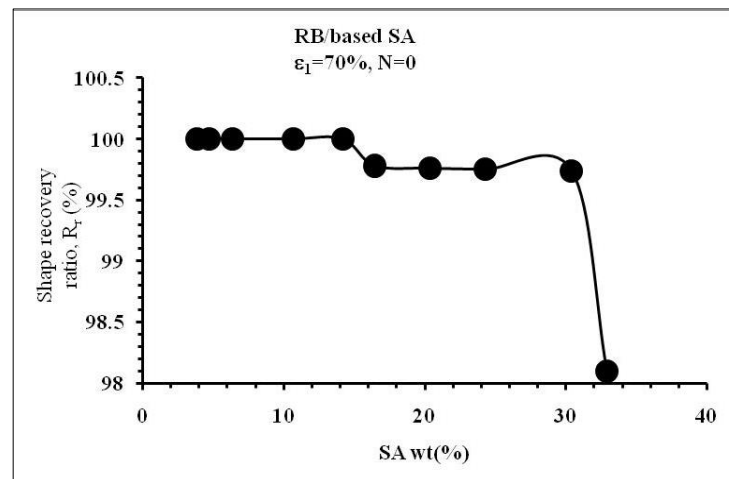


Figure (4-40): The Relation of The Shape Recovery Ratio to The Weight Percentage of Stearic Acid in (RB/based SA) Material.

Regarding the Figure (4-41), they show that the shape memory behavior improves with the increase in the stearic acid percentage. In general, the SM-behavior of RB/based SA can be classified according to the results shown) in Figure (4-41) in comparison with the ideal SM-behavior in which ($R_f = R_r = 100\%$), follows: -

- 1-SM-behavior is poor when $SM\text{-index} \leq 0.5$.
- 2-SM-behavior is good when $0.5 < SM\text{-index} \leq 0.7$.
- 3-SM-behavior is very good when $0.7 < SM\text{-index} \leq 0.8$.
- 4- SM-behavior is excellent when $SM\text{-index} > 0.8$.

5- SM-behavior is ideal when SM-index =1.

This classification is in agreement with the references [59,94]. So that, optimum shape memory properties are obtained when the swelling time is 120min.

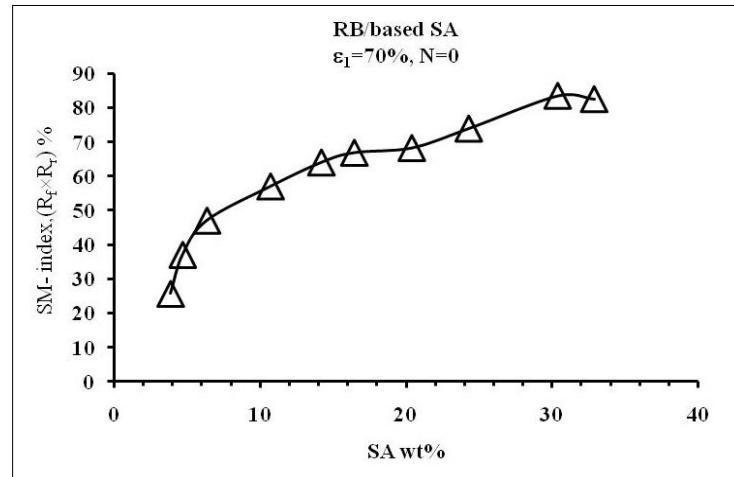


Figure (4-41): The Relation of The SM- index to The Stearic Acid Weight Percentage in (RB/based SA) Material.

4-7-2 Studying the Effect of the Imposed Applied Strain on the Behavior of Shape Memory

Figures (4-42) and (4-43) showed an increase in both the fixed strain in step 3 and the shape fixity ratio, R_f of (RB/based SA) after the SME activation stage has ended, with an increase of the applied strain in step1. Also, the results clarified in Figures (4-42) and (4-44) have showed an increase in the permanent plastic strain accumulation in step4, as well as a decrease in the original permanent shape recovery ratio, R_r with an increase in the applied strain in step1. The reason for this is due to the decrease in the number of elastic effective chains to be retained, especially at high strains, which leads to a decrease in the driving force for recovery, and this is consistent with the references [10,23,33,65].

As for Figure (4-45), it was found that there are no significant differences in the behavior of shape memory within this range of applied strains.

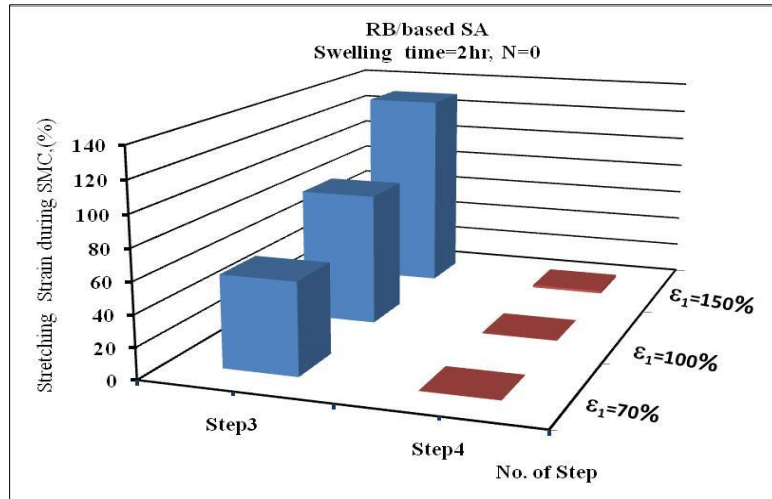


Figure (4-42): The Relation Between The Tensile Strain Measured During The Shape Memory Cycle, and The Number of Steps of The Shape Memory Cycle.

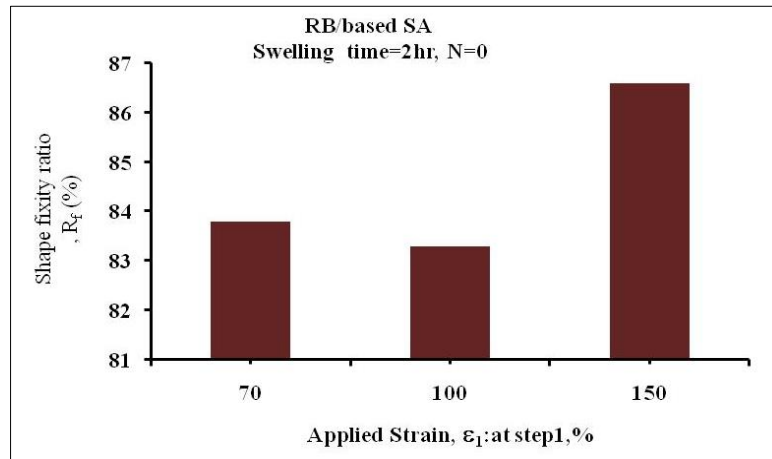


Figure (4-43): The Relation Between The Tensile Strain Measured During The Shape Memory Cycle, and The Number of Steps of The Shape Memory Cycle.

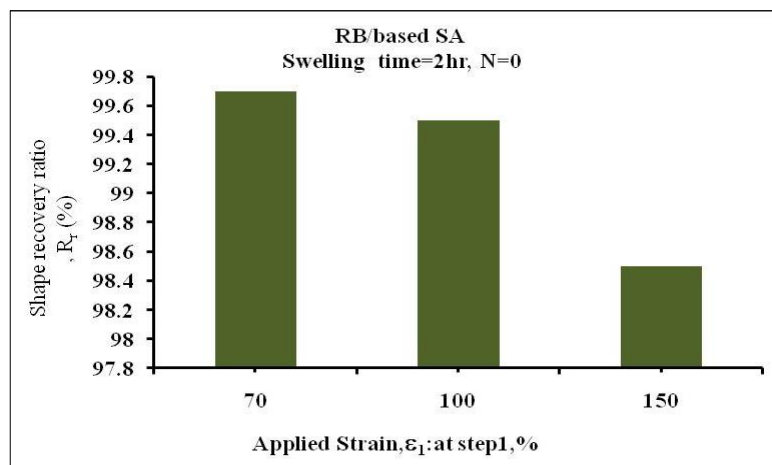


Figure (4-44): The Relation Between The Shape Recovery Ratio of (RB/based SA) and The Strain Applied in Step1.

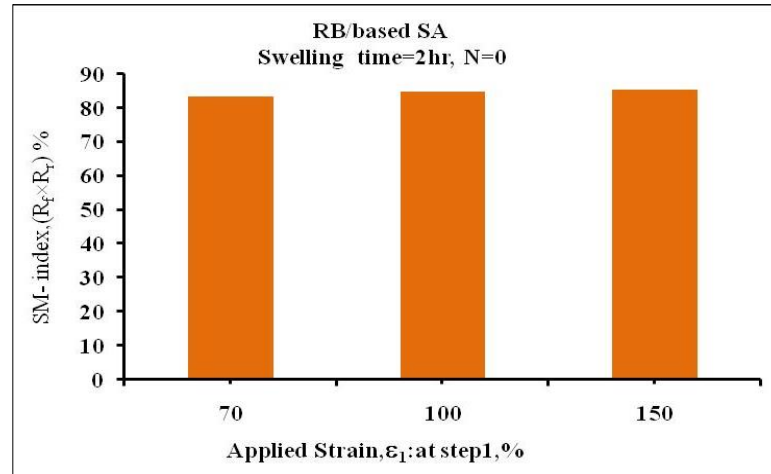


Figure (4-45): The Relation Between The SM-index of (RB/based SA) and The Strain Applied in Step1.

4-7-3 Studying the Effect of Shape Memory Cycle Number on Shape Memory Behavior

The results shown in Figure (4-46) indicate that the Stearic acid weight percentage (SA wt%) after the end of the shape memory cycle No. (N=0), has decreased from 30.4% to 30.27%; while this value decreased to 30.09% with an increase in the number of shape memory cycles from N=0 to N=1, according to following equation[23]:-

$$wt\% \text{ difference} = \frac{|wt_o - wt_n|}{0.5(wt_o + wt_n)} \times 100 \dots (4.9)$$

Where:

wt% difference: It is weight percent difference from the original weight.

wt_o and wt_n correspond to the sample's initial and nth cycle weight respectively.

The decrease in the value of Stearic acid weight percentage in the body of (RB/based SA) with the increase of the shape memory cycle number represents the amount of Stearic acid that is expelled from the body of (RB/based SA). This is due to the occurrence of the “Wax blooming” phenomenon, that is exacerbated during rapid shrinkage when moving from high temperature to low temperature

and back, rapidly, during the shape memory cycle by its two stages in order to reduce the strain generated by swelling.

As for the Figures (4-47) and (4-48), they show decrease in both; fixity strain in step 3 as well as shape fixity ratio with the increase in the number of shape memory cycles. The reason for this is due to the fact that decreasing the value of Stearic acid weight percentage (SA wt%) with the increase in the number of shape memory cycles leads to a decrease in the ability to restrict the movement of the entropic recovery force in step2 of the SME property activation stage, and an increase in the value of the spontaneously released elastic strain in step3 after the applied load removal due to the “elastic retraction phenomenon”. While Figure (4-51) shows that the permanent plastic strain accumulation increases with the increase in the number of cycles, this in turn reduces the ability of (RB/based SA) material to recover its permanent original shape, this is what shown by Figure (4-50).

While the Figure (4-51), show that the shape memory behavior (SM-behavior) of (RB/based SA) material can be described as good and very good, respectively, after three shape memory cycles have passed, and that these results are in agreement with what was reached by the references [10,15,23,26,33,59].

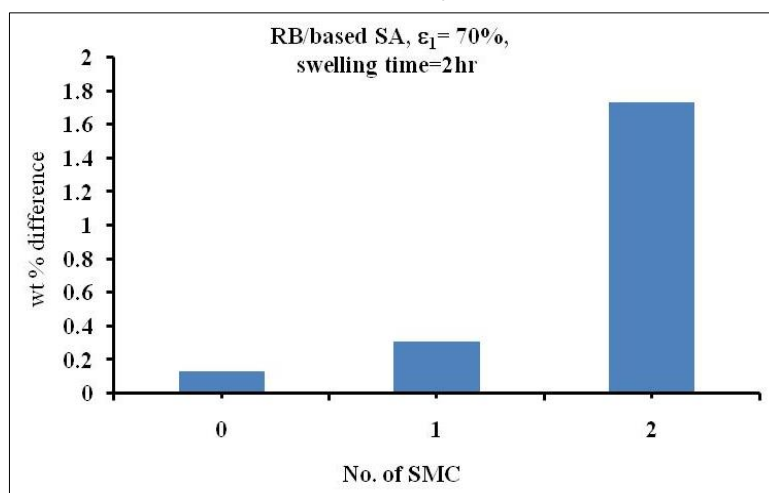


Figure (4-46): The Relation of The Stearic Acid Weight Percentage Difference With The Shape Memory Cycle Number.

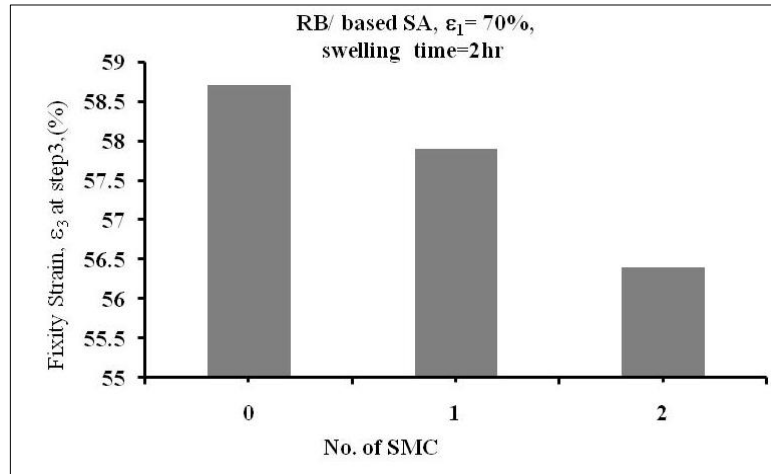


Figure (4-47): The Relation of The Fixity Strain in Step3 With The Shape Memory Cycle Number.

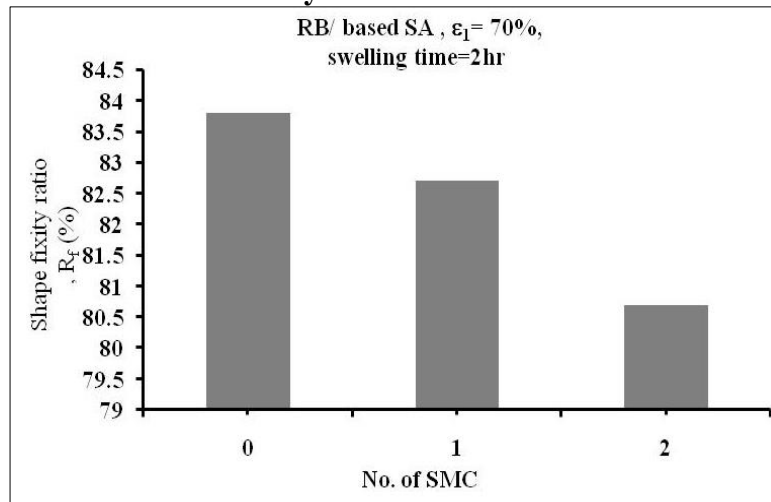


Figure (4-48): The Relation of The Shape Fixity Ratio of The Mechanically Deformed Shape With The Shape Memory Cycle Number.

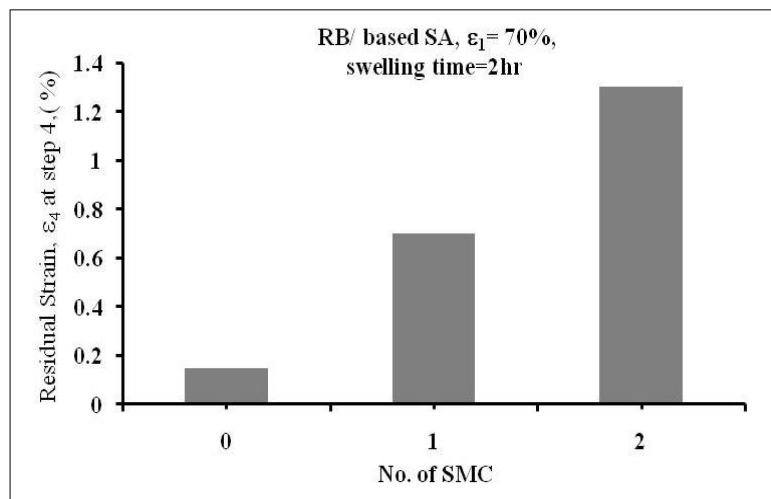


Figure (4-49): The Relation of The Permanent Plastic Strain With The Shape Memory Cycle Number.

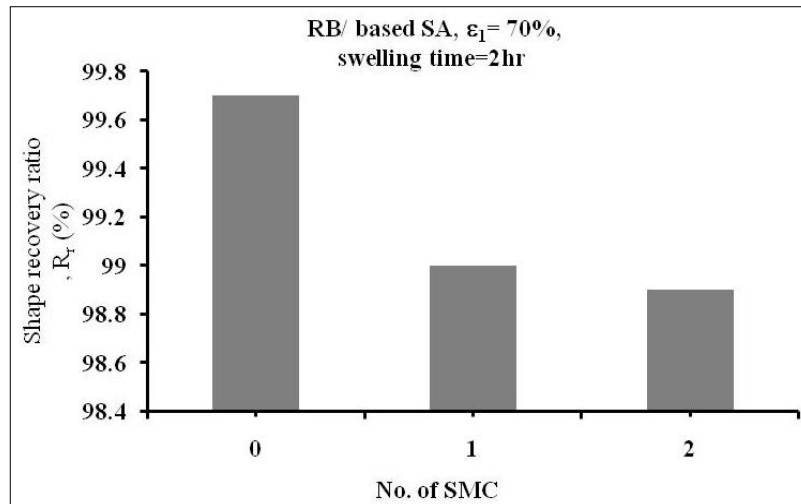


Figure (4-50): The Relation of The Shape Recovery Ratio With The Shape Memory Cycle Number.

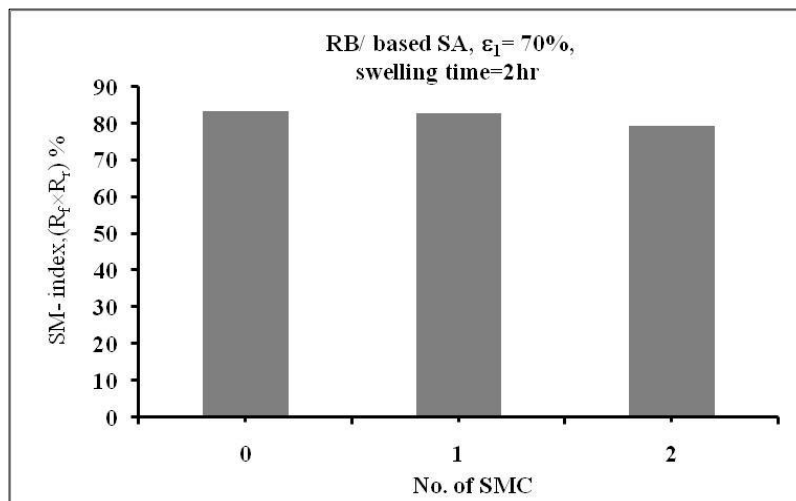


Figure (4-51): The Relation of The SM-index $(R_f \times R_r)$ % to The Shape Memory Cycle Number.

4-7-4 Study of the Effect of the Fatty Acid Nature on the Shape Memory Behavior

It is evident from Figure (4-52) that the swelling percentage of the commercial rubber band (Code Virgin RB) after immersion at 75°C in Palmitic acid molten is slightly more than the swelling percentage of this rubber band after immersion in Stearic acid molten at a temperature of 75°C as well. The reason for this is due to these fatty acids different nature in terms of chain length, this agrees with the reference [23,66].

As for the Figures (4-52) and (4-54), they show that there are differences, albeit a small amount, in the fixed strain in step 3 after the end of the hot classical shape memory cycle programming stage, as well as in the deformed shape fixity ratio of the rubber band (Code RB/based PA) impregnated Palmitic acid compared with the rubber band impregnated with Stearic acid (Code RB/based SA). While the results shown in Figures (4-55) and (4-56) showed that the plastic strain is non-reversible and the original shape recovery ratio is very close, and that the degree of recovery was at 75°C for each sample, (RB/based PA) and (RB/based SA), as this temperature is above the melting point of Palmitic acid (62.9°C) of Stearic acid (69.3°C). This is consistent with the findings of the references [22,23].

Also, it was shown in Figure (4-57) that the SM-behavior behavior of (RB/based PA) and (RB/based SA) can be described as very good this agrees with the references [59,86].

As for the cost, (RB/based PA) sample differs from the (RB/based SA) sample in the price of the fatty acid used in its preparation, where 25g of Palmitic acid reaches 9\$, while the 25g of Stearic acid reaches 2.5\$. In light of the economic cost, the use of Stearic acid is the most inexpensive way to convert vulcanized natural rubber products into shape memory smart rubber; this is a fact consistent with the absence of a significant difference in the shape memory behavior when using Palmitic acid in preparing this type of smart materials.

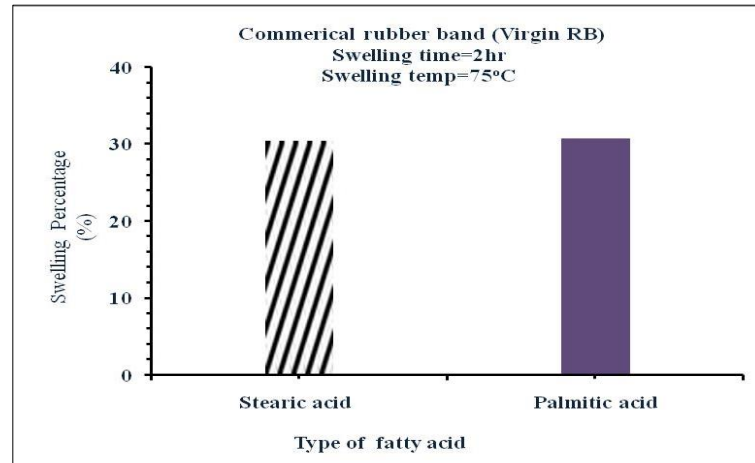


Figure (4-52): Effect of The Nature of The Fatty Acid on The Swelling Percentage of The Commercial Natural Rubber Band (Virgin RB) After Immersing With This Acid.

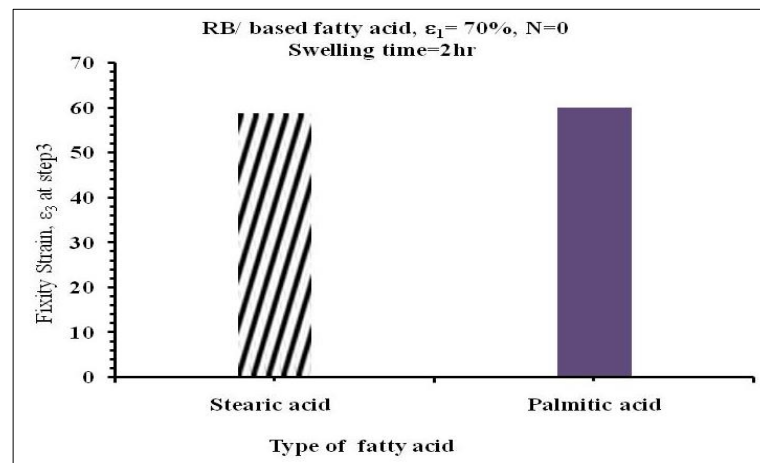


Figure (4-53): Effect of The Nature of The Fatty Acid on The Fixity Strain in Step 3 of The Deformed Shape Programming Stage.

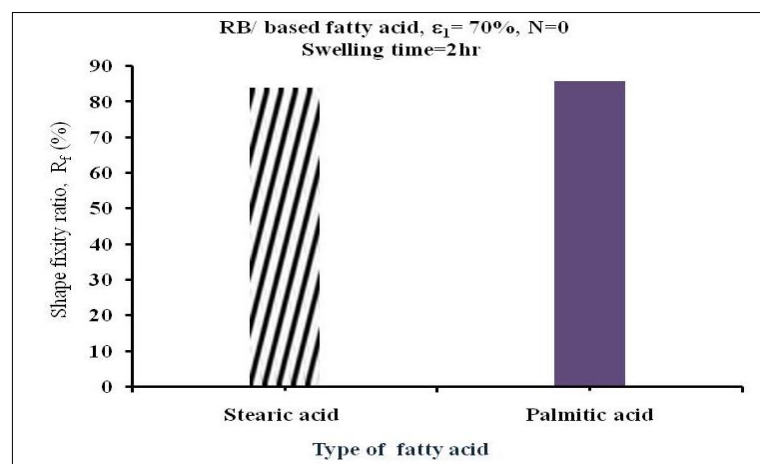


Figure (4-54): Effect of The Nature of The Fatty Acid on The Shape Fixity Ratio, R_f (%) of The Commercial Rubber Band Deformed Shape Impregnated With The Fatty Acid (Code RB/ based fatty acid).

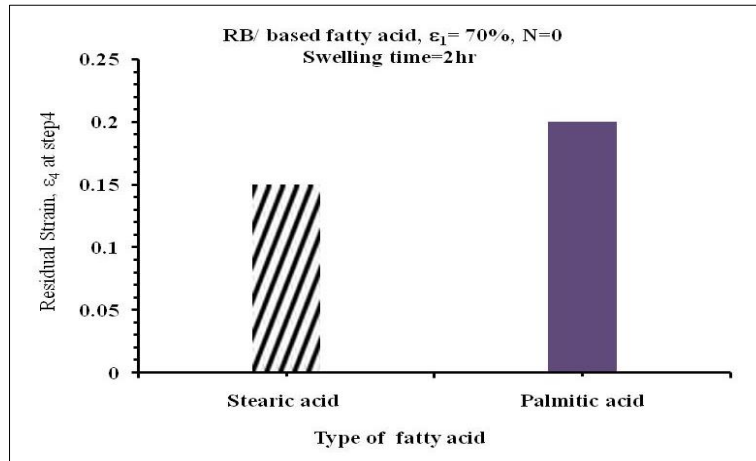


Figure (4-55): Effect of the nature of the fatty acid on the permanent plastic strain formed in the commercial rubber band impregnated with fatty acid (RB/ based fatty acid) after the end of the hot classical shape memory cycle.

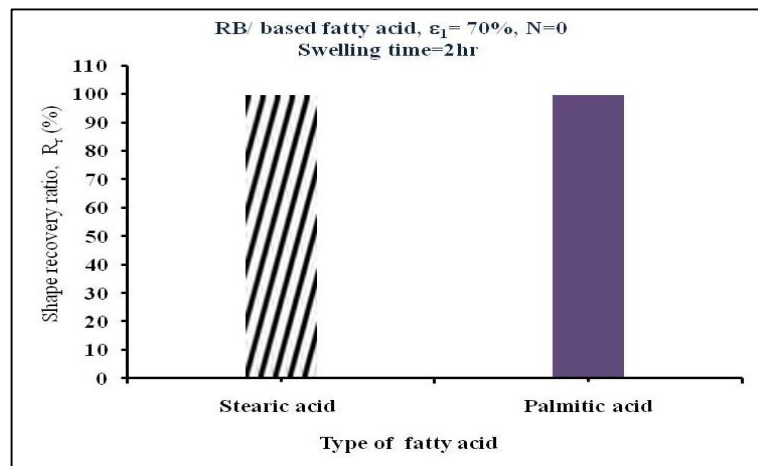


Figure (4-56): Effect of The Nature of The Fatty Acid on The Shape Recovery Ratio, R_r (%) of The Commercial Rubber Band Impregnated With Fatty Acid (RB/ based fatty acid).

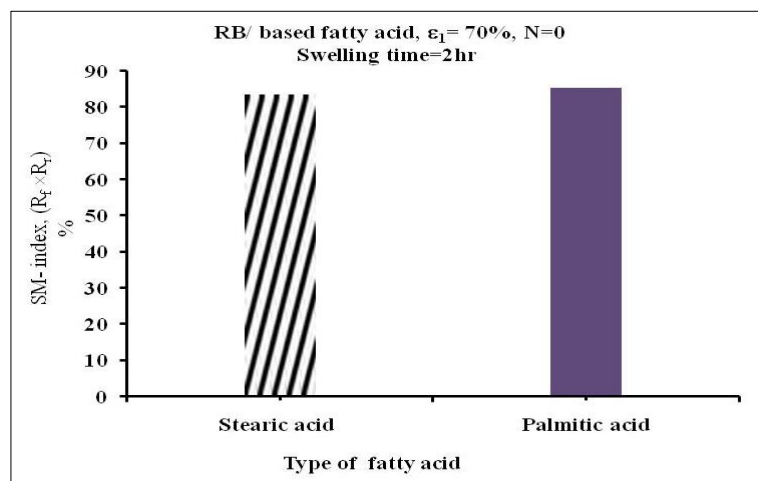


Figure (4-57): Effect of The Nature of The Fatty Acid on The SM-index $(R_f \times R_r)$ % of The Commercial Rubber Band Impregnated With Fatty Acid (RB/ based fatty acid).

4-7-5 Studying the Relation of the Cross- link Density to Shape Memory of the Smart Vulcanized Natural Rubber.

From Figure (4-58), it is clear that the increase in the sulfur ratio used in the vulcanization process of the smoked natural rubber (RSS) under study leads to an increase in the cross-link density of this rubber after vulcanization, which symbolized as (Virgin RSS); the reason is attributed to the increase in the molecular chains linkage in the form of cross-linkers with an increase in the amount of sulfur needed to obtain this cross-link, this result is consistent with the references [15,59,63,86,91,92].

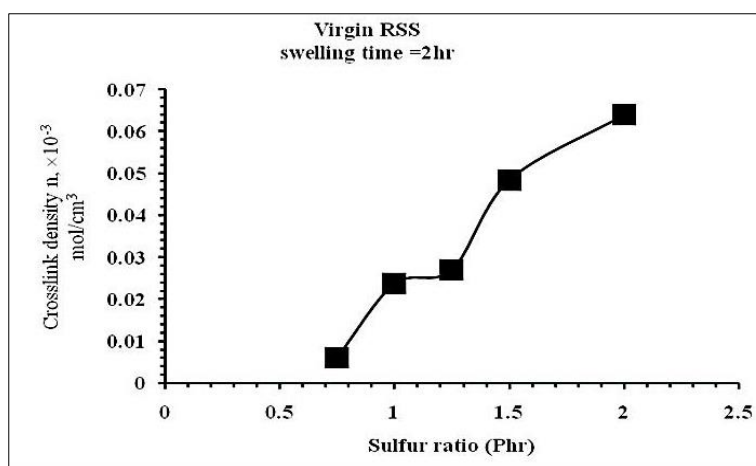


Figure (4-58): The Relation Between Cross-Link Density and Sulfur Ratio in Virgin RSS.

As Figure (4-59) shows, the increase in the sulfur ratio causes a decrease in the weight percentage of Stearic acid (SA) in Virgin RSS body after being immersed in the molten of this acid for a period of (2hr) in order to obtain a shape memory natural rubber (SMNR) type of RSS/Stearic acid (SA) blend (SMP), which was denoted as (RSS/based SA) after impregnation with the acid, Where (RSS/based SA) material with sulfur ratio of (0.75phr) gave the highest weight percentage of Stearic acid (SA) in its body compared to the rest of sulfur ratios. That can be attributed to the decrease in the spaces between the vulcanized rubber chains with an increase in the sulfur ratio, and this means a decrease in the areas

that stearic acid can penetrate into; this in turn negatively affects the swelling behavior of (RSS/SA) material in (SA) melt.

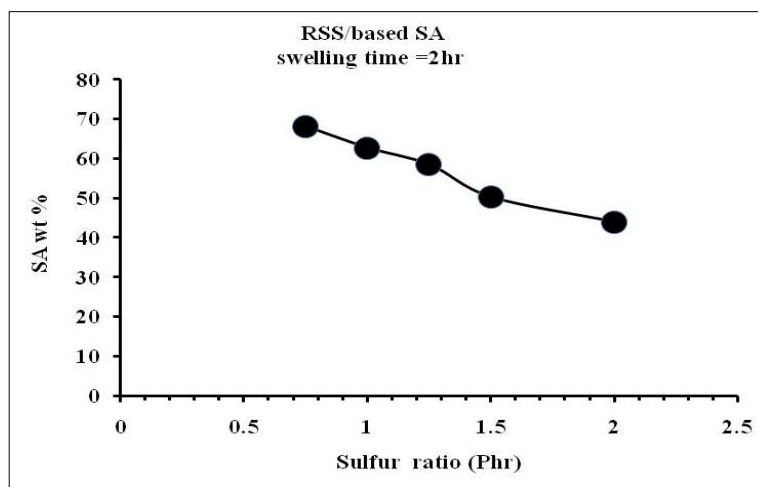


Figure (4-59): The Relation Between The Weight Percentage of Stearic Acid (SA) and Sulfur Ratio in (RSS/based SA).

It can be seen from Figure (4-60) the decline in the weight percentage of Stearic acid (SA) in the (RSS/based SA) body with an increase in the cross-link density.

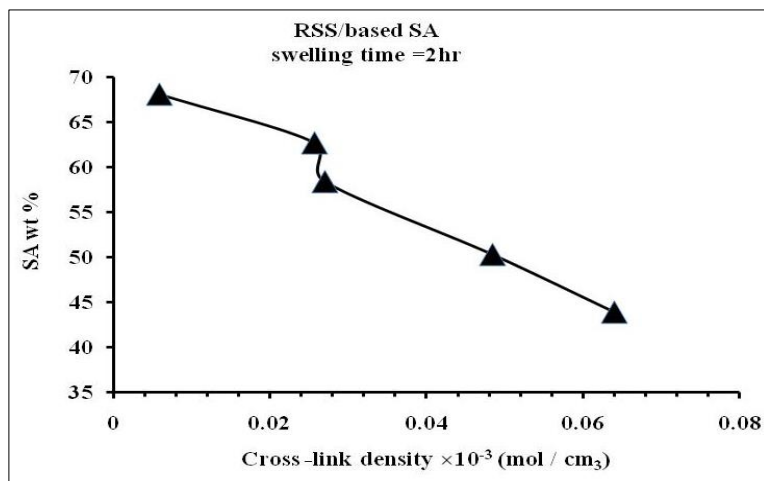


Figure (4-60): The Relation Between The Weight Percentage of Stearic Acid SA With The Cross-Link Density of (RSS/based SA).

Thus, it can be said that when the cross-link density is low, the number of cross-links will be small, which causes many paths to be provided for the osmotic of Stearic acid (SA) molten into this vulcanized rubber network through the

swelling process. But when the crosslinking density is big, the number of cross-links will be high, and (SA) molten osmotic paths in the vulcanized natural rubber network represented by (Virgin RSS) will definitely decrease, which reduces the transformation of Stearic acid (SA) into this network. This means that the force opposing the swelling depends on the cross-link density, as the force opposing the swelling increases with the increase in the cross-link density, and this is consistent with the findings of the researches [59,86,91,92]. By looking at Figure (4-61), it can be found that the fixed strain or the restricted strain in the mechanically deformed shape of (RSS/based SA) after the completion of the SME property activation stage of the shape memory cycle decreases in value with the increase in sulfur ratio.

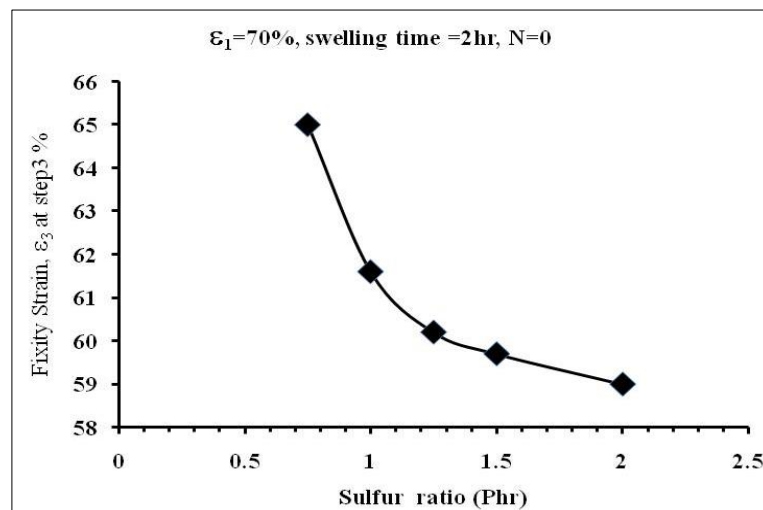


Figure (4-61): The Relation Between Fixed Strain and Sulfur Ratio in (RSS/based SA) After The End of The SME Activation Stage During The Classical Hot Shape Memory Cycle Based on Normal Cooling at Room Temperature.

The reason for this is attributed to the fact that the Stearic acid (SA) network acts as a switcher in the (RSS/based SA) material during the phase change from the crystalline state to the molten state or vice versa through the stages of the shape memory cycle. Where, in the first part of the hot classical shape memory cycle represented by the shape memory property activation stage (SME) and exclusively to step2, SA network freezing process occurs in the

(RSS/based SA) material while it is still under the influence of the applied load. The effects of this SA network freezing clearly appear in step3, by remaining the mechanical deformation after removing the applied load, by restricting the entropic recovery force of the cross-linkers of the vulcanized rubber network; that represents the stable phase or hard segment in (RSS/based SA) by freezing SA network on it. This means that SA network decreasing in the RSS/based SA body with increasing sulfur ratio will create a state of diminishing in the ability of this material to restrict the driving force to recover its original shape in the SME activation stage, which completely prevents the retention of the strain-induced crystals in step2. So that, the applied strain releasing process spontaneously increases in step 3 after the load is off the RSS/based SA, more than its fixation (the applied strain), in conjunction with the occurrence of the elastic retract, which is inversely proportional to the weight percentage of stearic acid (SA).

Where the activity of (RSS/based SA) material in retaining the mechanical deformation formed in step1 is measured by the weight percentage of Stearic acid (SA) in its body, that goes from the fact that the ability to restrict the driving force to recover the original shape (the entropic recovery force) depends on cross-linking which in turn decreases by weight percentage of SA in the body of (RSS/based SA). That assists in creating a diminishing state in its ability to restrict the driving force to recover the original shape at the SME property activation stage, which reduces the retained strain-induced crystals in step2;so this state is called the spontaneous elastic mechanical deformation release in step3.

As for Figure (4-62), it shows a decrease in the mechanically deformed shape fixity ratio, R_f of the material (RSS/based SA) with the increase in the sulfur ratio, that eventually leads to a weak memory of (RSS/based SA) for its new molecular architecture con Figure ration after the completion of the (SME) property activation stage, this result agrees with the references [10,18,23,26,27 and 75].

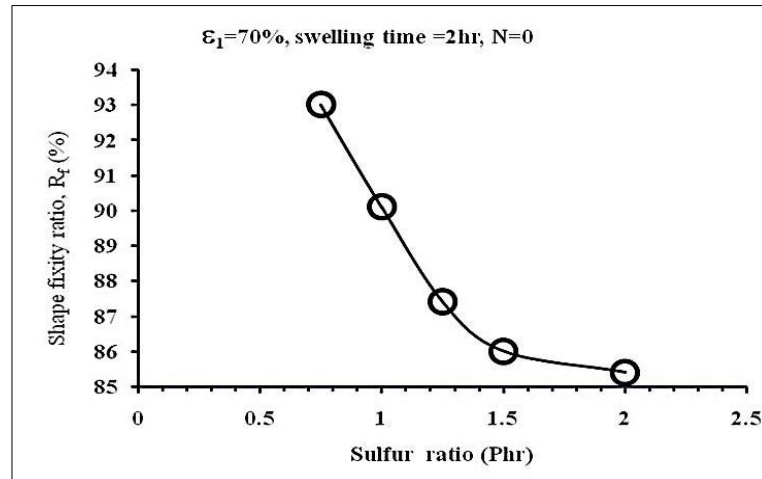


Figure (4-62): The Relation Between The Shape Fixity Ratio and The Sulfur Ratio in RSS/based SA After The End of The SME Property Activation Stage During The Hot Classical Shape Memory Cycle Based on Normal Cooling at Room Temperature.

Figure (4-63) shows that the accumulation of non-reversible plastic deformation decreases with the increase of sulfur ratio in RSS/based SA. The reason for this is due to the increase in the entropic recovery force due to the increase in the cross-link density with the increase in sulfur ratio in the body of the (RSS/based SA) material.

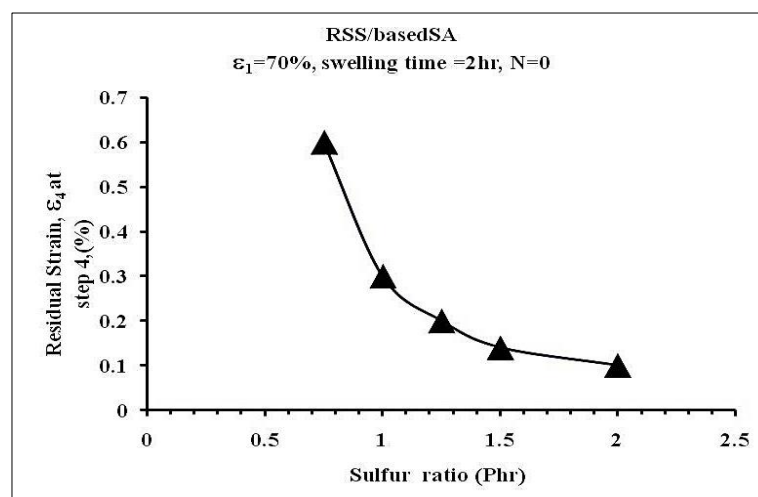


Figure (4-63): The Relation Between The Permanent Plastic Strain and The Sulfur Ratio in RSS/based SA After The End of The SME Property Deactivation Stage During The Hot Classical Shape Memory Cycle Based on Normal Cooling at Room Temperature.

As for Figure (4-64), it shows that the permanent original shape recovery ratio increases with the increase in the sulfur ratio in the (RSS/based SA) material

after subjecting it to the SME property deactivation stage, or the so-called recovery stage, which involved re-stimulating the SA network to transform from the crystalline state to the molten state by heating. So that the elastic strain restricted in the deformed shape of the (RSS/based SA) could be thermally released, allowing the (RSS/based SA) to return to its original shape it was in before subjecting it to the shape memory cycle, but in an amount that varies according to the sulfur ratio, this result is in agreement with the references [1,18,23,33,85].

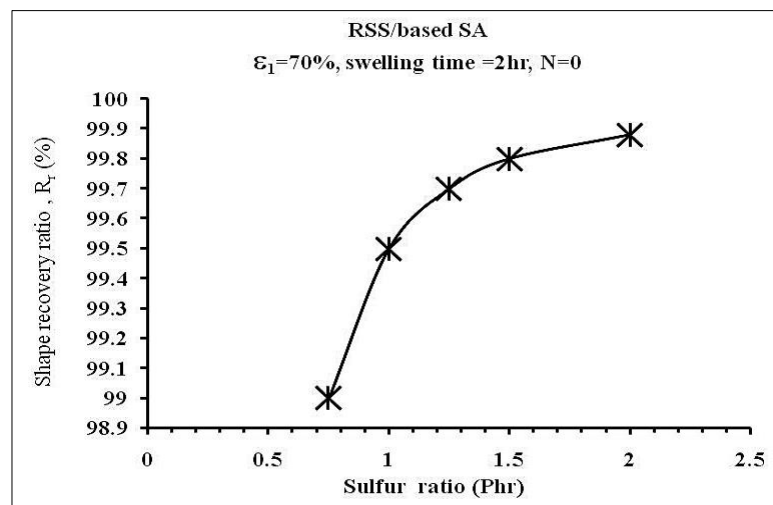


Figure (4-64): The Relation Between The Shape Recovery Ratio and The Sulfur Ratio in RSS/based SA After The End of The SME Property Deactivation Stage During The Hot Classical Shape Memory Cycle Based on Normal Cooling at Room Temperature.

In general, the material (RSS/based SA) with a sulfur ratio (0.75 phr) is distinguished from the rest of the samples by a high shape memory performance which is shown by the results of shape memory (SM)-index, ($R_f \times R_r$), shown in Figure (4-65) .

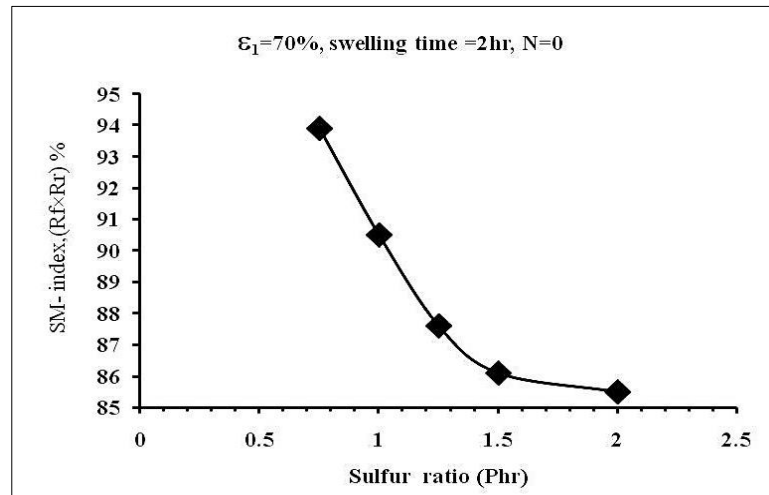


Figure (4-65): The Relation Between SM-index and Sulfur Ratio of The Material RSS/based SA.

Figure (4-66) shows the shape memory effect (SME) property demonstration macroscopically by the digital imaging (videography) that relies on photographic documentation of the original shape change of the (RSS/based SA) material of sulfur ratio (0.75Phr) represented by (straight- shape) to a new shapes represented by long-strip shape, U-shape, and spiral-shape by the (SME) property activation and, then returning to the original shape by (SME) property deactivation during the hot classical shape memory cycle.

Figure (4-66) and (4-67) also show that there is a direct relation between the shape recovery temperature and the shape recovery speed, where an increase in the recovery temperature leads to a decrease in the recovery time. So the temporary shape represented by the long strip–shape has returned to its original permanent shape in less time than what was needed by both U-shape and spiral-shape, with the use of hot water at a temperature of 90°C. It is worth noting that the followed method on how to prove SME property is consistent in terms of style with the researchers [28,93 and 94].

Before the start of SMC		After the prog. Stage is over		During recovery stage				After the prog. Stage is over
Original permanent shape		Temporary shape		Stimulus	Recovery process			Recovered permanent shape
Straight -shape		Long strip - shape  t = 0 s	at 90 °C	 t = 10 s			 t = 15 s	
				u- shape  t = 0 s	at 50 °C	 t = 6 s	 t = 26 s	 t = 41 s
		Spiral- shape  t = 0 s	at 75 °C	 t = 5 s	 t = 14 s	 t = 22 s	 t = 27 s	 t = 30 s

Figure (4-66): The Macroscopically Demonstration of The Shape Memory Effect (SME) Property by Digital Imaging for The RSS/based SA Sample.

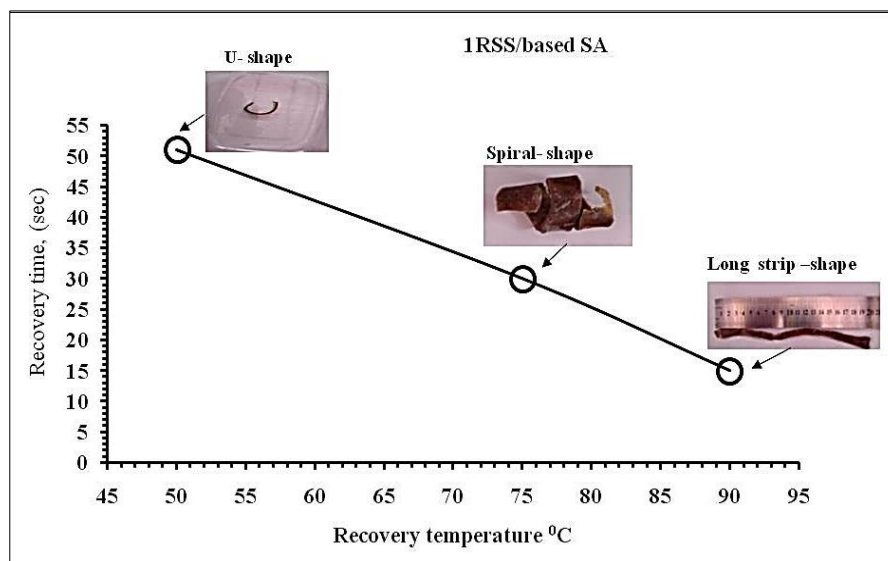


Figure (4-67): The Relation Between The Recovery Time and Recovery Temperature.

4-7-6 Studying the Effect of the Different Nature of the Smart Rubber Material on the Behavior of Shape Memory.

It is evident from Figure (4-68) that the cross link density reflects the nature of the specimens under study, where the crosslink density of the commercial natural rubber band represented by (Virgin RB) type (Latex) was higher than it is in the laboratory-smoked and vulcanized natural rubber represented firstly by the sample (1Virgin RSS) with a sulfur content of (0.75Phr) as the lowest value used in the vulcanization process, and secondly, by the sample (5Virgin RSS) with a sulfur content of (2Phr) as the highest value used in the vulcanization process. This result is consistent with the content of the commercial natural rubber band of silica as a reinforcing material, whose weight percentage reaches (3.49wt%), in addition to the weight percentage of sulfur that reaches (1.8wt%) according to the (EDS) examination data. On the other hand, the samples (1Virgin RSS) and (5Virgin RSS) do not contain any type of reinforcement, so the cross link density differs with each of:

- The nature of the rubber material.
- The sulfuric vulcanization agent content.
- Reinforcing materials content.

So that, the increment of content of each, vulcanization agent and reinforcement materials is positively reflected on the cross-link density, this agrees with the findings of references [74] and [28].

Figure (4-69) shows that the Stearic acid weight percentage in the sample (1RSS/based SA) is superior to the value of the Stearic acid weight percentage in the samples (5RSS/based SA) and (RB/based SA), respectively. The decrease in the Stearic acid weight percentage in the samples (5RSS/based SA) and (RB/based SA) is due to the decrease of the pathways through which this fatty

acid penetrates into these samples with the increase of the cross-link density. This result is consistent with the findings of the reference [22].

Looking at Figures (4-70) and (4-71), it has been found that the deformed shape fixity ratio and the original shape recovery ratio depend on the rubber material nature and the cross-link-density.

As shown from Figure (4-72), the shape memory behavior (SM-behavior) of (1RSS/based SA) can be described as excellent because it is close to the ideal behavior (Ideal-behavior).

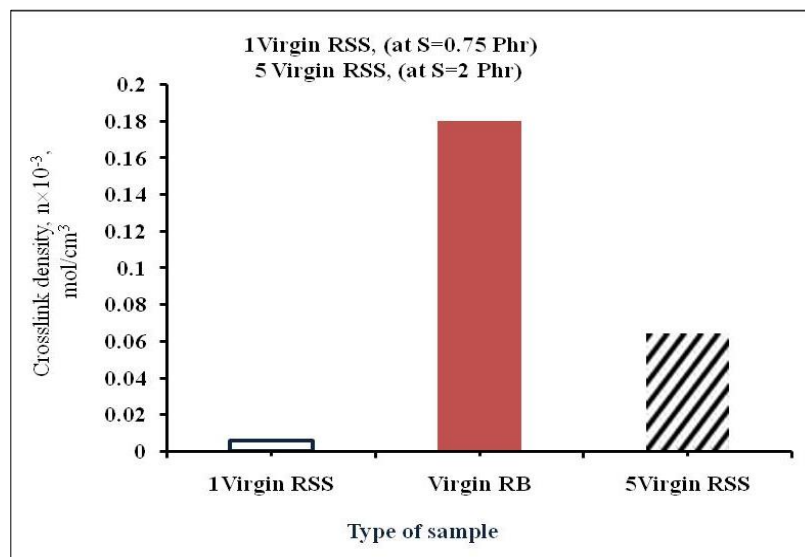


Figure (4-68): The Relation of The Cross Link Density to The Material Nature Under Study.

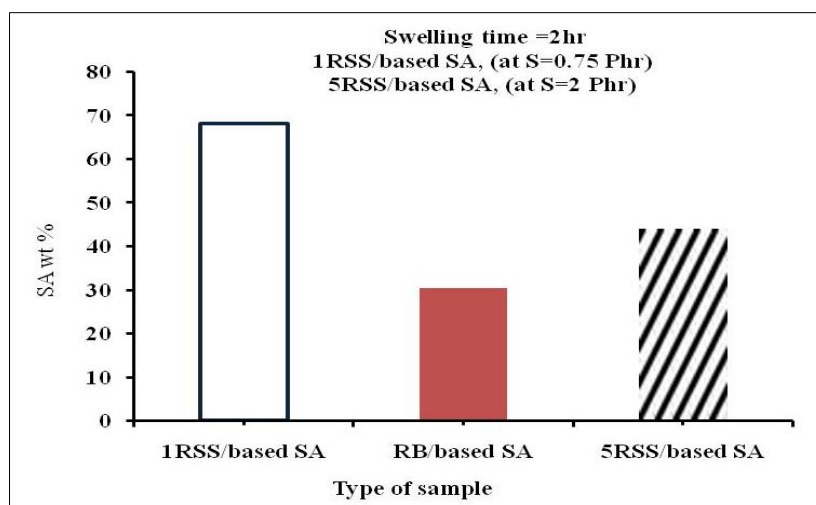


Figure (4-69): The Relation of The Stearic Acid Weight Percentage (SA wt%) to The Material Nature Under Study.

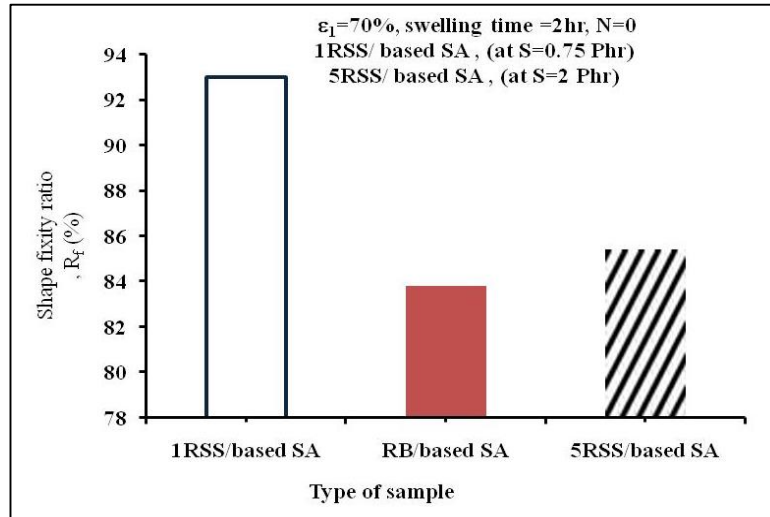


Figure (6-70): The Relation of The Shape Fixity Ratio, R_f (%) to The Material Nature Under Study.

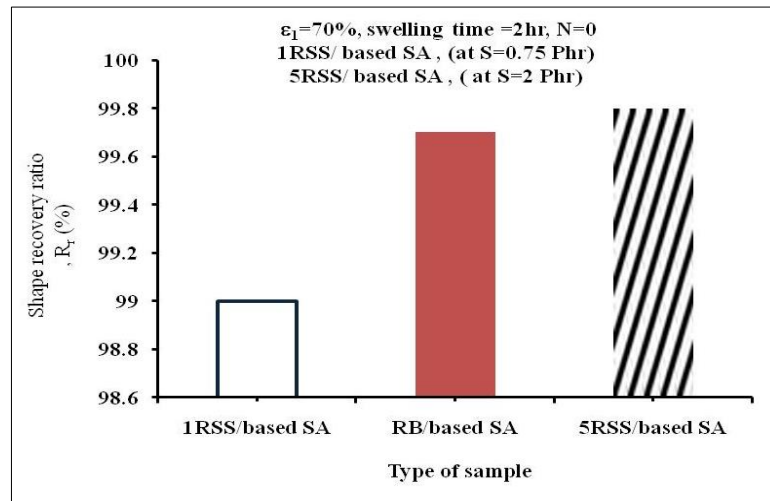


Figure (4-71): The Relation of The Shape Recovery Ratio, R_r (%) to The Material Nature Under Study.

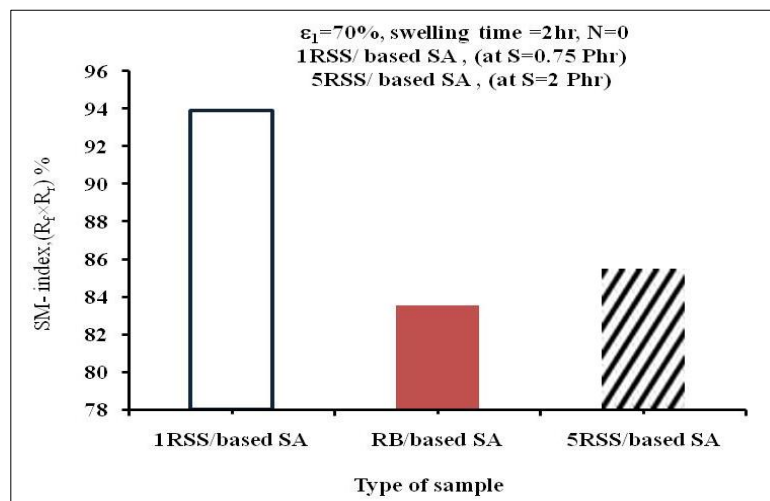


Figure (4-72): The Relation of The SM-index to The Material Nature Under Study.

4-8 Quasi-static short-time Mechanical Characterization of some Materials under Study Before Undergoing a Shape Memory Cycle.

The shape memory behavior of the materials under study after their impregnation with Stearic acid is related to the shape-memory cycle, where these materials are considered traditional (non-smart) despite their impregnation with fatty acid in the absence of the programming process, so, this process is directly responsible for appearing the shape memory effect (SME).

Figures from (4-73) to (4-78) show that the tensile strength at fracture of the commercial rubber band material (Code Virgin RB) and laboratory-vulcanized and smoked rubber material with a sulfur ratio of (0.75Phr) (Code 1 Virgin RSS), is slightly less than it is after impregnation of these samples with Stearic acid. The values of the maximum elongation gave a decrease with the impregnation of these samples with Stearic acid (SA). The reason of this is attributed to the fact that treatment by swelling using fatty acid is highly affecting the cross linking. This result is consistent with the reference [26].

While Figure (4-79) shows that the maximum crushing strength increases with impregnation with Stearic acid of both samples; the commercial rubber band sample (Code RB/based SA), and the laboratory-vulcanized smoked rubber sample (code 1RSS/based SA), but it differs according to the nature of the rubber under study.

For the Figure (4-80), it shows that the surface hardness decreases with the impregnation of both (Virgin RB) and (1 Virgin RSS) with Stearic acid, and the reason for this is due to the nature of the fatty acid that coats the rubber particles. Therefore, these static mechanical tests are means of describing the variability and difference in the mechanical properties of fatty acid swollen rubber as a conventional non-smart rubber due to the lack of programming and recovery stages in these means.

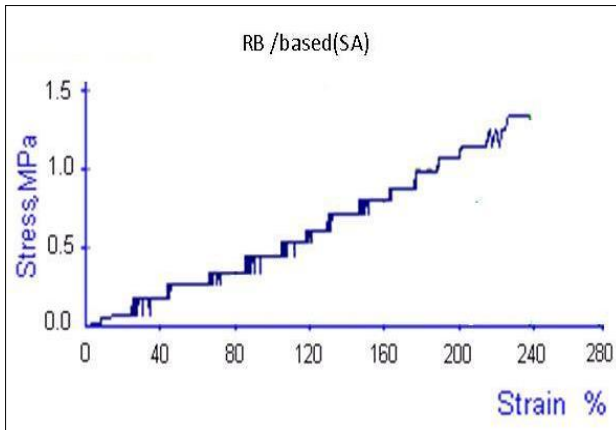


Figure (4-73): Stress-Strain Tensile Curve for RB without SA (Virgin RB) at Room Temperature.

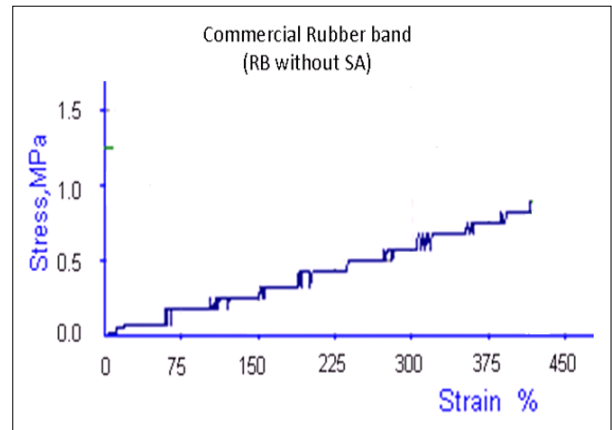


Figure (4-74): Stress-Strain Tensile Curve for (RB based/ SA) at Room Temperature.

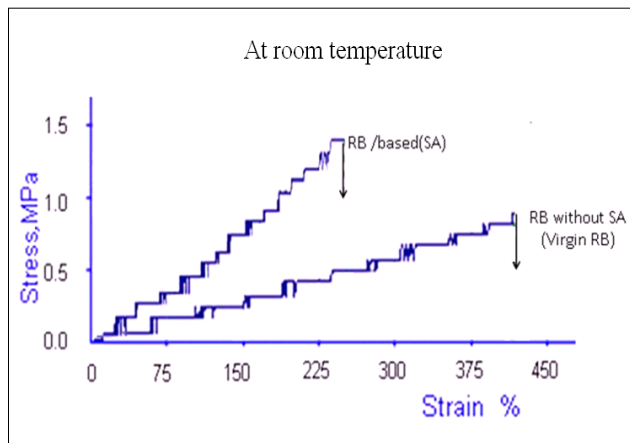


Figure (4-75):The Effect of The Rubber Bands Impregnation With Stearic Acid on The Tensile (Stress-Strain).

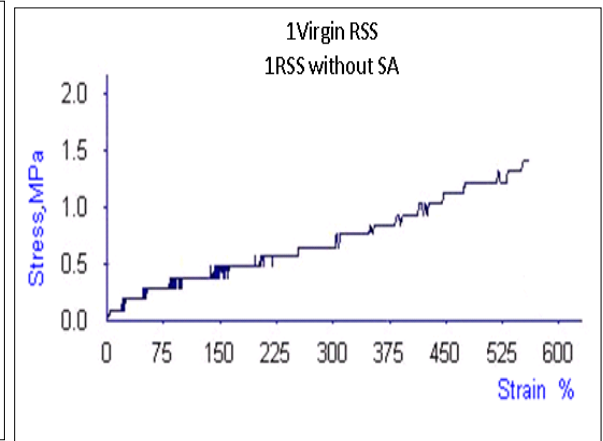


Figure (4-76): Stress-Strain Tensile Curve for (1Rss without SA) (1Virgin RSS) at Room Temperature.

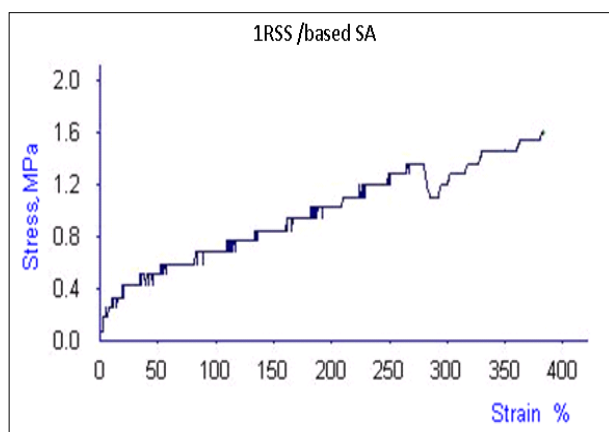


Figure (4-77): Stress-Strain Tensile Curve for (1Rss based/ SA) at Room Temperature.

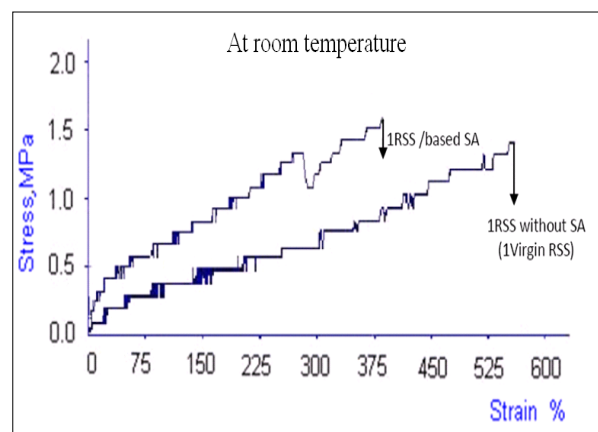


Figure (4-78): The Effect of The 1Virgin RSS Impregnation With Stearic Acid on The Tensile (Stress-Strain).

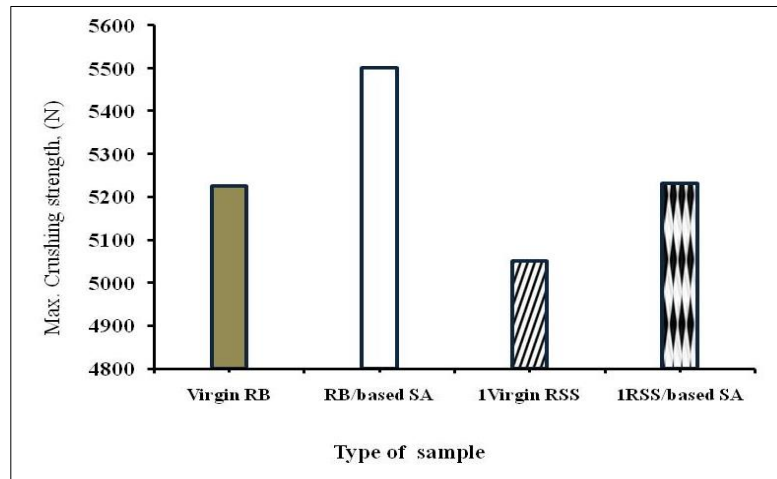


Figure (4-79): The Relation of The Max. Crushing Strength to The Type of Sample at Room Temperature.

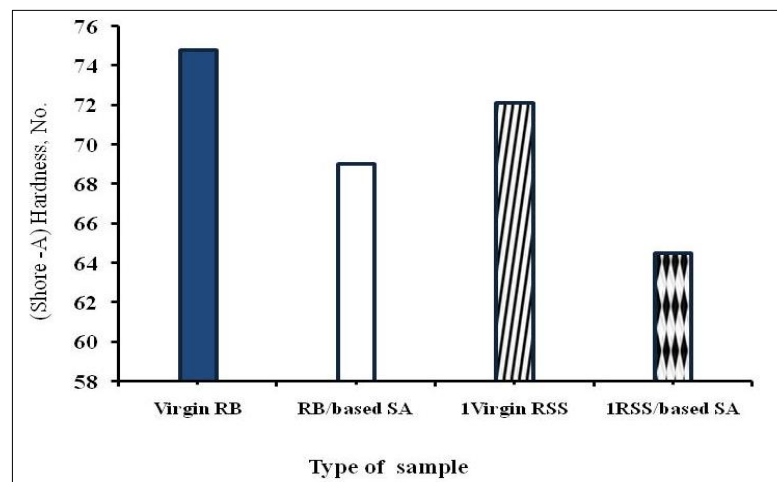


Figure (4-80): The Relation of The Surface Hardness to The Type of Sample at Room Temperature.

4-9 Factors Affecting Hot Classical Shape Memory Cycle Time.

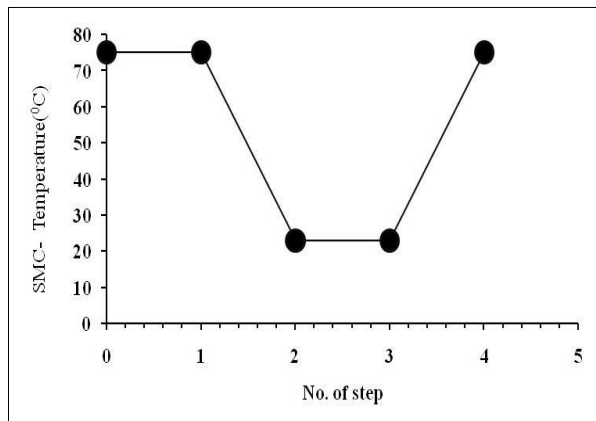
Determining the shape memory cycle time is one of the important factors for selecting the appropriate shape memory polymers for a particular application, which in turn depends on the properties of these materials and the experimental conditions.

4-9-1 Study the Effect of the Cooling and Heating facility on the Shape Memory Cycle Time Using the Thermal Elongation Device.

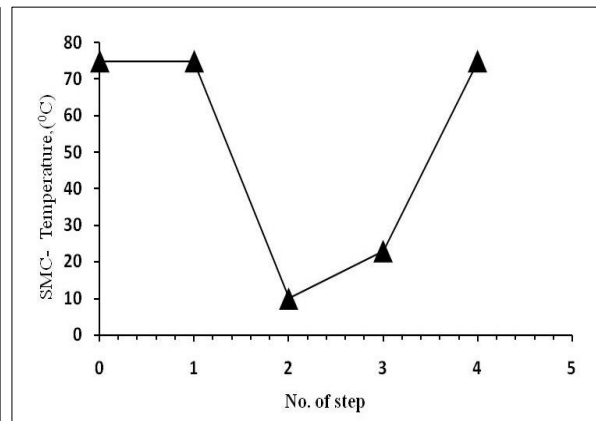
Figure (4-81) shows the difference in the temperature protocol for the hot classical shape memory cycle according to the difference in cooling facility used

in step2 for the smart rubber under study. This difference in cooling facility was reflected on the shape memory cycle time as shown in Table (4-3).

While Figures (4-82) and (4-83) show that there is no significant difference in the shape fixity ratio as well as shape recovery ratio with the change of the cooling facility in step2 of the shape memory cycle.



(a) When Cooling is to Room Temperature in Step2.



(b) When Cooling in Step2 is by Using Iced Water Spraying at a Temperature of 10°C.

Figure (4-81): Profile of The Classical Shape Memory Cycle Temperature Using Thermal Elongation Device for The Smart Rubber Under Study.

Table (4-3): The Difference of The Shape Memory Cycle Time of (RB/based SA) by Different SME Property Activation and Deactivation Instruments During the Hot Classical Shape Memory Cycle.

Measuring instrument of SM- behavior			Stages time of Hot- classical shape memory cycle (SMC)						Shape memory cycle time, t_{sm}	Advantages	Disadvantages
			Programming process				Recovery process				
			Step0	Step1	Step2	Step3	Stimulus	Step 4			
Thermal elongation device based on cooling:	abnormal	iced water spraying	11 min	1min:20s	10 min	10min	Hot air at 75°C	4min	36min:20s	SMC time less than 1h.	Hard, with continuous need for ice pieces, and consumes electrical power
	normal				30 min						
Modified Vernier caliper tool based on cooling:	abnormal	By immersing in iced water	30s	10s	30s	60s	Immersing in hot water at 75°C	30s	2min:40s	Easy measuring instrument with very short SMC time estimated by few seconds	continuous need for ice pieces

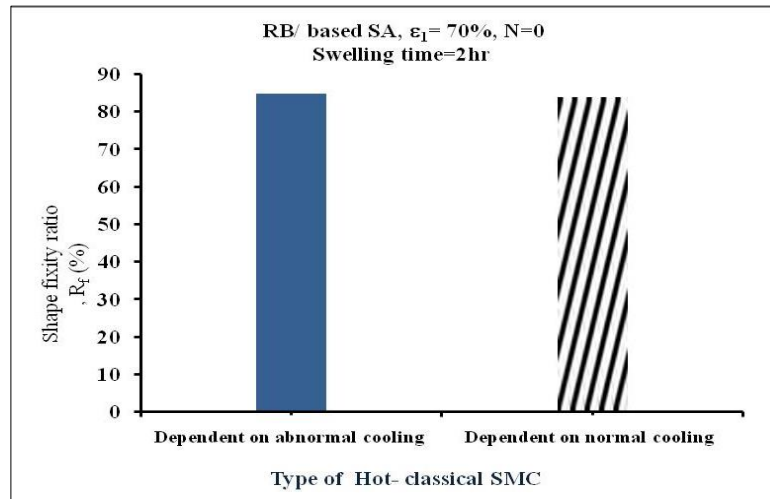


Figure (4-82): The Relation of The Shape Fixity Ratio, R_f (%) With The Type of Classical Shape Memory Cycle Using Thermal Elongation Device.

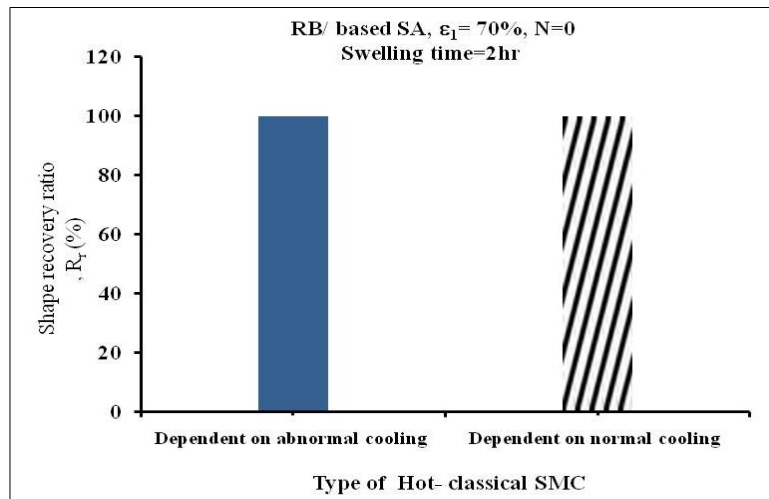


Figure (4-83): The Relation of The Shape Recovery Ratio, R_r (%) With The Type of Classical Shape Memory Cycle Using Thermal Elongation Device.

Figure (4-84) describes the hot classical shape memory cycle consisting of two stages as follows: -

- Programming stage, consisting of three steps, which are: -

- Step1: Loading at 75°C .
- Step2: Cooling under load.
- Step3: Remove loading.

- Recovery stage, consisting of one step, which is: -

- Step4: Recovery at 75°C .

It appears from Figure (4-85) that the shape recovery ratio increases with the increase in heating temperature from room temperature to 75°C.

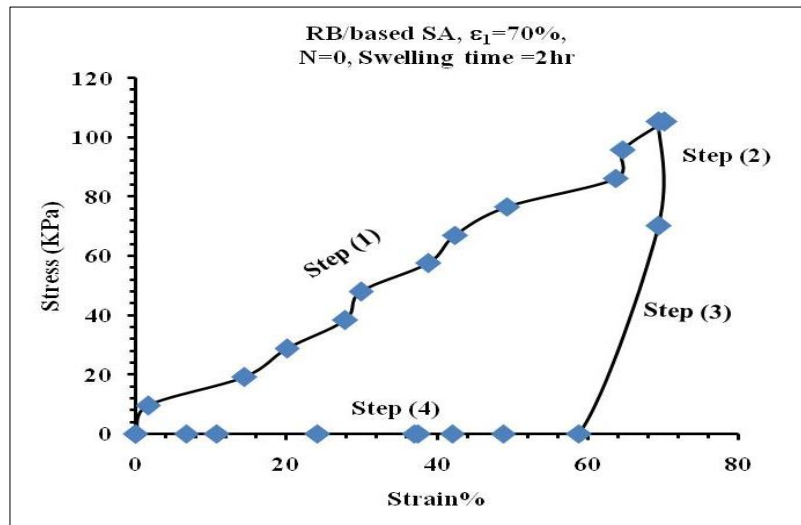


Figure (4-84): Characterization of Shape Memory Behavior During The Hot Classical Shape Memory Cycle.

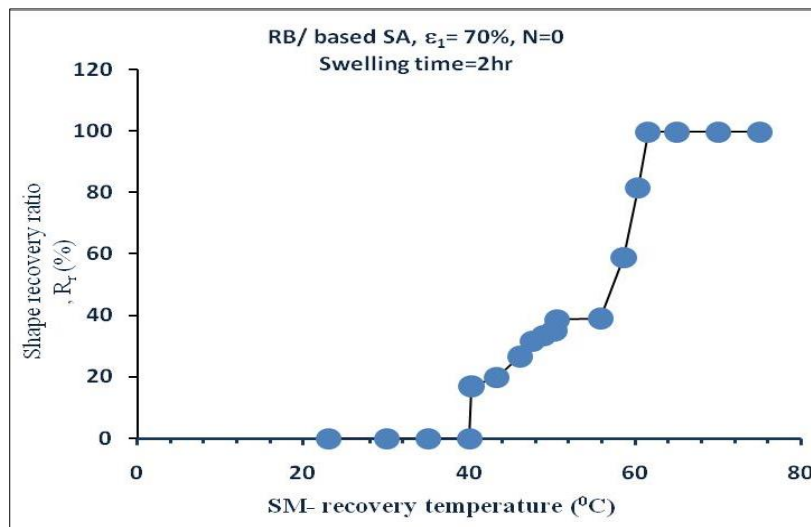


Figure (4-85): The Relation of The Shape Recovery Ratio to The Original Shape Memory Recovery Temperature (SM-recovery temperature).

In general, the hot classical shape memory cycle protocol based on normal cooling at room temperature aims to provide a way to show (SME) property without difficulty, so the shape memory cycle time will be higher than it is in the shape memory cycle protocol based on abnormal cooling and this is what shown by Table (4-3).

4-9-2 Studying the Effect of the Heating and Cooling Method on the Shape Memory Cycle Time Using the Modified Vernier Caliper Tool

One of the obvious facts in the smart rubber hot shape memory cycle under study is that the temperature profile using the modified Vernier caliper is the same as the temperature profile of the shape memory cycle under study using the thermal elongation device as shown in Figure (4-81-b); but this does not mean that the shape memory cycle time using these devices is identical, that is for the difference in heating and cooling methods during the SME property activation and deactivation stages of (RB/based SA). Where the data in Table (3) indicate that the use of heating method by immersion in hot water at a temperature of 75°C instead of hot air, the time of step0 is shortened from 11min to 30sec. Also, the use of cooling method by immersion in iced water instead of iced water spraying at the same temperature, shortens the time of step1 from 10min to 30sec during the deformed shape programming stage. While the process of immersion in hot water instead of hot air, it has shortened the recovery time from 4min to 30sec during the recovery stage.

In general, the reduction in the shape memory cycle time is a required and important step in the applications of shape memory smart materials, and this is confirmed by the reference [59].

As for Figures (4-86) and (4-87), they show that there is no significant difference in the shape fixity ratio as well as the shape recovery ratio with changing the measurement instrument of (SM-behavior), while Table (4-4) shows the advantages and disadvantages of the thermal elongation device and modified Vernier caliper, to study the SME property.

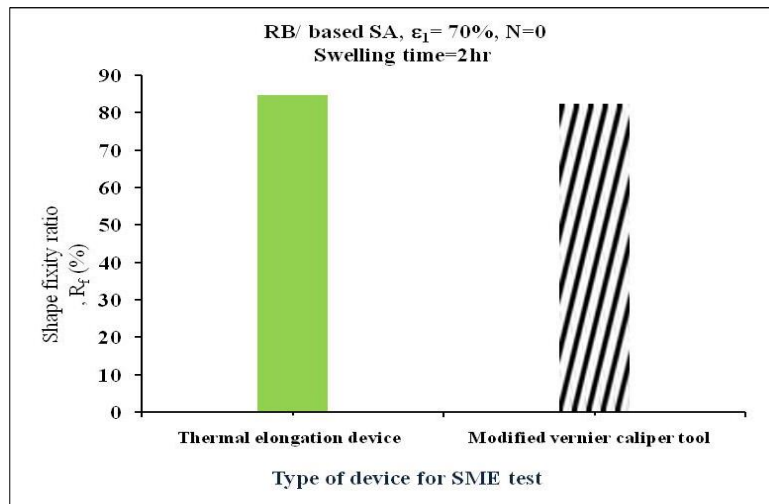


Figure (4-86): The Relation of The Shape Fixity Ratio to Device Type for SME Test.

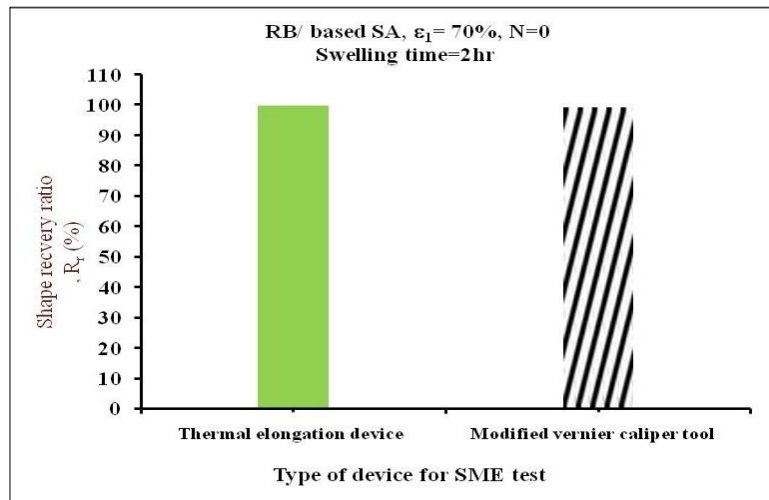


Figure (4-87): The Relation of The Shape Recovery Ratio to Device Type for SME Test.

Table (4-4): A Comparison Between The Thermal Elongation Device and The Modified Vernier Caliper Tool Used in The (SME) Property Test.

SME property test device type	Photographic image of the instrument	disadvantages	Advantages
<p>Thermal elongation device</p>		<ul style="list-style-type: none"> • Energy consumer • Long SMC time 	<ul style="list-style-type: none"> • Gives information about the SME property behavior during SMC. • Gives information about the beginning and end of the shape recovery.
<p>Modified Vernier caliper tool</p>		<ul style="list-style-type: none"> • Does not give information about SME property behavior. • Does not give information about the beginning and end of the shape recovery. 	<ul style="list-style-type: none"> • Easy to handle. • Short SMC time



5

Chapter Five
Conclusions and
Recommendations

5-1 Conclusions:

From the current study based on the hot classical shape memory cycle, the following conclusions were reached:

- 1- The vulcanized natural rubber non-impregnated with fatty acid did not exhibit shape-memory behavior.
- 2- From DSC test, the heat of fusion of the vulcanized natural rubber impregnated with fatty acid after SME property activation is greater than its melting temperature after deactivation of the SME property.
- 3- From XRD test, the degree of crystallization of the vulcanized rubber impregnated with fatty acid and subjected to the SME property activation stage, becomes greater than the temperature of crystallization after SME property deactivation.
- 4- The physical phenomena accompanying the shape memory cycle effect on the ability of the vulcanized rubber impregnated with fatty acid infixing its mechanically deformed shape and recovering its permanent original shape.
- 5- The elastic retraction plays a more negative role than thermal contraction in the mechanically deformed shape restriction process during the programming stage of the shape memory cycle.
- 6- The shape memory performance is related to the elastic stretching work energy restricted from the spontaneous reversal.
- 7- The non-reversible permanent plastic deformation reduces the shape memory behavior of the vulcanized natural rubber impregnated with fatty acid.
- 8- Increasing the cross-link density of the vulcanized natural rubber negatively effects on the process of its impregnation with fatty acid.
- 9- The shape memory behavior of the vulcanized rubber impregnated with fatty acid improves with the increase in fatty acid weight percentage.
- 10- Wax blooming phenomena occurs during the shape memory cycle.

11- The shape memory behavior of the vulcanized natural rubber impregnated with fatty acid weakens with the increase of shape memory cycle number, applied strain, and cross-link density.

12- The original shape recovery speed time during the recovery stage of the shape memory cycle increased with increasing thermal stimulation temperature.

13-Short-time quasi-static mechanical tests at room temperature are not valid in evaluating the shape memory behavior (SM-behavior).

14- The difference in the nature of the cooling and heating methods has a slight effect on the shape memory behavior, while it has a significant effect on the shape memory cycle time.

15- Thermal elongation device is an excellent mean to study the shape memory behavior in a detailed way, but it consumes electrical energy in compare to the modified Vernier instrument.

16-The prepared material was successfully used as a medical engineering equipment used in the field of cancer diseases.

5-2 Recommendations

- 1- Study of the materials applicability of this study in the field of medical equipment engineering.
- 2- Study of the shape memory properties of the materials of this study using other types of shape memory cycles
- 3- Preparation and characterization of shape memory smart rubber from the industrial elastomeric products.
- 4- Studying the two-way shape memory effect (2w-SME) for the materials of this study.
- 5- Study the multiple programming shape memory cycle for the materials of this study.
- 6- Preparation and characterization of shape memory epoxy resins.
- 7- Preparation and characterization of shape-memory cross-linked polyethylene.
- 8- Preparation and characterization of polyurethane shape memory polymers.
- 9- Preparation and characterization of masks used in the field of treating cancer patients, with a small thickness, with a high value of fixity shape ratio.

References

References

References: -

- 1- G. Li, "Self –Healing composites: shape memory polymer – Based structures", published by John wiley and Sons, 2015.
- 2- W. D. Callister, Jr. and David G. Rethwisch, "Materials Science and Engineering an introduction 9th Edition ", published by John wiley and Sons, 2014.
- 3- V. K. Wadhawan," Smart structure Blurring the Distinction Between the living and Nonliving", published in the united states by Oxford University press Inc, New York, 2007.
- 4- D. Michelle Addington, Daniel Schodek,"Smart Materials and Technologies For the Architecture and Design Professions", Published by Routledge and Taylor and Francis group, 2004.
- 5- L. Peponi, M.P. Arrieta, A. Mujica-Garcia and D. Lopez ,"6 - Smart Polymers", Modification of Polymer Properties, Published by Elsevier Inc, 2017.
- 6- M. Addingron and D.L.Schedek, " Smart materials and new technologies for the architecture and design professions", Published by Elsevier, 2005.
- 7- S. K. Melly, L. Liu, Y. Liu & J. Leng,"Active composites based on shape memory polymers: overview, fabrication methods, applications, and future prospects", Journal of Materials Science, Vol .55, pp .10975–11051,2020, <https://doi.org/10.1007/s10853-020-04761-w>.
- 8- F. Quadrini ,Leandro Iorio,Denise Bellisario and Loredana Santo ,"Durability of Shape Memory Polymer Composite Laminates under Thermo-Mechanical Cycling ", Journal of Composites Science, Vol. 6,No. 91, pp.2-12, 2022; <https://doi.org/10.3390/jcs6030091>.
- 9- A. Kausar, " Shape memory polymer/graphene nanocomposites: State-of-the-art", journal e-Polymers ,Vol.22 ,No.1, 2022, <https://doi.org/10.1515/epoly-2022-0024>.

References

- 10- D. R. Askeland, Pradeep P. Fulay, "Essentials of Materials Science and Engineering ", Second Edition, Published by RPK Editorial services, ASCO type setters USA, 2009.
- 11- Y.Wah Chung, Monica Kapoor, "Introduction to Materials Science and Engineering - 2nd edition" , Published by CRC Press, 2022.
- 12- S. Zhu, " Study on Smart Materials Using in Civil Engineering", Advances in Social Science, Education and Humanities Research, Vol.631, pp.1462-1466, 2022,
<https://doi.org/10.2991/assehr.k.220105.269>.
- 13- M. Bashir, Chih Fang Lee and Parvathy Rajendran, "Shape memory materials and their applications in aircraft morphing: an introspective study", ARPN Journal of Engineering and Applied Sciences, Vol.12, No. 19, pp. 5434 – 5446, 2017.
- 14- A. Basit, "Development and characterization of shape memory polymer composite actuator for morphing structures", thesis submitted to fulfil the requirement for the degree of Doctor of philosophy (PhD) in mechanics, University de Haute Alsace (UHA) Laboratoire de physique et Mecanique Textiles (LPMT), 2016.
- 15- H. Holman , Minoo Naozer Kavarana , Taufiek Konrad Rajab, "Smart materials in cardiovascular implants: Shape memory alloys and shape memory polymers, "Artificial Organs, Vol.45, No.5, pp.454-463, 2021.
- 16- A. Lendlein , Steffen Kelch, "Shape-Memory Polymers", Angewandte international Edition Chemie, Vol.41, No.12, pp. 2034-2057, 2002.
- 17- M. J. Haskew and John G. Hardy, "A Mini-Review of Shape-Memory Polymer-Based Materials : Stimuli-responsive shape-memory polymers", Johnson Matthey Technology Rev., Vol. 64, No.4, pp.425-442, 2020.

References

- 18- A. Shojaei and Guoqiang Li, "Thermomechanical constitutive modelling of shape memory polymer including continuum functional and mechanical damage effects", Proceedings of the Royal Society , 2014, <http://rspa.royalsocietypublishing.org/subscriptions>.
- 19- A. Reghunadhan, Keloth Paduvilan Jibin , Abitha Vayyaprontavida Kaliyathan , Prajitha Velayudhan , Michał Strankowski , and Sabu Thomas,"Shape Memory Materials from Rubbers", Journals Materials Vol. 14 No.23, pp .1-19, 2021, <https://doi.org/10.3390/ma14237216>.
- 20- C. F. Jasso-Gastinel, Jose M. Kenny, "Modification of polymer properties", Published by Elsevier, 2017.
- 21- T..Mu, Liwu.Liu, Xin.Lan,Yanju.Liu,Jinsong.Leng,"Shape memory polymers for composites",Composites Science and Technology,Vol. 160, , pp.169-198, 2018, <https://doi.org/10.1016/j.compscitech.2018.03.018>.
- 22- M. Behl, Andreas Lendlein,"Shape-Memory Polymers", Journal materials today,Vol. 10, No. 4, pp. 20-28, 2007, [https://doi.org/10.1016/S1369-7021\(07\)70047-0](https://doi.org/10.1016/S1369-7021(07)70047-0).
- 23- S. Pisani , Ida Genta , Tiziana Modena , Rossella Dorati , Marco Benazzo and Bice Conti, "Shape-Memory Polymers Hallmarks and Their Biomedical Applications in the Form of Nanofibers", International Journal of Molecular Sciences, Vol. 23, No. 3,pp.2-20, 2022, <https://doi.org/10.3390/ijms23031290>.
- 24- D.L. Safranski, Jack C Griffis, "Shape-memory polymer device design", Published by Elsevier Inc, 2017.
- 25- W.M. Huang, Bin Yang, Yong Qing Fu, "Polyurethane Shape Memory Polymers". Published by CRC press Taylor and Francis Group , LLC.2012.
- 26- T. Ramani, "Thermo-mechanical characterization of carbon-reinforced shape memory polymer", Thesis Submitted in partial fulfill of the

References

- requirements for the degree of Master of Science in Civil Engineering in the Graduate College of the University of Illinois at Urbana-Champaign, 2017.
- 27- S. Kirwa Melly, Liwu Liu, Yanju Liu, Jinsong Leng, "Active composites based on shape memory polymers: overview, fabrication methods, applications, and future prospects", *Journal of Materials Science* Vol.55, pp. 10975-11051, 2020.
- 28- I. A. Rousseau and Tao Xiea, "Shape memory epoxy: Composition, structure, properties and shape memory performances", *Journal of Materials Chemistry*, Vol.20, No. 17, pp. 3431-3441, 2010.
- 29- S.Cai- Li, Li-Nong Lu, Wei Zeng, "Thermostimulative shape-memory effect of reactive compatibilized high-density polyethylene/poly(ethylene terephthalate) blends by an ethylene-butyl acrylate-glycidyl methacrylate terpolymer", *Journal of Applied Polymer Science* ,Vol.112 , No.6 ,pp. 3341 - 3346,2009.
- 30- P. A. Quiñonez, Leticia Ugarte, Diego Bermudez, Paulina Chinolla, "Design of Shape Memory Thermoplastic Material Systems for FDM-Type Additive Manufacturing", *Materials*, Vol.14, No.15, pp.6-19,2021.
- 31- S.N.Saud AL-Humair, H.Sh.Majdi, A.N.Saud Al-Humair and M.H.Al-Maamori, " Future Prospects: Shape Memory Features in Shape Memory Polymers and Their Corresponding Composites", chapter in Book , "Smart and Functional Soft Materials ", Edited Xufeng Dong, publish with Intechopen. 2019, doi: <http://dx.doi.org/10.5772/intechopen.84924>.
- 32- J. A. Jacobs and Thomas F. Kilduff, "Engineering Materials Technology : Structures, Processing, Properties, and Selection - 5th edition" ,University of Michigan, Pearson/Prentice Hall, 2005.
- 33- K. Han Kiu , "study of adhesion properties of natural rubber, epoxidized natural rubber, and ethylene-propylene diene terpolymer-based adhesives",

References

- A thesis submitted in fulfil of the requirements for the Degree of Master of Science, Universiti Sains Malaysia, 2007.
- 34- S. K.K." Natural rubber latex filler masterbatch by soap sensitised coagulation preparation processing and evaluation". A thesis submitted in fulfilment of the requirements for the degree of Doctor of Faculty of Technology, Cochin University of Science and Technology , India 2014.
- 35- A. C Rustan, Christian A Drevon, "Fatty Acids: Structures and Properties", Encyclopedia of life Sciences , 2005,
<https://doi.org/10.1038/npg.els.0003894>.
- 36- A. Mortensen, Fernando Aguilar, Riccardo Crebelli, Alessandro Di Domenico, Birgit Dusemund, Maria Jose Frutos, Pierre Galtier, David Gott, Ursula Gundert-Remy, Jean-Charles Leblanc, Oliver Lindtner, Peter Moldeus, Pasquale Mosesso, Dominique Parent-Massin, Agneta Oskarsson, Ivan Stankovic, Ine Waalkens-Berendsen, Rudolf Antonius Woutersen, Matthew Wright, Maged Younes, Polly Boon, Dimitrios Chrysafidis, Rainer Gurtler, Paul Tobback, Petra Gergelova, Ana Maria Rincon and Claude Lambr, "Re-evaluation of fatty acids (E 570) as a food additive", EFSA Journal, Vol.15 No.5, pp. 1-49, 2017
<https://efsa.onlinelibrary.wiley.com/doi/full/10.2903/j.efsa.2017.4785>.
- 37- S. Pimple, Shilpa Nagapurkar, "Shape Memory Polymers in Deployable Architecture", International Journal of Engineering Research, Vol.7, No. 3, pp. 321-324, 2018, doi : 10.5958/2319-6890.2018.00085.5.
- 38- J. Li, Qiuhua Duan, Enhe Zhang, Julian Wang ."Applications of Shape Memory Polymers in Kinetic Buildings" Hindawi, Advances in Materials Science and Engineering, Vol. 2018, pp.1-13, Article ID 7453698, 2018
<https://doi.org/10.1155/2018/7453698>.

References

- 39- M. O. Goka , Mehmet Z. Bilira, Banu H. Gurcumb," Shape-Memory Applications in Textile Design", Procedia - Social and Behavioral Sciences, Vol.195, pp. 2160 – 2169 , 2015,
<https://doi.org/10.1016/j.sbspro.2015.06.283>.
- 40- L. Sun, W.M. Huang, T.X. Wang, H.M. Chen, C. Renata, L. W. He, P. Lv, C.C. Wang," Elastic polymeric shape memory materials for comfort fitting: a brief review of recent progress", Materials & Design, Volume Vol. 136, pp. 238-248,2017,
<https://doi.org/10.1016/j.matdes.2017.10.005>.
- 41- D. J. Maitland, Landon Nash,"Shape Memory Polymer Technology", Nsert to Endovascular Today , Vol. 20, No. 4, pp. 74-78, 2021,
<https://evtoday.com/articles/2021-apr/shape-memory-polymer-technology>.
- 42- M. C. Serrano, Guillermo A. Ameer, "Recent Insights Into the Biomedical Applications of Shape-memory Polymers", Macromolecular bioscience, Vol.12, No.9,pp. 1156-1171, 2012,
<https://doi.org/10.1002/mabi.201200097>.
- 43- M. Bothe."Shape Memory and Actuation Behavior of Semicrystalline Polymer Networks", presented by Dipl.-Phys. Martin Bothe from Tuebingen from Faculty II – Mathematics and Natural Sciences of the Technical University of Berlin for obtaining the academic degree Doctor of Science, Berlin 2014.
- 44- X. Chen, "Synthesis of 10-Carboxy-N-decyl-N, N'-dimethydecyl-1-ammonium bromide as organogelator & room temperature shape memory programming of stearic acid/natural rubber bilayer blend", A thesis, The graduate Faculty of The University of Akron, pp. 1-73 , 2017.
- 45- F. Li, Yan Chen, Wei Zhu, Xian Zhang, Mao Xu,"Shape memory effect of polyethylene/nylon 6 graft copolymers", journal of Polymer Vol.39, No.26, pp. 6929-6934,1998,

References

- [https://doi.org/10.1016/S0032-3861\(98\)00099-8](https://doi.org/10.1016/S0032-3861(98)00099-8).
- 46- F. Li, Richard C. Larock, "New soybean oil–styrene–divinylbenzene thermosetting copolymers. v. shape memory effect", *Journal of Applied Polymer science* , Vol.84, No. 8, pp. 1533-1543, 2002.
- 47- S. Rezanejad, Mehrdad Kokabi, "Shape memory and mechanical properties of cross-linked polyethylene/clay nanocomposites", *European Polymer Journal*, Vol. 43, No. 7, pp.2856-2865, 2007.
- 48- B. Heuwers, D. Quitmann, F. Katzenberg, J. C. Tiller, "Stress-Induced Melting of Crystals in Natural Rubber: a New Way to Tailor the Transition Temperature of Shape Memory Polymers", *Macromolecular Rapid Communications* , Vol. 33, No. 18, pp. 1517-1522, 2012.
- 49- B. Heuwers, A. Beckel, A. Krieger, F. Katzenberg, J. C. Tiller, "Shape-Memory Natural Rubber: An Exceptional Material for Strain and Energy Storage" *Macromolecular Chemistry and Physics*, Vol. 214, pp. 912–923, 2013.
- 50- R. Hoehner, T. Raidt, M. Rose, F. Katzenberg, J. C. Tiller, "Recoverable strain storage capacity of shape memory polyethylene", *Journal of polymer science/ part B: polymer Physics* ,Vol. 51, No.13, pp. 1033-1040, 2013.
- 51- J. Shin, "Shape Memory Elastomers and Fatty Acid Organogels: Functional Materials from Small Molecule Additives", A Thesis of Master , The Graduate Faculty of The University of Akron, 2013.
- 52- N. R. Brostowitz, R. A. Weiss, and K. A. Cavicchi, "Facile Fabrication of a Shape Memory Polymer by Swelling Cross-Linked Natural Rubber with Stearic Acid", *American Chemical Society, (ACS) Macro Lett*, Vol. 3, No.4, pp. 374–377, 2014.
- 53- A. Wang and Guoqiang Li, "Stress memory of a thermoset shape memory polymer", *Journal of Polymer Science*, Vol. 132, No. 24, pp1-11,2015, <https://doi.org/10.1002/app.42112>.

References

- 54- F. Xie, C. Huang, F. Wang, L. Huang, R. A. Weiss, J. Leng, Y. Liu, "Carboxyl-Terminated Polybutadiene–Poly(styrene-co-4-vinylpyridine) Supramolecular Thermoplastic Elastomers and Their Shape Memory Behavior," *Macromolecules*, Vol. 49, No.19, pp.7322–7330, 2016. <https://doi.org/10.1021/acs.macromol.6b01785>.
- 55- L. Xia, Jiayu Xian, Jieting Geng, Yan Wang, Feifei Shi, Zuoyan Zhou, Na Lu, Aihua Du, Zhenxiang Xin, " Multiple shape memory effects of trans-1,4-polyisoprene and low-density polyethylene blends", *Journal of Polymer International*, Vol.66, No.10, pp.1382-1388, 2017 <https://doi.org/10.1002/pi.5387>.
- 56- J. Sze- Huawee, Ai Bao Chai , Jee -Hou Ho, " Fabrication of shape memory natural rubber using palmitic acid," *Journal of King Saud University – Science*, Vol.29, No.4, pp, 494-501, 2017.
- 57- M. Pantoja, Z. Lin, and M. Cakmak, and K. A. Cavicch, "Structure-property relationships of fatty acid swollen, crosslinked natural rubber shape memory polymers", *Journal of polymer science, part B: polymer physics*, Vol.56, pp.673-687, 2018.
- 58- R. Abishera, R. Velmurugan, KV. Nagendra Gopal, "Free, partial, and fully constrained recovery analysis of cold-programmed shape memory epoxy/carbon nanotube nanocomposites: Experiments and predictions", *Journal of Intelligent Material Systems and Structures*, pp.1-13, 2018, <https://doi.org/10.1177/1045389X18758187>.
- 59- G. Capiel, Norma E. Marcovich, Mirna A Mosiewicki, " From the synthesis and characterization of methacrylated fatty acid based precursors to shape memory polymers", *Journal of Polymer International*, Vol.68, No.3, pp.546-554, 2018.
- 60- N. M. Setyadewi and I .N. Indrajati, "Shape Memory Behavior Of Shape Memory Natural Rubber", *IOP. Conf. Series: Materials Science and*

References

- Engineering. Vol.553, pp.1-5, 2019, doi:10.1088/1757-899X/553/1/012050.
- 61- N.M. Setyadewi, I.N. Indrajati and N. Darmawan." Mechanical properties and curing characteristics of shape memory natural rubber", IOP Conf. Series: Materials Science and Engineering ,Vol.541 , pp. 1-5 ,2019, doi:10.1088/1757-899X/541/1/012012.
- 62- L. Xia, Shuai Chen, Wenxin Fu and Guixue Qiu ,"Shape Memory Behavior of Natural *Eucommia ulmoides* Gum and Low-Density Polyethylene Blends with Two Response", *Polymers*, Vol 11, No.4, pp.1-11, 2019, <https://doi.org/10.3390/polym11040580>.
- 63- T. Sengsuk, Sililak Intom, Ladawan Songtipya, Jobish Johns, Krisadakon Chawengsaksopak," Shape Memory Thermoplastic Natural Rubber for Forensic Applications", IOP Conference Series: Materials Science and Engineering, Vol.553,2019, [doi:10.1088/1757-899X/553/1/012045](https://doi.org/10.1088/1757-899X/553/1/012045).
- 64- N. Maryam Setyadewi, Hesty Mayasari, " The Effect of Different Types of Carbon Black on Thermal Characteristics of Shape Memory Natural Rubber Vulcanizate", *Indonesian Polymer Journal* , Vol.22, No.2, pp. 1-3, 2019.
- 65- W. Wu, Chuanhui Xu, Zhongjie Zheng, Baofeng Lin and Lihua Fua, " Strengthened, recyclable shape memory rubber films with a rigid filler nano-capillary network" ,*Journal of Materials Chemistry A*, No. 12, pp.1-15, 2019, [Doi:10.1039/C9TA01266D](https://doi.org/10.1039/C9TA01266D).
- 66- Q. Yang, Wenjie Zheng, Wenpeng Zhao, Chuang Peng, Juntao Ren, Qizhou Yu, Yanming Hu and Xuequan Zhang, " One-way and two-way shape memory effects of a high-strain cis-1,4-polybutadiene–polyethylene copolymer based dynamic network via self-complementary quadruple hydrogen bonding" , *Polymer Chemistry*, No. 6, 2019, doi:10.1039/C8PY01614C.

References

- 67- L. Zhou, " Investigation of The Shape Memory Behaviour of Stearic Acid Swollen, Crosslinked EPDM Elastomers ", Thesis submitted Fulfillment Of the Requirement for the Degree Master of Science, University of Akron ,2019.
- 68- J. Teng, Zhenqing Wang, Jingbiao Liu, Xiaoyu Sun, " Thermodynamic and shape memory properties of TPI/HDPE hybrid shape memory polymer", Polymer Testing, Vol. 81, pp.1-28, 2020,
<https://doi.org/10.1016/j.polymertesting.2019.106257>.
- 69- Y. Ren, Zhuan Zhuan Zhang, Wenlong Xia, Qifeng Zhou, Xiaofeng Song," Water-responsive shape memory PLLA via incorporating PCL-(PMVS-s-PAA)-PCL-PTMG-PCL-(PMVS-s-PAA)-PCL",European Polymer Journal, Vol.147, pp.1-4, 2021,
<https://doi.org/10.1016/j.eurpolymj.2020.110252>.
- 70- R. Zhang, Jing Tian, Yihui Wu, Weimin Chou, Jiayuan Yang, Ping Xue , " An investigation on shape memory behaviors of UHMWPE -based nanocomposites reinforced by grapheme nanoplatelets",PolymerTesting,Vol.99,pp.1-33,2021,
<https://doi.org/10.1016/j.polymertesting.2021.107217>.
- 71- C. B. Cooper, Shayla Nikzad, Hongping Yan, Yuto Ochiai, Jian-Cheng Lai, Zhiao Yu, Gan Chen, Jiheong Kang, and Zhenan Bao,"High Energy Density Shape Memory Polymers Using Strain-Induced Supramolecular Nanostructures", ACS Central Science, Vol.7, No.10, pp.1657–1667, 2021,
<https://doi.org/10.1021/acscentsci.1c00829>.
- 72- N. Lehman, Ladawan Songtipya, Jobish Johns and Korakot Maliwankul,"Shape memory thermoplastic natural rubber for novel splint applications", eXPRESS Polymer Letters, Vol.15,No.1,pp.28-38,2021,
<https://doi.org/10.3144/expresspolymlett.2021.4>.

References

- 73- F. Quadrini , Leandro Iorio, Denise Bellisario and Loredana Santo," Durability of Shape Memory Polymer Composite Laminates under Thermo-Mechanical Cycling", Journal of Composites Science, Vol.6,No. 91, pp.1-12, 2022, <https://doi.org/10.3390/jcs6030091>.
- 74- J. Ming Yang, Pradeep Kumar Panda, Chia Jing Jie, Pranjyan Dash, Yen-Hsiang Chang,"Poly (vinyl alcohol)/chitosan/sodium alginate composite blended membrane: Preparation, characterization, and water-induced shape memory phenomenon", Polymer Engineering and Science, Vol.62, No.5 , pp.1526-1537,2022, <https://doi.org/10.1002/pen.25941>.
- 75- Y. Yang Kow1,Ai Bao Chai, Jee Hou Ho ,"Relationships between swelling temperature and shape memory properties of palmitic acid-based shape memory natural rubber", Journal of Rubber Research, Vol. 23,No.10, pp. 13–22,2020, doi:10.1007/s42464-019-00031-w.
- 76- A. Biswas, Akhand Pratap Singh, Dipak Rana,Vinod K. Aswal and Pralay Maiti," Biodegradable toughened nanohybrid shape memory polymer for smart biomedical applications" Nanoscale,Vol.10,No.,21,. pp . 9917-9934, 2018, <https://doi.org/10.1039/C8NR01438H>.
- 77- S. Song, Jiachun Feng and Peiyi Wu," A New Strategy to Prepare Polymer-based Shape Memory Elastomers", Macromolecular. Rapid Communications, Vol. 32 ,No.19 , pp.1569-1575, 2011 , <https://doi.org/10.1002/marc.201100298>.
- 78- Y.Yan Cui , Bao-Jian Dong , Bao-Long Li and Shu-Cai Li,"Properties of Polypropylene/Poly(ethylene terephthalate) Thermostimulative Shape Memory Blends Reactively Compatibilized by Maleic Anhydride Grafted Polyethylene-Octene Elastomer", International Journal of Polymeric Materials and Polymeric Biomaterials ,Vol. 62,No.13, pp. 671-677,2013, <https://doi.org/10.1080/00914037.2013.769225>.

References

- 79- T. Xie, "Recent advances in polymer shape memory", *Polymer*, Vol. 52, No. 22, pp. 4985–5000, 2011, doi:10.1016/j.polymer.2011.08.003.
- 80- H. Liu, Shu-Cai Li, Yi Liu, Mahmood Iqbal, "Thermo stimulative shape memory effect of linear low-density polyethylene/polypropylene (LLDPE/PP) blends compatibilized by crosslinked LLDPE/PP blend (LLDPE-PP)", *Journal of Applied Polymer Science*, Vol. 122, No. 4, pp. 2512 – 2519, 2011, <https://doi.org/10.1002/app.34345>.
- 81- B. Kumar, Nuruzzaman Noor, Suman Thakur, Ning Pan, Harishkumar Narayana, Siu-cheong Yan, Faming Wang, and Parth Shah, "Shape Memory Polyurethane-Based Smart Polymer Substrates for Physiologically Responsive, Dynamic Pressure (Re)Distribution", *ACS Omega*, Vol. 4, No. 13, pp. 15348–15358, 2019, <https://doi.org/10.1021/acsomega.9b01167>.
- 82- N. Zheng, Guangqiang Fang, Zhengli Cao, Qian Zhao, Tao Xie, "High Strain Epoxy Shape Memory Polymer," *Polymer Chemistry*, Vol. 6, No. 16, pp. 3046–3053, 2015, doi:10.1039/c5py00172b.
- 83- Y. Liu, Ying Li, Guang Yang, Xiaotong Zheng, and Shaobing Zhou, "Multi-Stimulus-Responsive Shape-Memory Polymer Nanocomposite Network Cross-Linked by Cellulose Nanocrystals", *ACS Applied Materials and Interfaces*, Vol. 7, No. 7, pp. 4118–4126, 2015, <https://doi.org/10.1021/am5081056>.
- 84- Y. Chen, Kunling Chen, Youhong Wang, and Chuanhui Xu, "Biobased Heat-Triggered Shape-Memory Polymers Based on Polylactide/Epoxidized Natural Rubber Blend System Fabricated via Peroxide-Induced Dynamic Vulcanization: Co-continuous Phase Structure, Shape Memory Behavior, and Interfacial Compatibilization", *Industrial & Engineering Chemistry Research*, Vol. 54, No. 35, pp. 8723–8731, 2015, <https://doi.org/10.1021/acs.iecr.5b02195>.

References

- 85- R. Abbas and Mohammed Al-Maamori, "Design and performance Evaluation of the Shape memory characterization machine for (SMPs)", American Institute of physics, AIP Conference Proceedings 2437, 020064 , 2022. <https://doi.org/10.1063/5.0092357>.
- 86- W. C. Chen , S. M. Lai , M. Y. Chang and Zong-Ching Liao, "Preparation and Properties of Natural Rubber (NR)/Polycaprolactone (PCL) Bio-Based Shape Memory Polymer Blends", Journal of Macromolecular Science, Part B, Physics, Vol. 53, No.4, pp. 645-661, 2014, <https://doi.org/10.1080/00222348.2013.860304>
- 87- K.L. Mok1 and A.H. Eng, "Characterisation of Crosslinks in Vulcanised Rubbers: From Simple to Advanced Techniques" ,Malaysian Journal of Chemistry, Vol. 20, No.1, pp. 118 – 127.2018.
- 88- I. Surya, Syahrul Fauzi Siregar, " Cure Characteristics and Crosslink Density of Natural Rubber/Styrene Butadiene Rubber Blends" Journal Teknik Kimia USU, Vol. 3, No. 4 , pp. 1-5,2014.
- 89- F. Abbas Hadi Fuliful." Preparation and study of Characterization of Acid Resistant rubber composites and their Applications, A thesis Submitted to fulfill the requirement for the degree of Doctor philosophy (PhD) science / physics, University of Babylon – College of science , 2020.
- 90- G. Capiel, N. E. Marcovich, M. A. Mosiewicki, " Shape memory polymer networks based on methacrylated fatty acids," European Polymer Journal , Vol.116, pp. 321-329,2019.
- 91- G. Tamura, Y. Shinohara, A. Tamura, Y. Sanada, M. Oishi, I. Akiba, Y. Nagasaki, K. Sakurai and Y. Amemiya, " Dependence of the swelling behavior of a pH-responsive PEG-modified nanogel on the cross-link density", Polymer Journal , Vol.44, pp. 240–244,2012.
- 92- T. Komatsu, " Vulcanization Accelerators", International Polymer Science and Technology, Vol. 36, No. 7, pp. 49-55, 2009.

References

- 93- S.kai Hu, Si Chen, Xiu-ying Zhao, Ming-ming Guo and Li-qun Zhang , " The Shape-Memory Effect of Hindered Phenol (AO-80)/Acrylic Rubber (ACM) Composites with Tunable Transition Temperature," *Materials*, Vol.11,No.12, 2018,<https://doi.org/10.3390/ma11122461>.
- 94- S. Kirwa Melly, Liwu Liu, Yanju Liu and Jinsong Leng, "Active composites based on shape memory polymers: overview, fabrication methods, applications, and future prospects", *Journal of Materials Science*, Vol. 55, pp. 10975–11051,2020, <https://doi.org/10.1007/s10853-020-04761-w>.

Appendix

Ministry of Health
Babil Health Directorate
Imam Sadiq Educationl Hospital
e- Imam Sadigh@gmail.com

جمهورية العراق



وزارة الصحة
دائرة صحة محافظة بابل

مستشفى الإمام الصادق (ع) التعليمي
شعبة الأمور الإدارية والمالية
وحدة الموارد البشرية

العدد
التاريخ / ٢٠٢٢ / ٩ / ٩

إلى/جامعة بابل / كلية هندسة المواد

م/إجابة

إشارة الي كتابكم المرقم ٣٠٩٢ في ٢٠٢٢/٩/١ المتضمن بيان راي حول
البحث الموسوم preparation and characterization of shape memory polymer materials in industrial application
نود اعلامكم باننه تم فحص المادة في مركز الاشعاع في مستشفانا وهي تعد
بادنه جيدة جدا للحاجة الماسة لها في علاج مرضى السرطان لكون الاقنعة
استهلاكية وغالية الثمن ويمكن الاستفادة منها مستقبلا مع ملاحظة مايلي
١- سمك المادة بحاجة ان يكون اكثر من ٢-٣ ملم
٢- حرارة التصلب تكون بدرجة حرارة الغرفة خلال وقت اقصر
٣- مقدار الصلابة للمادة بعد الجفاف بحاجة لزيادة لتقليل حركة المريض
اثناء العلاج

للتفضل بالاطلاع ٠٠٠ مع الاحترام

الدكتور
ماجدي ياس خضير السعدي
مدير مستشفى الإمام الصادق التعليمي
رئيس مجلس الإدارة
مدير مستشفى الإمام الصادق التعليمي

رئيس مجلس الإدارة

٢٠٢٢/٩/٩

نسخه منه الى:

- مكتب مدير المستشفى .
- معاون الإداري / قسم الاشعاع
- الموارد البشرية / الأرشيف .



Ref. No :

Date: / /

العدد : ٢٠٩٢

التاريخ : ٢٠٢٢ / ٩ / ١



السلي / دائرة صحة بابل / قسم البحث والتطوير / مستشفى الامام الصادق / وحدة الامراض السرطانية

م / دراسة

تهديكم كلية هندسة المواد اطيب تحياتها و تود بيان رأيكم حول امكانية الاستفادة من البحث الموسوم :

(Preparation and Characterization of Shape Memory Polymer Materials in Industrial Application)

(تحضر وتوصيف مواد بوليميرية ذات ذاكرة الشكل في التطبيقات الصناعية) لطالبة الدراسات العليا / الدكتوراه/ قسم هندسة البوليمرات والصناعات البتروكيميائية (رولا عبد الخضر عباس) وبإشراف الاستاذ الدكتور (محمد حمزة المعموري)

مع الاحترام

أ.د عماد علي دشر الحيدري
عميد كلية هندسة المواد وكالة
٢٠٢٢ / ٩ / ١

المرفات

- نسخة من البحث



نسخة منه المرز -
- الشؤون العلمية - مع الاذونات
- الاصدار العامة -

Design and performance evaluation of the shape memory characterization machine for (SMPs)

Cite as: AIP Conference Proceedings 2437, 020064 (2022); <https://doi.org/10.1063/5.0092357>
Published Online: 17 August 2022

Rola Abdul Al Khader Abbas and Mohammed Hamza Al-Maamori



View Online



Export Citation



Lock-in Amplifiers
up to 600 MHz



Zurich
Instruments



AIP Conference Proceedings 2437, 020064 (2022); <https://doi.org/10.1063/5.0092357>

2437, 020064

© 2022 Author(s).

Certificate of Participation

Awarded to

Author/s: Kola Abbas and Mohammed Al-Maamori

Title: Design And Performance Evaluation of the Shape Memory
characterization Machine for (SMCs)

Speaker: Kola Abbas

International Conference on
Technologies and Materials for Renewable Energy, Environment and Sustainability
TARREC21 or Int'l Conf. Athens - Greece. 28-29-30 May, 2021.



European Academy for Sustainable Development
EASD, Decree S18550004-S230Z, 57, France
Chalix-Touma Salame

A handwritten signature in black ink, appearing to read "Chalix-Touma Salame".

The Classification of the Stress-Strain Curve Zones on the Basis of their Validity to Study the Shape Memory Effect (SME) Property

Rola Abdul Al Khader Abbas^a, Mohammed Hamza Al-Maamori^b

University of Babylon, College of Materials Engineering-Polymer and the Petrochemical Industries

^a100153@uotechnology.edu.iq

^bmat.mohammed.hamzah@uobabylon.edu.iq

Keywords: SM- rubber, Rubber band, Stearic acid, Tensile test, Classical Tensile programming, Stress- Strain curve.

Abstract. This study attempts to emphasize a pre-step for determining the permitted deformations (strains) extents. This is for changing the original molecular architecture shape for the materials under study (rubber band/stearic acid (RB/ based SA) and Rubber band without stearic acid (RB without SA). It is necessary as a basic controlling step in the choosing process of the appropriate programming method to show the shape memory effect (SME) property. By this property, the polymers are either described as shape memory effect (SME) or conventional polymers. If the material was proved to have the shape memory effect (SME) property, then it will be allowed to predict many thermo-mechanical properties. So for these materials, the (stress-strain) curve zones have been classified according to the ability of the deformation memory, which can be erased and programmed again after the immediate removal of the applied tensile force. This can be achieved by calculating the residual strain ratio. The comparative results showed that the elastic and plateau zones were classified respectively as valid for the study of the (SME) property. While for the Hardening strain and fracture zones, they were classified as bad and very bad respectively for the study of this property.

Introduction

The light weight, high capability for shape recovery (multiple recovery), ease of manufacture, excellent chemical stability, high capability for recycling, reusing at low cost, and giving a broad extent of deformations in the molecules shape allowing the designing and tailoring of these thermo-mechanical properties according to desire or need all these features have made the shape memory polymers (SMPs) to be active materials more than the rest materials in a set of applications such as micro-biomedical, equipment, components, deployable, aerospace, actuation devices, etc. [1][2][3][4][5].

The shape memory materials are a class of the smart materials which have the ability to return from the fixity temporary shape to the permanent original shape at any point of time by applying the right stimulus to them [1], this is known as the shape memory effect (SME). As examples for this type of smart materials: shape memory polymers (SMPs), shape memory alloys (SMAs), and Shape memory ceramics (SMCs) [2].

As well as, these polymers (SMP) are considered as not smart materials in the absence of a process called as “programming” or “training”. Programming is considered as the direct responsible in showing the shape memory effect property that is not inherent in this type of polymers [5][6][7]. As mentioned, it can be said that the (SMP) polymer is a conventional not smart polymer if there are no exceptional conditions that assist in controlling it through what is named “programming cycle” [6].

Hence the transformation process of the SMP polymer from conventional to smart polymer should be connected to the programming cycle to get a basic idea about the prediction possibility through experiment in wide levels of the molecular architecture shapes. For a single polymer, they are dominant for a period of time, may be last forever as long as it is not stimulated by the right stimulus depending on the researcher or the design requirements [3][8]. So the method of showing the shape



Available online at www.sciencedirect.com

ScienceDirect

Energy Reports 8 (2022) 204–217



www.elsevier.com/locate/egy

TMREES22-Fr, EURACA, 09 to 11 May 2022, Metz-Grand Est, France

The role of the melting and crystallizing of the stearic acid network in retaining and releasing the mechanical deformation energy during the hot classical shape memory cycle

Rola Abdul Al Khader Abbas*, Mohammed Hamza Al-Maamori

College of Materials Engineering - Polymer and the Petrochemical Industries, University of Babylon, Iraq

Received 14 June 2022; accepted 25 June 2022

Available online xxxx

Abstract

Shape memory natural rubber (SMNR) was prepared using a technique, Elastomer/small molecule blend shape memory polymers (SMPs), by impregnating the commercial natural rubber band (RB) with molten stearic acid (SA) for 2 h and at a temperature of 75 °C, to form commercial natural rubber band RB/based stearic acid (SA) blend SMP, (RB/based SA). Then the success and obstacles indications have been observed in fixing the applied strain of the value of 70% and shape recovery during the hot classical shape memory cycle. This cycle is dependent on the normal cooling at room temperature. That is done by studying the relation of the applied strain with the physico-mechanical phenomena accompanying the activation and deactivation stage of the SME property during this thermo-mechanical cycle. The results of the SME property examination showed that the occurrence of the thermal contraction and elastic retraction is directly responsible for the loss of a part of the elastic applied strain. The value of the applied strain that was restricted is 58.7% instead of 70% after the end of the activation stage, while the plastic strain accumulation was the direct responsibility for the material not being back to its original shape at 100% after the end of the deactivation stage. At the same time, this study shows that the relation of these phenomena to the stretching work energy during the thermo-mechanical cycle is a relationship that falls under the dominance of the first law of thermodynamics and that the shape memory of RB/based SA is only related to the elastic stretching work energy.

© 2022 The Authors. Published by Elsevier Ltd. This is an open access article under the CC BY-NC-ND license

(<http://creativecommons.org/licenses/by-nc-nd/4.0/>).

Peer-review under responsibility of the scientific committee of the TMREES22-Fr, EURACA, 2022.

Keywords: Shape memory effect; Commercial natural rubber band; Stearic acid; Energy conservation law; Shape-memory natural rubber

1. Introduction

The lightweight, high capability for shape recovery (multiple recoveries), ease of manufacture, excellent chemical stability, high capability for recycling, reusing at low cost, and giving a broad extent of deformations in the shape of the molecule allow to obtain excellent thermo-mechanical properties. To get such desired properties, considerable attention has been made toward researching and manufacturing the shape memory polymers (SMPs) to be active

* Corresponding author.

E-mail address: 100153@uotechnology.edu.iq (R.A.A.K. Abbas).

<https://doi.org/10.1016/j.egy.2022.06.119>

2352-4847/© 2022 The Authors. Published by Elsevier Ltd. This is an open access article under the CC BY-NC-ND license (<http://creativecommons.org/licenses/by-nc-nd/4.0/>).

Peer-review under responsibility of the scientific committee of the TMREES22-Fr, EURACA, 2022.

The Relation of the Cross-link Density to Shape Memory of the Smart Vulcanized Natural Rubber

Rola Abdul Al Khader Abbas ^{a)}, Mohammed Hamza Al Maamori ^{b)}

College of Materials Engineering- Polymer and The Petrochemical Industries, University of Babylon, Iraq

^{a)} rola.alsaffi@gmail.com

^{b)} prof.almaamori@gmail.com

Abstract. Shape-memory natural rubber (SMNR) was prepared from the impregnation process of the smoked natural rubber type (ribbed smoke sheet, RSS) (after laboratory vulcanization (Virgin RSS) with different ratios of sulfur ranging from 0.75 to 2Phr) with stearic acid (SA) molten for a period of 2hr, so as to obtain shape memory rubber samples represented by (RSS/based SA). Then the process of testing the shape memory behavior was conducted by subjecting these samples under study to the hot classical shape memory cycle based on normal cooling at room temperature. The comparative results of calculating the shape memory parameters practically once and through digital imaging again, have showed that the impregnation of the vulcanized natural rubber with stearic acid leads to its transformation from a traditional vulcanized rubber to a shape memory rubber. This study also showed that the cross-link density increase is negatively affects the shape memory of this smart rubber.

Keywords: Natural rubber, stearic acid, shape memory behavior, cross-link density, hot classical shape memory cycle.

INTRODUCTION

The term “rubber materials”, or what are sometimes called “polydiene elastomers”, refers to a group of polymers that exhibit an elastic behavior, as these materials quickly return to their initial dimensions and original shape after the applied stress is removed. These materials are processed in two stages, in the first stage called primary processing, from which a suitable and marketable raw material is obtained, while in the second stage, the raw material is transformed into a final product by the process of vulcanization that links the chains of these materials to each other with three-dimensional linkages called “cross-link” [1-3]. Polydiene elastomers can be divided into two types:

1- Natural rubber (NR): It is a flexible hydrocarbon polymer (polyisoprene) with a chemical formula ($\text{CH}_2\text{CCH}_3\text{CH}=\text{CH}_2$), extracted from the sap of some plants called (Hevea brasiliensis). Where, the raw natural rubber is classified into several types differ from each other by the drying method and the percentage of rubber and color, among the most important of these types are [2-3]:

- Preserved and concentrated latex.
- Ribbed smoked sheet.
- Pale latex crepe and sole crepe.
- Field coagulum crepe.
- Technically specified rubber.

2-Synthetic rubber: It is obtained by controlling the polymerization process of certain chemicals. There are different types of synthetic rubber, each of which differs from the other according to the primary chemicals used and which are being polymerized. The most important types of synthetic rubber are the following:

- Synthetic cis- polyisoprene (PI).



European Academy for Sustainable Development "EURACA"
Decree. 818 559 064 - 8230Z



Acceptance Letter

TMREES Conference Series
Technologies and Materials for Renewable Energy, Environment and Sustainability
TMREES-2022 The 17th Int'l Conf. France, May 9 to 11, 2022.

Tuesday, April 26, 2022

Speaker: ...Rola Abbas.... / **Oral-Visio /ID:** #.1158../**SN:** 2207...
Authors: ...Rola Abbas and Mohammed Al Maamori.....
Paper Title: ...The Relation of the Cross-link Density to Shape Memory of the Smart Vulcanized Natural Rubber.....
Country: ...Iraq.....// **Affiliation:** ...University of technology.....
Publishers: *Accepted for American Institute of Physics (APC)*
Indexed: *Scopus, Web of Science (WOS), International Scientific Indexing (ISI)*
Metrics: *H-Index: 75 ISSN: 0094-243X, E-ISSN: 1551-7616*

Dear **Rola Abbas**,

We are pleased to inform you that your submission has been reviewed and received a positive recommendation by the Program Committee.

Your paper has been Accepted for American Institute of Physics (APC)! And thank you for your interest in the Tmrees2022-France International Conference (www.tmrees.org).

On behalf of the Conference Chairs Committee, we would like to formally invite you to participate the Tmrees2022-France International Conference on Technologies and Materials for Renewable Energy, Environment and Sustainability to present your paper by **Remote Video Presentation**.

We would like to inform you that presentations will be realized, thus you are kindly invited to register in advance to book a slot for your presentation:

www.tmrees.org

Date Time: May 9 to 11, 2022, 10:00 AM to 06:00 PM (Paris time)

We look forward to meeting you in **TMREES-2022 The 17th Int'l Conf. France, May 9 to 11, 2022**.

Best Regards,

On behalf of the General Chairs
Prof. Panagiotis Papageorgas
Department of Electrical
And Electronics Engineering
University of West Attica
Athens, Greece

European Academy for Sustainable Development

Certificate of Participation

Awarded to

Author/s: Kola Abbas and Mohammed Al Maamori

Title: The Relation of the Cross-link Density to Shape Memory of the Smart Vulcanized Natural Rubber

International Conference on
Technologies and Materials for Renewable Energy, Environment and Sustainability.
TARRES22 Fr Int'l Conf. Metz-Grand Est - France, 09-10-11 May, 2022.



European Academy for Sustainable Development
EURACA, Decree 818550064-8230Z, 57-France

Characterization of the Commercial Rubber Band as a Shape Memory Smart Material by Swelling process with fused stearic acid

Rola Abdul Al Khader Abbas
rola.alsaffi@gmail.com

Mohammed Hamza Al-Maamori
University of Babylon/ College of Materials Engineering- Polymer and The Petrochemical Industries

Abstract:

This study attempted to focus the light on the characterization possibility of the vulcanized, chlorinated, natural rubber products (as the commercial rubber band used in this study) as a shape memory smart material in the case of impregnating it with fused stearic acid by swelling mechanism.

Where in this study, the ability of the commercial rubber band on fixing the stretching strain chosen in this study which is of 70% after removing the applied load off the rubber band, was measured after impregnating it with stearic acid(SA) material of weight ratio (30.4%) and swelling time=2hr. At the same time, measuring the ability of that rubber band on rid of this mechanical deformation once it is thermally stimulated and returning to its original shape (before the deformation) by subjugating it to the hot classical shape memory cycle (based on normal cooling at room temperature) with its two stages represented by the shape memory effect (SME) property activation and deactivation stages. Also, the techniques of differential scanning calorimetry (DSC) and x-ray diffraction (XRD) were used to know the agreement between these tests and the SME property test results (thermomechanical cycle test).

Through the practical results of all the tests depending on the diagnosis, it was shown that the direct responsibility for the characterization of the commercial rubber band as a shape memory smart material is the stearic acid (SA) material, which acted as a lock in the rubber band structure that can be opened and closed with a temperature change within the melting range of (SA).

Keywords: Rubber band, stearic acid, DSC, XRD, shape memory polymer.

1- Introduction:

After the emergence of the concept of smart materials and the concept of shape memory, which led mankind to countless pioneering inventions, which led to rapid technological development in the twenty-first century, it is possible that this technological growth accelerates more and more in the coming years [1-5].

The “smart” characteristic in these materials refers to their ability to sense changes in their environments and then respond to these changes by changing one of their properties by the influence of this external environment such as temperature, light, pressure or it may be electricity and other stimuli, this property change can be repeated many times [1][4].An example of these materials is shape-memory materials (SMMs), which are named by this because they can undergo a change in dimensions in response to a variety of stimuli. This type of shape change smart materials can be divided into three basic types, which are [5-9]:

Certificate

THIS CERTIFICATE IS GRANTED TO

**Rola Abdul Al Khader Abbas and
Mohammed Hamza Al-Maamori**

This document certifies that the paper “Characterization of the Commercial Rubber Band as a Shape Memory Smart Material by Swelling Process with Fused Stearic Acid” by the authors Rola Abdul Al Khader Abbas and Mohammed Hamza Al-Maamori is accepted* for publication in the journal “Materials Science Forum” (ISSN print 0255-5476, ISSN web 1662-9752) and will be published in accordance with the publishing schedule in 2022 year.

November 30, 2022

Scientific team

*Before the publication all of the manuscripts accepted by editors undergo an additional internal quality check. They are verified for the absence of the plagiarism and redundant publication. The accepted manuscripts which do not pass this quality check are rejected from the publication in the journal.

الخلاصة:-

تم تحضير بوليمرات ذات ذاكرة الشكل (SMPs) Shape –memory polymers بطريقة انتفاخ (swelling) المطاط الطبيعي المفلكن بالحامض الدهني Fatty acid وفق تقنية Elastomer/ small molecular blend SMP، حيث استعملت في هذه الدراسة الحالية نوعان من المنتجات المطاطية كطور ثابت Stationary phase أو ما يطلق عليه أيضا بـ (الجزء الصلب Hard segment) في تحضير مطاط طبيعي ذكي ذات ذاكرة الشكل وهي:-

1-المنتج المطاطي التجاري المتمثل بالمطاط الطبيعي والذي رمز له في هذه الدراسة بالرمز (Virgin RB).

2-المنتج المطاطي المختبري المتمثل بالمطاط الطبيعي نوع 5-RSS (Ribbed smoke sheet) المفلكن مختبرياً بنسب مختلفة من الكبريت تراوحت ما بين (0.75-2 phr) والذي رمز له بالرمز Virgin RSS، بينما استعمل نوعان من الأحماض الدهنية الطبيعية والمشبعة والتي تتمثل بحامض السيتريك (Stearic acid) وحامض البالمتيك (Palmitic acid) بنسب وزنية مختلفة تراوحت ما بين (3.8- 43.9%) لزمن انتفاخ تراوح ما بين (5-180min) كطور تبادلي (Switching phase) او ما يطلق عليه أيضا (Soft segment)، ولغرض تشخيص وتوصيف خصائص تأثير ذاكرة الشكل الأحادية الاتجاه One-way shape memory effect (1w-SME) بالاعتماد على دورة ذاكرة الشكل الكلاسيكية الساخنة، أجريت مجموعة من الاختبارات التي تمكنا من التحقق (verification) من سلوك ذاكرة الشكل (Shape memory behavior (SM-behavior)) لتقييم اثر تشرب (impregnation) المطاط المفلكن بالحامض الدهني على سلوكيتها كمواد ذكية ذات ذاكرة الشكل وهي:-

• اختبار تأثير ذاكرة الشكل (SME) الكمي لحساب معاملات ذاكرة الشكل عملياً والمتمثلة بـ (Shape fixity ratio, $R_f\%$), (Shape recovery ratio, $R_r\%$) and (Shape memory index, SM-index) ، باستعمال جهاز الاستطالة الحراري (المصمم من قبلي والمصنع بالتعاون مع ورشة صناعية هندسية محلية) وآلة الورنية المطورة من قبلي.

• اختبار تأثير ذاكرة الشكل التصويري المرئي باستعمال تقنية Video-Image.

• اختبار ذاكرة الشكل السطحية باستعمال جهاز Surface –shape memory (المصمم من قبلي والمصنع بالتعاون مع ورشة صناعية هندسية محلية).

• Differential Scanning Calorimeter (DSC) .

• X-ray diffraction (XRD)

علاوة على ذلك اجري فحص (Energy dispersive ray spectroscopy (EDS) و Field emission scanning electron microscopy (FE-SEM) و Fourier transform infrared و spectrometry analysis (FT-IR)) واختبار قياس كثافة التشابك الترابطي (Crosslink density) وبعض الفحوصات الميكانيكية الشبه الساكنة القصيرة الزمن مثل مقاومة الشد و الصلادة السطحية و مقاومة السحق (Max crushing strength) بدرجة حرارة الغرفة. وقد تم مناقشة النتائج المستحصلة بالتفصيل. هذه الدراسة أوضحت إن قدرة المطاط المفلكن والمشرب بالحامض الدهني في التثبيت المؤقت (Temporary fixation) للانفعال المسلط يرتبط ببعض الظواهر الخاصة التي تحدث وفق بروتوكول الدورة الترموميكانيكية الساخنة مثل التقلص الحراري (Thermal contraction) والتراجع المرن (Elastic retract) وتراكم الانفعال اللدن plastic ألدائي، حيث تلعب هذه الظواهر دوراً سلبياً في عملية تقييد الشكل المشوه ميكانيكياً خلال مرحلة برمجة الشكل (مرحلة تنشيط Activation stage خاصة و Shape memory effect, SME) وعليه فإن القيمة الفعلية التي تم احتجازها في هذه الدورة هي 58.7% بدلاً من 70% وان R_f تصل قيمتها الى 83.8% وبالتالي تؤثر سلباً على احتجاز طاقة شغل الاستطالة حيث تقل من 73.71KJ/m^3 الى 61.65KJ/m^3 كما أوضحت هذه الدراسة ارتباط أداء ذاكرة الشكل بطاقة شغل الاستطالة المرنة المقيد عن الانعكاس التلقائي خلال مرحلة تنشيط خاصية SME من دورة ذاكرة الشكل (SMC). إضافة إلى ما ذكر فقد تم دراسة العوامل الأساسية المؤثرة على سلوك ذاكرة الشكل (SM-behavior)، وهي: النسبة المئوية الوزنية للحامض الدهني و عدد دورة ذاكرة الشكل و الانفعال المسلط و كثافة التشابك الترابطي، وقد تبين إن SM-behavior يتحسن عندما ترتفع النسبة المئوية الوزنية للحامض الدهني في كتلة المطاط المفلكن بينما تضعف SM-behavior مع زيادة كل من (الانفعال المسلط ورقم دورة ذاكرة الشكل و كثافة التشابك الترابطي) ومن ناحية أخرى حصول ظاهرة تزهير الشمع (Wax blooming) خلال دورة ذاكرة الشكل.

كما ترصد بيانات هذه الدراسة زيادة زمن سرعة استعادة الشكل الأصلي خلال مرحلة الاستعادة (مرحلة تعطيل خاصية SME) من دورة ذاكرة الشكل (SMC). Shape memory cycle. مع زيادة درجة حرارة التحفيز الحراري حيث يتم الوصول الى النسبة المئوية لاستعادة الشكل الأصلي (R_f) و المقدره بـ 99.7% كما لوحظ الاختلاف الطفيف في SM-behavior مع تغير طبيعة وسائل التبريد والتسخين، إلا إن هذا التغير يؤثر تأثيراً كبيراً على زمن دورة ذاكرة الشكل.

وأخيراً فإن الفحوصات الميكانيكية الشبه الساكنة القصيرة الزمن وبدرجة حرارة الغرفة هي وسائل لوصف التباين في الخصائص الميكانيكية للمطاط المفلكن قبل وبعد تشربه بالحامض الدهني، وان المطاط المفلكن والمشرب بالحامض الدهني باستخدام هذه الفحوصات التقليدية لا يظهر سلوك ذاكرة الشكل بالرغم من تشربه بالحامض الدهني ، حيث يسلك سلوكاً مشابهاً للمطاط المفلكن التقليدي الغير الذكي. وان سبب عدم إظهار سلوك ذاكرة الشكل لعدم توفر الظروف الاستثنائية في هذه الأجهزة و التي تساعد في إجراء دورة ذاكرة الشكل لغرض تنشيط وتعطيل خاصية SME ، لكون هذه الخاصية غير متأصلة بالمواد البوليميرية ذات ذاكرة الشكل بشكل عام.



جمهورية العراق
وزارة التعليم العالي والبحث العلمي
جامعة بابل
كلية هندسة المواد
قسم هندسة البوليمرات والصناعات البتروكيمياوية

تحضير وتوصيف مواد بوليمرية ذات ذاكرة الشكل في التطبيقات الصناعية

أطروحة

مقدمة إلى قسم هندسة البوليمرات والصناعات البتروكيمياوية / كلية هندسة المواد/جامعة
بابل وهي جزء من متطلبات نيل درجة دكتوراه في فلسفة تقانات المواد البوليمرية.

من قبل الباحث

رولا عبد الخضر عباس الصافي

بإشراف

أ. د. محمد حمزة دحام المعموري